Biogeochemical cycling of nutrient silicon in a human-impacted large lake nearshore environment (Hamilton Harbour Area of Concern, Lake Ontario, Canada)

by

Christine Ridenour

A thesis

presented to the University of Waterloo

in fulfillment of the

thesis requirement for the degree of

Master of Science

in

Earth Sciences (Water)

Waterloo, Ontario, Canada, 2017

Author's Declaration

This thesis consists of material all of which I authored or co-authored: see Statement of Contributions included in the thesis. This is a true copy of the thesis, including any required final revisions, as accepted by my examiners.

I understand that my thesis may be made electronically available to the public.

Statement of Contributions

This thesis consists of a series of co-authored chapters. As the first author of each chapter, I was primarily responsible for study designs, execution, data analysis and interpretation, and writing the chapters. The following summarizes the contributions of the co-authors of each chapter.

Chapter 2: Christine Ridenour, Chris Parsons, and Philippe Van Cappellen

Philippe Van Cappellen, Chris Parsons and I designed the research. Chris Parsons and I collected sediment cores. I designed the experimental setup with assistance from Chris Parsons. I ran the experiment and analysed samples. I analysed and interpreted the results. Chris Parsons and I wrote the chapter.

Chapter 3: Christine Ridenour, Chris Parsons, Chris Marvin, Mark Fitzpatrick, and Philippe Van Cappellen

Philippe Van Cappellen, Chris Parsons and I designed the research. Chris Marvin assisted with logistics of suspended sediment and bottom sediment sample collection and provided use of his lab at the Canada Center for Inland Waters for sediment core incubation experiments. Mark Fitzpatrick provided data on phytoplankton community composition in Hamilton Harbour. I performed all laboratory analysis on water, suspended sediment and bottom sediment samples. I collected sediment cores with assistance from Chris Parsons and performed sediment core incubation experiments. I analysed the data, constructed the mass balance model, and interpreted the results. Philippe Van Cappellen, Chris Parsons and I wrote the chapter.

Abstract

The biogeochemical cycling of nutrient silicon (Si) through rivers, wetlands, lakes, and artificial reservoirs regulates the magnitude and bioavailability of Si delivered downstream and to the ocean (Frings et al. 2014; Maavara et al. 2014; Laruelle et al. 2009; Struyf & Conley 2012). Lakes are areas of Si retention along the land to ocean continuum due to uptake of dissolved Si (DSi) by silicon-requiring phytoplankton, such as diatoms, and burial of biogenic Si (BSi) as siliceous frustules in sediments (Frings et al. 2014). The nearshore zones of lakes and the coastal ocean directly receive nutrient inputs from the watershed, which may lead to eutrophication (Haffner et al. 1983; Jickells 1998; Mackenzie et al. 2000; Strayer & Findlay 2010). Enrichment with the nutrients phosphorus (P) and nitrogen (N) can enhance DSi uptake, which can ultimately lead to Si depletion and limitation of siliceous phytoplankton growth in the water column (Schelske & Stoermer 1971; Schelske & Stoermer 1972). Sediments can play an important role in water column nutrient dynamics through acting as a source or a sink of Si and P (Orihel et al. 2017; Nriagu 1978; Schelske 1985). Interactions between dissolved Si and P in pore waters and oxygenation at the sediment-water interface may influence the release of Si and P from sediments (Tuominen et al. 1998; Hartikainen et al. 1996; Tallberg & Koski-Vahala 2001; Koski-Vähälä et al. 2001; Tallberg et al. 2008; Siipola et al. 2016; Lehtimäki et al. 2016). Relatively little is known about Si cycling in the sediments and water column of nearshore zones of large lakes, such as the Laurentian Great Lakes, and it's response to eutrophication.

This thesis examined the biogeochemical cycling of reactive Si in the Hamilton Harbour Area of Concern, a highly eutrophic and human impacted nearshore area of Lake Ontario. The Hamilton Harbour Area of Concern includes Cootes' Paradise marsh and Hamilton Harbour. The mechanisms influencing internal loading of Si and P were investigated in sediments collected from Cootes' Paradise marsh (Chapter 2). Sediment core flow through systems were used to test the effects of oxic and anoxic conditions at the sediment-water interface, and the relative concentrations of Si and P in pore waters on the internal loading of Si and P. Both P and Si appeared to be retained and released by iron(Fe)(III) oxide minerals through adsorption to or coprecipitation with Fe(III) oxides under oxic conditions, and reductive dissolution of Fe(III) oxides and release of sorbed P and Si under anoxic conditions. Compared to oxic conditions, anoxic release of P increased by 8 times while anoxic release of Si increased by only 1.4 times. Thus, sorption to and release from Fe(III) oxides was proportionally a more important mechanism of internal loading for P than Si, leading to greater P retention under oxic conditions and release under anoxic conditions relative to Si. In contrast, dissolution of biogenic Si was likely the dominant source of Si release under oxic and anoxic conditions, however anoxic conditions increased Si release by approximately 40%. The decoupling of Si and P cycles under oxic and anoxic conditions resulted in the Si:P ratio of anoxic release being low (mean Si:P < 16) relative to the Si:P ratio of oxic release (mean Si:P >23), which may potentially contribute to Si limitation of siliceous phytoplankton growth in the water column.

A reactive Si mass balance model was constructed for Hamilton Harbour to determine if Hamilton Harbour is a net source or sink of reactive Si, and if Si is stoichiometrically limiting to diatom growth with respect to P. This was achieved through quantification of reactive Si inputs, outputs, and transformations within

the water column and sediments through field sampling and experimental work, followed by mass balance modelling. Si limitation was determined by calculation of Si:P ratios in the water column of Hamilton Harbour throughout the growing season of 2016, and stoichiometric limitation was defined as a Si:P ratio less than 16:1 (Redfield 1958; Brzezinski 1985). Hamilton Harbour was found to be a net sink of reactive Si, retaining approximately 16% of total reactive Si inputs. Internal loading, water exchange between Hamilton Harbour and Lake Ontario, and discharge from wastewater treatment plants were the largest fluxes of Si to the Hamilton Harbour water column. Si was stoichiometrically and likely physiologically limiting to siliceous phytoplankton growth between May and November 2016, which is in contrast to the assumption of P limitation of phytoplankton growth and may be contributing to the seasonally recurring harmful algal blooms in Hamilton Harbour (Hiriart-Baer et al. 2009).

This research demonstrates that freshwater nearshore zones, such as coastal wetlands and embayment's are important areas of nutrient cycling that can alter nutrient fluxes from the watershed to the open lake. Coastal wetland sediments may act as a source or sink of Si and P to the water column depending on redox conditions at the sediment-water interface. Different mechanisms of internal loading decouples the Si and P cycles in sediments. The nearshore zones of large lakes can reduce Si export offshore and downstream through nutrient retention. Anthropogenic sources of Si such as wastewater treatment plant effluent can be a larger source of Si than tributaries and groundwater, and as such humans are directly affecting the biogeochemical cycling of Si in nearshore zones. Cultural eutrophication in nearshore zones can lead to Si limitation, which may have critical implications for ecosystem functioning and repercussions for nutrient cycles offshore and downstream. This knowledge enhances our understanding of the effects of human activities and cultural eutrophication on biogeochemical Si cycling along the land to ocean continuum. This knowledge may better inform ecosystem modelling and the impacts that climate change may have on Si biogeochemistry, such as spreading hypoxic zones (Rabalais et al. 2010). Through furthering our understanding of factors influencing phytoplankton dynamics, this knowledge may be beneficial to remediation efforts and the protection of nearshore zones in freshwater lakes.

Acknowledgements

I am grateful to the Queen Elizabeth II Graduate Scholarship in Science and Technology and the University of Waterloo for funding this research.

I am indebted to Tanya Long of the Ontario Ministry of Environment and Climate Change; Craig McGinaly of Arcelor-Mittal Dofasco; Mike Spicer and Mukesh Patel of Halton Region; Bert Posedowski, Mark Soloman, and Nelson Vidal of the City of Hamilton; Mark Fitzpatrick of Fisheries and Oceans; and Chris Marvin, Julia Jia, Debbie Burniston, Katrina Barnwell, Dave Depew, Jacqui Milne, Daniel Abby and Carley Smiley of Environment and Climate Change Canada for providing data, samples, and/or assistance with sample collection, without which this thesis would not have been possible.

I thank Marianne Vandergriendt for all her help and guidance in the many hours spend in the lab, as well as Shuhuan Li for her assistance with chemical extractions. I also thank Sarah Legemaate, Tatjana Milojevic, Danny Oh, Steph Slowinski, Lu Huang, Sophie Ehrhardt and Brooke McNeil for lending a helping hand at a time of need.

I am grateful to my supervisors Chris Parsons and Philippe Van Cappellen, and to the entire Ecohydrology Research Group for their guidance, support, mentorship and friendship throughout my time at the University of Waterloo.

I thank Chris Parsons and Christina Smeaton for taking me on as an undergraduate student and giving me my first taste of research, without which I may not have pursued graduate school and learned everything I have about science and myself over the past few years.

Dedication

To my family and my boyfriend Francis for their unwavering support and faith in me.

Table of Contents

List of Figures

List of Tables

List of Abbreviations

Si	Silicon
DSi	Dissolved silicon
RPSi	Reactive particulate silicon
P	Phosphorus
SRP	Soluble reactive phosphorus
TDP	Total dissolved phosphorus
N	Nitrogen
Fe	Iron
TDFe	Total dissolved iron
Mn	Manganese
TDMn	Total dissolved manganese
S	Sulfur
TDS	Total dissolved sulfur
ICP-OES	Inductively coupled plasma-optical emission spectrometry
IC	Ion chromatography
UV-Vis	Ultra violet visible spectrophotometer

Chapter 1

General Introduction

1.1 The global biogeochemical silicon cycle

1.1.1 Forms of silicon in the environment

Nutrient silicon (Si) exists in dissolved and particulate forms in nature. Dissolved Si (DSi) is originally produced through the chemical weathering of silicate minerals in the earth's crust and is predominantly in the form of orthosilicic acid (H_4SiO_4) below pH 9.7 (Dietzel 2000). Particulate Si includes 1) biogenic Si (BSi) produced through the biological assimilation of DSi, 2) DSi adsorbed to the mineral surfaces (adsorbed Si), 3) Si contained in primary and secondary crystalline silicate minerals such as quartz, feldspars, micas and clays, and 4) Si coprecipitated in minerals such as iron(III) oxides (Tallberg et al. 2012; Mayer & Jarrell 2000; Sauer et al. 2006 and references therein). DSi, BSi, adsorbed Si and coprecipitated Si are bioavailable or potentially bioavailable and therefore are considered reactive forms of Si (Tallberg et al. 2012).

1.1.2 Silicon cycling along the land to ocean continuum

The past few decades of research have revealed that there is the strong biological component of the Si cycle all along the land to ocean continuum (Figure 1.1) (Frings et al 2014). Of the 14.6 Tmol Si yr^{-1} estimated to be produced through chemical weathering, only slightly more than half of this (7.7 Tmol Si yr^{-1}) reaches the coastal ocean due to biological assimilation and retention of Si in soils, lakes and artificial reservoirs (Laruelle et al. 2009). Annual fixation of DSi on the continents is comparable to the annual fixation of DSi in the global ocean (Conley 2002). In soils and freshwater aquatic environments, DSi is assimilated by terrestrial and aquatic plants, testate amoebae, freshwater sponges, and siliceous phytoplankton including diatoms, chrysophytes and silicoflagellates to build internal or external siliceous structures (Figure 1.2) (Epstein 1994; Aoki et al 2007; Conley 1988; Yang et al 1993). Terrestrial and aquatic plants can accumulate BSi in significant amounts in siliceous deposits known as phytoliths (Figure 1.2a), which provide rigidity and may improve plant resistance to biotic and abiotic stress (Epstein 1994; Struyf & Conley 2009; Schoelynck et al. 2010; Schoelynck & Struyf 2016). Testate amoebae, which have siliceous tests (shells) (Figure 1.2b), have been estimated to assimilate as much Si as higher plants (Aoki et al. 2007). DSi and BSi are heavily recycled in soils, and export to rivers, lakes, and reservoirs has a strong biological control (Figure 1.1) (Derry et al. 2005; Conley 2002).

Diatoms are an important primary producer in freshwater and marine aquatic environments and require DSi to build siliceous frustules (shells) (Figure 1.2c) (Willen 1991; Treguer et al. 1995). Lakes and reservoirs are areas of Si retention due to uptake of DSi primarily by diatoms and burial of BSi in sediments (Frings et al. 2014; Maavara et al. 2014; Taylor Maavara et al. 2015). Frings et al. (2014) estimated the global retention of Si by lakes to be 1.3 Tmol DSi yr^{-1} and artificial reservoirs 0.23 Tmol DSi yr^{-1}, which combined equates to 21-27% of the global riverine DSi load. Maavara et al. (2014) estimated the global retention of Si by artificial reservoirs to be 0.16 Tmol

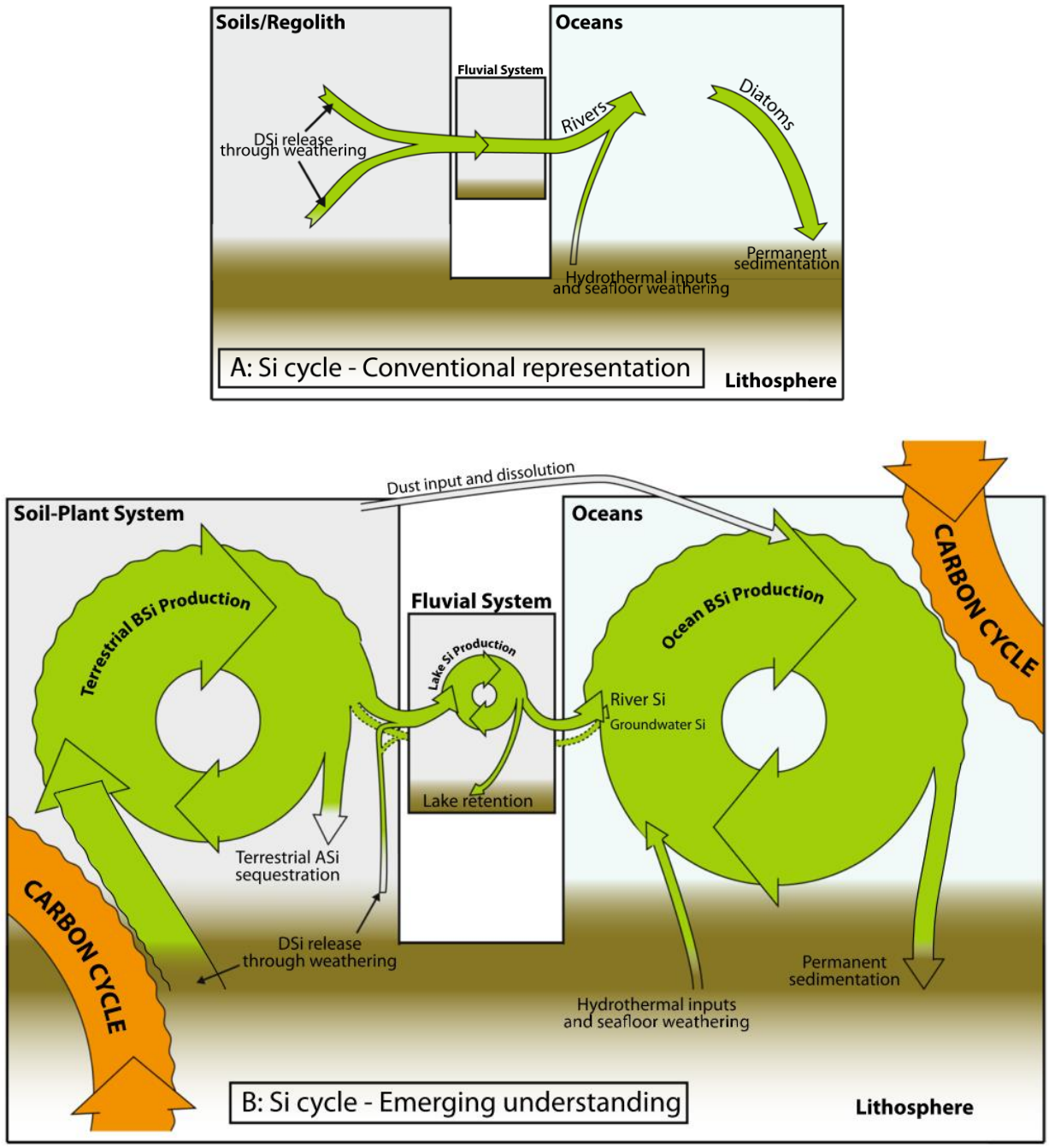

Figure 1.1. Past (top) versus present (bottom) conceptualisation of Si cycling along the land to ocean continuum where biological processes play a major role in Si cycling and retention. Consumption of CO_2 through chemical weathering of silicate minerals and transport of organic carbon to the deep ocean through sedimentation and burial of BSi link the Si and carbon cycles. Figure taken from Frings et al. (2014) Lack of steady-state in the global biogeochemical Si cycle: Emerging evidence from lake Si sequestration. *Biogeochemistry*, 117:255-277.

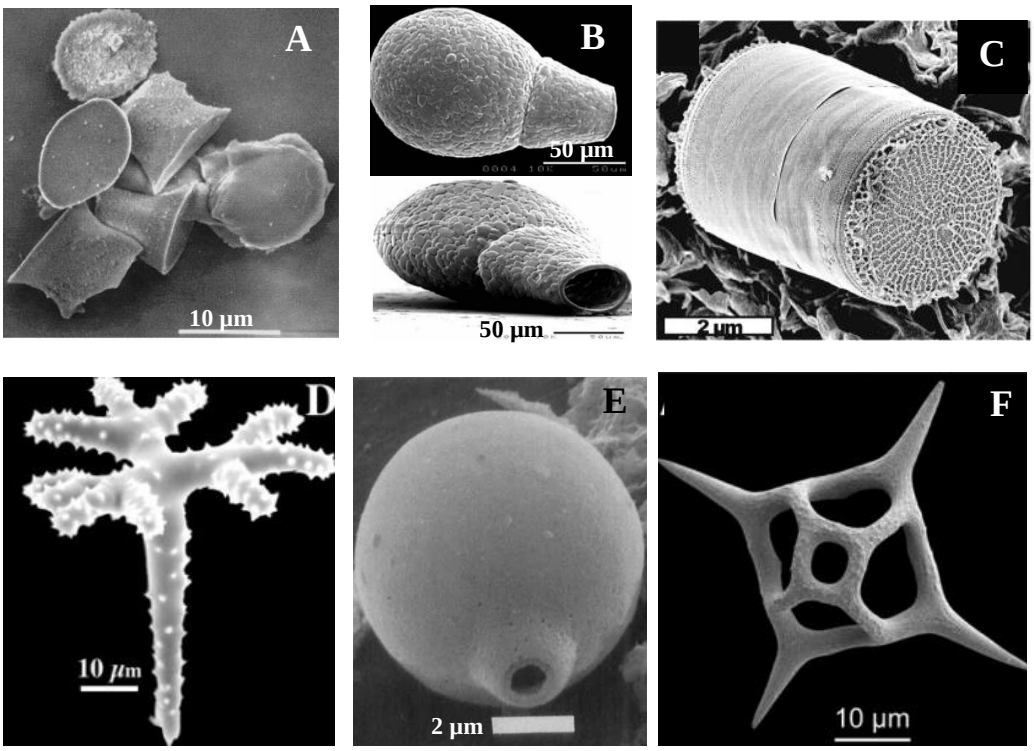

Figure 1.2. Scanning electron microscope images of siliceous structures of plants and organisms.
A. Silica cell phytolith from wheat *Triticum aestivum.* Image taken from Ball et al. (1999) Identifying inflorescence phytoliths from selected species of wheat (*Triticum monococcum*) and barley (*Hordeum vulgare and H. spontaneum*) (Gramineae). *American Journal of Botany*, 86(11):1615-1623.
B. Testate amoebae test. Image taken from Mitchell et al. (2008) Testate amoebae analysis in ecological and paleoecological studies of wetalnds: Past, present and future. *Biodiversity and Conservation*, 17(9):2115-2137.
C. Diatom frustule. Image taken from Hildebrand et al. (2009) 3D imaging of diatoms with ion-abrasion scanning electron microscopy. *Journal of Structural Biology*, 166:316-328.
D. Sponge spicule. Image taken from Uriz et al. (2003) Siliceous spicules and skeleton frameworks in sponges: Origin, diversity, ultrastructural patterns, and biological functions. *Microscopy Research and Technique*, 62:279-299.
E. Chrysophyte stomatocyst. Image taken from Duff et al. (1992) Chrysophyte cysts in 36 Canadian high arctic ponds. *Nordic Journal of Botany*. 12(4):471-499.
F. Silicoflagellate. Image taken from McCartney et al. (2014) Fine structure of silicoflagellate double skeletons. *Marine Micropaleontology*, 113:10-19.

DSi yr^{-1} and 0.37 Tmol reactive Si yr^{-1} (dissolved + particulate), which is equivalent to 5.3% of the global reactive Si load to rivers.

Upon reaching the ocean, a substantial portion of the Si delivered is retained in the nearshore coastal zone and on the continental shelf (Laruelle et al. 2009). Burial of BSi was estimated to be 1.4 Tmol Si yr^{-1} in nearshore coastal zone sediments, and 1.7 Tmol Si yr^{-1} on the continental shelf, which combined is approximately 40% of the total marine burial (Laruelle et al. 2009).

BSi deposited in lacustrine and marine sediments may be resuspended, dissolved and thereby recycled to DSi, or buried (Van Cappellen 2003). In this way sediments can act as both a sink and a source of reactive Si. Globally, freshwater and marine sediments are a net sink of Si as net sedimentation (gross sedimentation minus

resuspension) exceeds recycling over an annual time scale (Laruelle et al. 2009). However, the recycling rate of BSi at the sediment-water interface is high and only 3% of BSi is permanently buried in ocean sediments (Treguer et al. 1995).

1.1.3 Cycling of silicon in sediments and interactions with phosphorus

The internal loading of Si can contribute over 40% of the total annual DSi to lakes and thus may be an important flux in the overal Si budget and for sustaining the growth of siliceous phytoplankton (Johnson & Eisenreich 1978; Nriagu 1978; Schelske 1985). In sediments, there are several potentially mobile Si pools: DSi in pore water, Si adsorbed to mineral surfaces, Si coprecipitated with amorphous minerals such as iron(Fe)(III) oxides, and BSi (Siipola et al. 2013; Tallberg et al. 2012; Mayer & Jarrell 2000). Studies on sediment Si release have predominantly focused on BSi, as this tends to be the largest potentially bioavailable pool of Si in sediments (Tallberg et al. 2008; Tallberg et al. 2012). Temperature, pH and salinity have all been shown to increase BSi dissolution rates (Kamatani 1982; Loucaides et al. 2008a). However, Si adsorbed to or coprecipitated with Fe(III) oxide minerals may be influenced by redox conditions at the sediment-water interface, and by other anions competing for sorption sites such as phosphate (PO_4^{3-}) (Siipola et al. 2016; Hartikainen et al. 1996; Tuominen et al. 1998; Tallberg & Koski-Vahala 2001; Tallberg et al. 2008).

Both silicate (SiO_4^-) and phosphate can be specifically adsorbed to the surfaces of Fe(III) oxide minerals by ligand exchange, and thus the two anions may compete for sorption sites if they become limited (Hingston et al. 1967; Obihara & Russell 1972). The ability for each anion to compete for sorption sites is influenced by pH as the charge at the mineral surface and the charge of each anion changes with pH due to dissociation (Figure 1.3) (Brinkman 1993; Lumsdon and Evans 1994). The point of zero net proton charge (PZNPC) is the pH at which the charge on the mineral surface is 0 (Lumsdon & Evans 1994). As pH decreases or increases away from the PZNPC, the charge on the mineral surface becomes increasingly positive and negative respectively (Figure 1.3) (Lumsdon & Evans 1994). Experimentally determined PZNPC for Fe(III) oxide minerals such as goethite, hematite, and hydrous ferric oxides range from 7.5 to 9.38 (Lumsdon & Evans 1994). Phosphoric acid and silicic acid dissociate and become increasingly negatively charged at pKa values of 7.1 and 12.7 for phosphoric acid, and 9.8 and 13.2 for silicic acid (Figure 1.3). Therefore, sorption of P to Fe(III) oxide minerals is preferred over Si below pH 9, as the charge on the mineral surface is positive below the PZNPC and the charge on phosphoric acid is more negative (-1 or -2) than that of silicic acid (0) (Figure 1.3) (Brinkman 1993). This results in a stronger attraction between the mineral surface and phosphoric acid than silicic acid (Figure 1.3) (Brinkman 1993). Whereas, at pH greater than 9, Si sorption to Fe(III) oxide minerals is preferred over P, as the charge on the mineral surface becomes negative above the PZNPC and phosphoric acid is more negatively charged (-2 or -3) than silicic acid (-1 or -2) (Figure 1.3) (Brinkman 1993). This causes strong repulsion between the mineral surface and phosphoric acid, which is less so between the mineral surface and silicic acid (Figure 1.3) (Brinkman 1993).

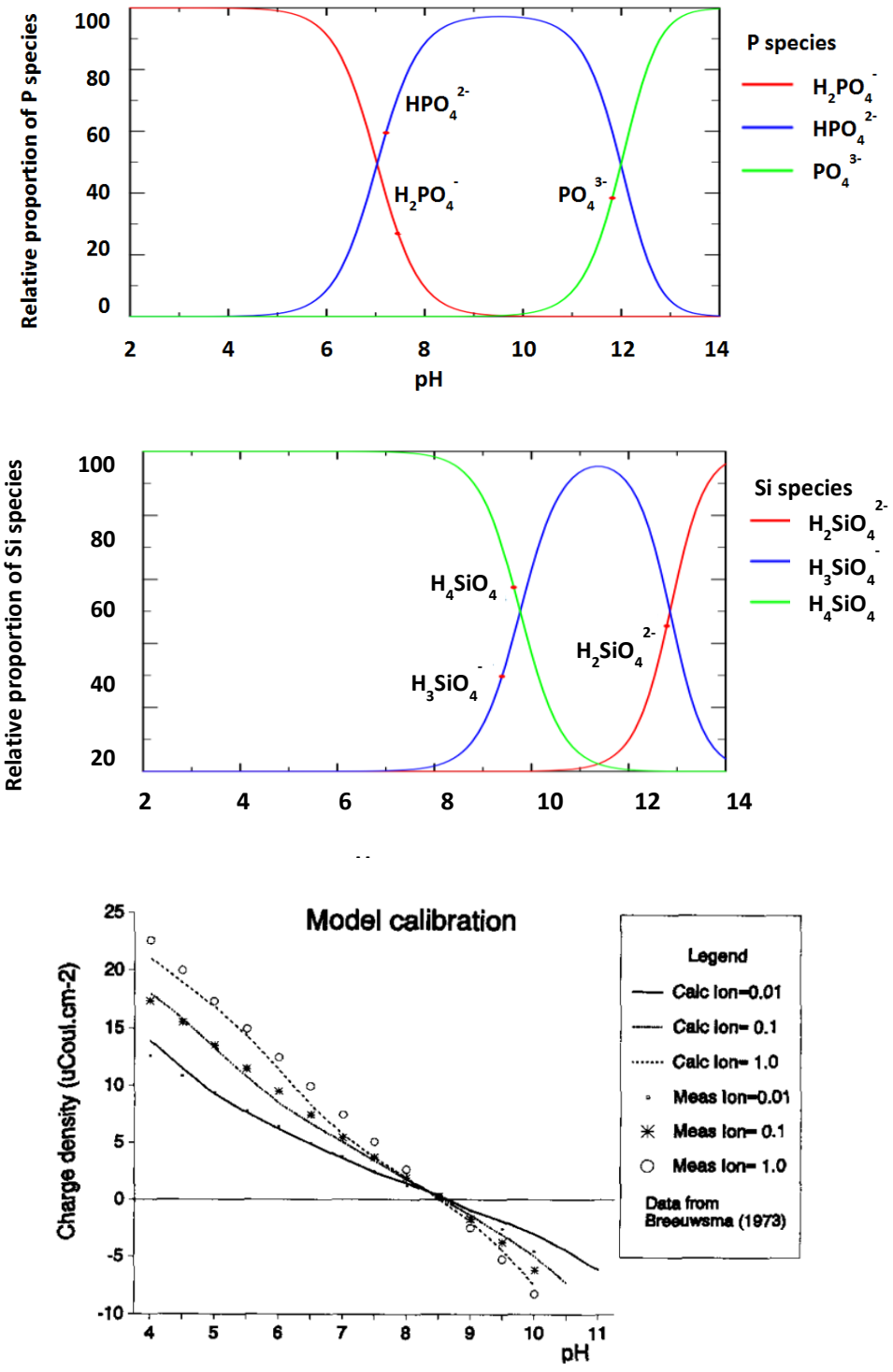

Figure 1.3. Speciation of phosphoric (top) and silicic acid (middle) and the charge density on the surface of hematite (bottom) across a range of pH. Phosphoric acid has pKa's at 7.1 and 12.7, and silicic acid has pKa's at 9.7 and 13.2. Speciation diagrams were made using PHREEQC and PHREEPLOT and the included thermodynamic database (Parkhurst and Appelo 1999; Kinniburgh and Cooper 2011). Bottom figure taken from Brinkman (1993) A double-layer model for ion adsorption onto metal oxides, applied to experimental data and to natural sediments of Lake Veluwe, the Netherlands. *Hydrobiologia*, 253:31-45.

Previous studies suggest that high concentrations of Si are able to desorb and/or prevent sorption of P thereby increasing P release from sediments to the interstitial water (Tallberg and Koski-Vahala 2001; Tallberg et al. 2008; Tuominen et al. 1998; Siipola et al. 2016; Koski-Vähälä et al. 2001). The deposition and dissolution of a large diatom bloom may provide high enough Si concentrations for this to occur in nature (Tallberg 1999). Competitive sorption may have important implications for the recycling of both Si and P in freshwater and marine sediments, particularly in areas of nutrient loading where there may be substantial accumulation of Fe-bound P in sediments (Søndergaard et al. 2003). Competitive sorption between P and Si has only been demonstrated in lake sediments in Finland and coastal marine sediments of the coast of France (Tallberg and Koski-Vahala 2001; Tallberg et al. 2008; Tuominen et al. 1998; Siipola et al. 2016; Koski-Vähälä et al. 2001). Thus, competitive sorption has not been investigated in eutrophic wetland sediments or in areas outside Europe. As well, the relative importance of competitive sorption in the context of other physical, chemical, and biological processes potentially influencing release of Si and P from sediments, such as groundwater discharge, anoxic conditions and bioturbation, has not been thoroughly investigated (Boström et al. 1988).

Due to the association of Si with Fe(III) oxides, anoxic conditions may result in the release of Si through the reduction of solid Fe(III) to aqueous Fe(II) and subsequent dissolution of Fe(III) oxide minerals. Fe(III) oxides can be reductively dissolved by both chemical (abiotic) and biological (biotic) means (Schwertmann 1991; Lovely et al. 1991). In aquatic sediments, the dominant mechanism of Fe(III) reductive dissolution is the dissimilatory reductive dissolution of Fe(III) to Fe(II) by anaerobic microorganisms using Fe(III) as a terminal electron acceptor (Lovely et al. 1991). Reductive dissolution of Fe(III) oxides and release of sorbed P is the classic model of internal P loading from anoxic sediments (Einsele 1936; Einsele 1938; Mortimer 1941; Mortimer 1942), but this mechanism has not been studied as thoroughly for Si (Siipola et al. 2016).

There is some evidence that suggests that anoxic conditions may increase Si release from sediments (Danielsson 2014; Rabalais et al. 2010; Siipola et al. 2016; Lehtimäki et al. 2016). In the Baltic Sea and the northern Gulf of Mexico, bottom water DSi concentrations were negatively correlated with dissolved oxygen concentrations, suggesting increased Si release or less Si removal from sediments under hypoxic/anoxic conditions (Danielsson 2014; Rabalais et al. 2010). However, the effect of anoxia on sediment Si release is not well understood as very few studies have investigated this (Siipola et al. 2016; Lehtimäki et al. 2016). Siipola et al. (2016) found that DSi release from the loosely sorbed and redox-sensitive fractions of Si in sediment decreased under anoxic conditions compared to oxic, which may have been due to resorption of Si to aluminum oxides and formation of colloidal mixed Fe-Si oxides. As well, on a monthly time scale, Siipola et al. (2016) found that DSi release from sediments was slower under anoxic compared to oxic conditions. However, over a period of 7 months, Lehtimäki et al. (2016) found that the total amount of DSi released from BSi was higher under hypoxic conditions compared to oxic, which may have been related to the microbial community. Understanding how oxygen depletion affects the Si cycle is critical knowledge currently lacking given that hypoxic areas in coastal zones are growing in size due to eutrophication (Rabalais et al 2010).

1.2 Human perturbations to the biogeochemical silicon cycle

The cycling of Si through terrestrial and aquatic ecosystems is being altered by human activities, the cumulative effects of which are difficult to predict. Reservoirs have been found to retain approximately 5% of river reactive Si loads and decrease export of the reactive Si species downstream (Maavara et al. 2014; Frings et al. 2014; Humborg et al 2000). Deforestation has been shown to initially increase Si fluxes to rivers, but over time leads to decreased Si fluxes with sustained soil disturbance due to depletion of soil Si pools (Conley et al. 2008; Struyf et al. 2010). Agriculture removes BSi from the terrestrial ecosystem through crop harvest (Vandevenne et al. 2012). Urbanization and development may increase the export of DSi to rivers compared to forested watersheds as the removal of vegetation decreases DSi uptake by plants (Carey & Fulweiler 2012). Wastewater treatment plant (WWTP) effluent contains Si from sewage and household detergents and thus is an anthropogenic point source of Si (Sferratore et al. 2006; Maguire & Fulweiler 2016; Maguire & Fulweiler 2017; Van Dokkum et al. 2004). Cultural eutrophication has altered the nutrient stoichiometry (P:N:Si) of many rivers and receiving waters around the world, which may lead to Si limitation of diatom growth and harmful algal blooms (Justic et al. 1995; Dubravko Justic et al. 1995; Danielsson et al. 2008; Viaroli et al. 2013).

1.2.1 Eutrophication and silicon limitation

In freshwater environments, P is typically the limiting nutrient to primary productivity (Blomqvist et al. 2004). Enrichment of water bodies with P can enhance the growth of diatoms and increase DSi uptake, which over time leads to depletion of water column DSi concentrations and a switch from P limitation to Si limitation of diatom growth (Schelske & Stoermer 1971; Schelske & Stoermer 1972). Si limitation of diatom growth also limits the uptake of P from the water column by diatoms, thereby increasing the pool of available P for non-siliceous phytoplankton, which can lead to a shift in phytoplankton community composition from a diatom-dominated to a non-diatom dominated system (Schelske & Stoermer 1971; Schelske & Stoermer 1972).

The Redfield-Brzezinski Si:P ratio of 16:1 is often taken as the stoichiometric delineation between P limitation (Si:P > 16:1) and Si limitation (Si:P < 16:1) of diatom growth, which is based on the average content of marine diatoms grown under non-limiting conditions (Redfield 1958; Brzezinski 1985). Therefore, increases in P concentration and/or decreases in Si concentration lower the Si:P ratio. Laboratory studies have shown that the transition from diatom to non-diatom dominance occurs between Si:P ratios of 3:1 to 30:1, with diatoms dominating at high Si:P ratios, non-siliceous phytoplankton dominating at low Si:P ratios, and diatoms and non-siliceous phytoplankton coexisting at intermediate Si:P ratios (Sommer et al. 2002; Sommer 1983; Sommer 1985; Peterson Holm & Armstrong 1981). Similar results were obtained in a mesocosm experiment where diatom dominance occurred at concentrations greater than 2 µmol Si L^{-1}, dominance by other phytoplankton species only occurred below 2 µmol Si L^{-1}, and an initially flagellate-dominated community switched to a diatom-dominated community within a few days after adding Si to a concentration above 2 µmol L^{-1} (Egge & Aksnes 1992).

Nutrient enrichment followed by Si depletion and shifts in phytoplankton community composition have been found in many areas including Lake Michigan (Schelske & Stoermer 1971; Schelske & Stoermer 1972;

Schelske et al. 1986), Chesapeake Bay (Conley & Malone 1992), the Bay of Brest (Chauvaud et al. 2000), the northern Gulf of Mexico (Dubravko Justic et al. 1995), the Guadiana estuary (Rocha et al. 2002), the East River-Long Island Sound system (Gobler et al. 2006), the Baltic Sea (Danielsson et al. 2008), the Black Sea (Garnier et al. 2002), the northern Adriatic Sea (Dubravko Justic et al. 1995), and the North Sea (Peeters et al. 1991). The risk of Si limitation may increase in the future for many coastal areas due to continued enrichment of P and N coupled with decreasing Si delivery to oceans due to Si retention in reservoirs (Garnier et al. 2010; Turner et al. 2003). However, retention of Si in freshwater bodies including lakes, rivers, and wetlands may also play an important role in shifting nutrient ratios, but few studies of Si cycling and limitation in lakes have been conducted in comparison to marine coastal areas.

Shifts in phytoplankton community composition towards non-diatom dominance may have negative consequences for aquatic food webs. Diatoms are generally a quality food source for zooplankton and fish, while flagellates are a poor food source and are not grazed (Officer & Ryther 1980). In the Mississippi continental shelf, copepod zooplankton abundance decreased and the risk of flagellate phytoplankton blooms increased when the Si:DIN (dissolved inorganic nitrogen – the sum of ammonia, nitrite, and nitrate) ratio dropped below the 1:1 Redfield ratio (Turner et al. 1998). Non-diatom dominance can alter energy transfer to higher trophic levels and may result in lower fish production:primary production ratios than in diatom dominated systems such as coastal upwelling areas (Sommer et al. 2002). Further, flagellate blooms persist for longer periods of time, and lack of grazing may lead to higher deposition of organic matter to sediments and anoxic conditions (Officer & Ryther 1980).

However it should be noted that not all diatom blooms are beneficial to aquatic ecosystems (Wright et al. 1989). Blooms of the marine species *Pseudo-nitzschia* can release domoic acid, a neurotoxic amino acid, causing Amnesic Shellfish Poisoning events (Wright et al. 1989). Domoic acid is thought to be produced during times of nutrient stress when growth slows or ceases (Bates & Trainer 2006). Studies suggest that domoic acid production is enhanced by Si or P limitation with respect to N when light is non-limiting, although low concentrations of domoic acid have also been found to be produced in the absence of nutrient limitation (Bates & Trainer 2006; Terseleer et al. 2013; Thorel et al. 2014). As well, Parsons et al (2002) found that *Pseudo-nitzschia* abundance increased with decreasing Si:N ratios. Thus, increasing N concentrations in the ocean through cultural eutrophication may also increase the occurrence of harmful diatom blooms (Bates & Trainer 2006; Terseleer et al. 2013; Parsons et al. 2002).

1.3 The large lake nearshore environment

The nearshore zone of large lakes such as the Laurentian Great Lakes is the transition from the watershed to the open lake (Haffner et al. 1983). Nearshore zones receive nutrient inputs from the watershed from sources such as atmospheric deposition, groundwater, rivers and surface runoff, and also through exchange with offshore waters (Figure 1.4) (Haffner et al. 1983; Mackenzie et al. 2000). Biogeochemical processes in the nearshore zone both retain and release nutrients through biological uptake and burial, and regeneration in the water column and sediments (Figure 1.4) (Strayer & Findlay 2010). Changes in nutrient supply from watershed sources or offshore exchange are likely to affect nutrient cycling and stoichiometry in the nearshore zone (Strayer & Findlay 2010;

Mackenzie et al. 2000). Such changes occur in nearshore zones impacted by human activities where nutrient inputs are dominated by anthropogenic sources such as sewage, and urban and agricultural runoff (Strayer & Findlay 2010). Nearshore zones with restricted exchange with offshore waters are the most seriously affected by human impacts as these areas have longer residence times sufficient to enable phytoplankton growth, and lower dilution of watershed inputs by inflowing offshore waters (Haffner et al. 1983; Jickells 1998). Many nearshore zones experience high human pressure through urbanization, industry, and recreation, and use of the nearshore zone as a water source, a waste disposal site, and for transportation (Strayer & Findlay 2010). These pressures and demands on nearshore zones will increase in the future with increasing global population (Strayer & Findlay 2010).

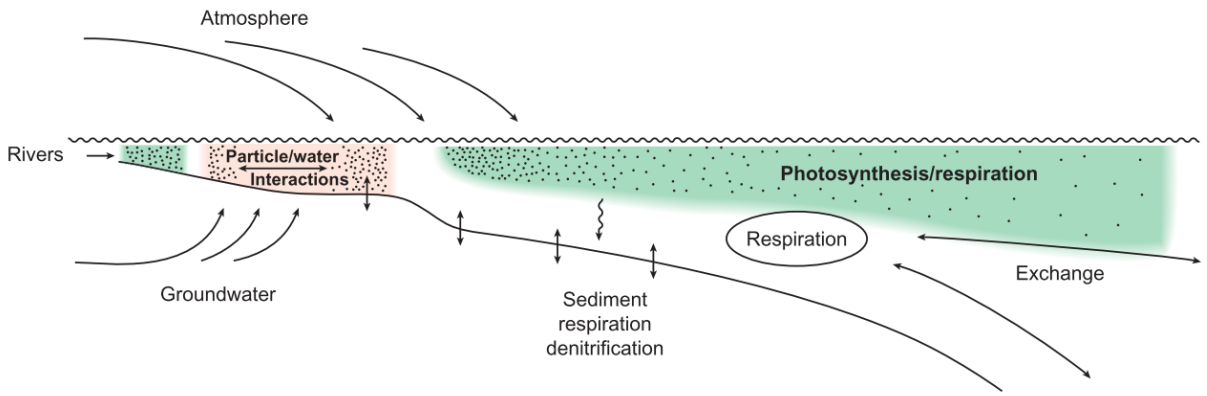

Figure 1.4. Schematic diagram showing nutrient sources, sinks, and internal cycling in coastal zones. Figure taken from Jickells (1998) Nutrient biogeochemistry of the coastal zone. *Science*, 281:217-222.

1.3.1 Hamilton Harbour Area of Concern

At the western end of Lake Ontario, Hamilton Harbour and the adjoining Cootes' Paradise marsh were identified as one of 43 Great Lakes Areas of Concern in 1987 by the Canada-U.S. International Joint Commission, due to several beneficial use impairments (International Joint Commission United States and Canada 1987; Hiriart-Baer et al. 2009; Hiriart-Baer et al. 2016). Industry, agriculture, and urbanization have all contributed to the degradation and eutrophic state of both Cootes' Paradise marsh and Hamilton Harbour (Barica 1989; Hiriart-Baer et al. 2009; Hiriart-Baer et al. 2016; Chow-Fraser et al. 1998).

Cootes' Paradise marsh is a hypereutrophic urban wetland that experiences excessive green filmentous algae growth every summer (Chow-Fraser et al. 1998; Parsons et al. 2017). Prior to the building of the Dundas WWTP in 1919, raw sewage was discharged into West Pond of Cootes' Paradise marsh (Kelton & Chow-Fraser 2005). Successive WWTP upgrades from a primary to a secondary treatment plant in 1962, a tertiary treatment plant

in 1978, and addition of sand filters in 1987 have reduced P loading from the WWTP from 45 kg d^{-1} in the 1970s to less than 4 kg d^{-1} in the 1990s (Chow-Fraser et al. 1998). However, after many years of high external P loading, Cootes' Paradise sediments have high concentrations of legacy P and internal loading of P contributes more than 20% of total P sources, delaying the progress of remediation efforts (Parsons et al. 2017; Chow-Fraser et al. 1998; Kelton & Chow-Fraser 2005).

Cootes' Paradise marsh flows into Hamilton Harbour, an urbanized eutrophic embayment with a history of industrial activity, sediment contamination, high nutrient loading, hypolimnetic anoxia, and nuisance and harmful algal blooms (Hiriart-Baer et al. 2009; Hiriart-Baer et al. 2016; Barica 1989). In 1985, loadings of P and N to Hamilton Harbour were 609 kg d^{-1} and 7076 kg d^{-1} respectively, with concentrations in the range 40-200 µg L^{-1} of total P and 50-4000 µg L^{-1} of ammonia (Barica 1989). High nutrient loading combined with a sufficiently long residence time resulted in extensive eutrophication of Hamilton Harbour (Haffner et al. 1983). At that time, diatom communities were maintained year round (Haffner et al. 1983). In response to remediation efforts such as WWTP upgrades and watershed best management practices, total P concentrations have significantly declined since 1987 but no significant improvements occurred between 1999 and 2016, and total P concentrations in surface water remain high (surface total P concentrations averaged 39.7 ± 3.4 µg L^{-1} in 2012) and above the target concentration of 20 µg L^{-1} (Hiriart-Baer et al. 2016). Chlorophyll *a* concentrations have not significantly changed since 1987, which may be due to high P concentrations and therefore a lack of nutrient limitation altogether (Hiriart-Baer et al. 2016). Today, diatom growth tends to be restricted to blooms in the spring and fall with summer growth being dominated by chlorophytes, crypotophytes, dinophytes and sometimes cyanobacteria (Dermott et al. 2007; Munawar et al. 2017). Cyanobacteria growth accounted for over 60% of phytoplankton biomass in late July of 2006 (Munawar et al. 2017). Low diatom abundance may be the result of Si limitation due to nutrient enrichment, but may also be influenced by other factors such as water temperature and top-down control by zooplankton grazing (Dermott et al. 2007).

1.4 Thesis outline

This thesis investigates the biogeochemical cycling of Si in a human impacted large lake nearshore environment – the Hamilton Harbour Area of Concern (AOC), Lake Ontario, Canada including Cootes' Paradise marsh and Hamilton Harbour.

Chapter 2 investigates the mechanisms of internal loading of P and Si from Cootes' Paradise sediments including 1) oxic and anoxic conditions at the sediment-water interface, and 2) the concentrations of dissolved P and Si in pore waters. This was investigated through sediment core flow through systems under oxic and anoxic conditions where different concentrations of P and Si were introduced to the sediment and the release of P and Si from sediment measured.

Chapter 3 investigates the biogeochemical cycling of reactive Si in Hamilton Harbour in order to determine if 1) Hamilton Harbour is a net source or sink of Si and 2) Si is stoichiometrically limiting to diatom growth with respect to P. A reactive Si mass balance model that accounted for Si inputs, outputs, and internal cycling in

Hamilton Harbour was constructed through extensive field sampling and experimental work. Water column molar Si:P ratios were calculated throughout the growing season of 2016 to determine stoichiometric Si limitation.

Chapter 4 summarizes research findings, discusses study limitations and proposes areas of future research.

Chapter 2

Mechanisms of internal loading of phosphorus and silicon in a eutrophic coastal wetland (Cootes' Paradise, Ontario, Canada)

2.1 Introduction

Internal loading from sediments can be a substantial source of the nutrients phosphorus (P) and silicon (Si) to freshwater bodies, with internal P loading often exceeding 30% of the external total P (TP) load, and internal Si loading exceeding 40% of the total annual Si inputs in some cases (Orihel et al. 2017; Schelske 1985; Nriagu 1978). Many physical, chemical and biological factors influence sediment release rates of P and Si, which can vary both temporally and spatially (Orihel et al. 2017; Spears et al. 2008; Srithongouthai et al. 2003; Cowan et al. 1996). One such factor is competition between phosphate (PO_4^{3-}) and other anions for sorption sites on the surfaces of iron(Fe)(III) oxide minerals, such as hydroxyl ions, arsenate, sulfate, bicarbonate, oxalate, and dissolved Si (DSi) in the form of silicate (SiO_4^-) (Orihel et al. 2017 and references there in). DSi is of particular importance as it is generally present in sediment pore water in high concentrations relative to phosphate (Sholkovitz 1973; Gaillard et al. 1987; Urban et al. 1997). Competition between phosphate and DSi may influence the retention and release of both nutrients in sediments (Hartikainen et al. 1996; Koski-Vähälä et al. 2001; Tallberg & Koski-Vahala 2001; Tallberg et al. 2008; Tuominen et al. 1998).

Phosphate and DSi have a high affinity for the sorption sites on the surfaces of Fe(III) oxide minerals (Slomp et al. 1996). At the common pH in aerated freshwater systems, Fe primarily exists as low solubility Fe(III) oxide minerals (Schwertmann 1991). Fe(III) oxides have a pH dependent surface charge which enables both phosphate and DSi to specifically adsorb to the surface through ligand exchange (Hingston et al. 1967; Obihara & Russell 1972; Brinkman 1993). Thus, in the oxic zone of surficial sediments, phosphate and DSi in pore water may adsorb or coprecipitate with Fe(III) oxides (Hingston et al. 1967; Obihara & Russell 1972; Brinkman 1993). Under anoxic conditions, Fe(III) oxides can be reductively dissolved through the reduction of solid Fe(III) to aqueous Fe(II) by anaerobic microorganisms, which can use Fe(III) as a terminal electron acceptor after depletion of oxygen, nitrate, and manganese (IV) oxides (Lovely & Phillips 1988; Lovely et al. 1991). Consequently, under anoxic conditions, adsorbed and coprecipitated P and Si can be released to the pore water and may diffuse across the sediment-water interface to the water column (Boström et al. 1988).

The retention and release of P from Fe oxides under oxic and anoxic conditions is a well-known mechanism of internal loading first described by Einsele (1936; 1938) and Mortimer (1941; 1942) (Hupfer & Lewandowski 2008). Similar concentrations of Fe-bound P and Si have been measured in sediments but far less attention has been given to the role of Fe(III) oxides on Si retention and release in sediments (Hartikainen et al. 1996; Tallberg et al. 2008; Tallberg et al. 2009; Tallberg et al. 2012). There have been few studies investigating the effect of anoxia on DSi release from sediment, and the findings have been unclear (Siipola et al. 2016; Lehtimäki et al. 2016). Siipola et al. (2016) performed sediment sequential extractions under oxic and anoxic conditions and found that DSi release from the loosely sorbed and redox-sensitive fractions of Si in sediment decreased under anoxic conditions compared to oxic. The authors proposed resorption to aluminum oxides and formation of colloidal mixed Fe-Si oxides as possible explanations. Siipola et al. (2016) also performed a water extraction on sediment for 28 days and found that DSi release from sediments was slower under anoxic compared to oxic conditions. Lehtimäki et al. (2016) found that biogenic Si (BSi) dissolution rates were initially faster under oxic than hypoxic conditions, in agreement with

Siipola et al. (2016), but that the total amount of DSi released over 7 months was higher under hypoxic conditions. Lehtimäki et al. (2016) also found that microbial activity enhanced BSi dissolution under both oxic and anoxic conditions and suggested that the increased BSi dissolution under hypoxic conditions was due to the differences in microbial communities under oxic and hypoxic conditions (Lehtimäki et al. 2016).

If sorption sites on Fe(III) oxides become limited phosphate and DSi may compete for sorption sites and laboratory studies have shown increased dissolved P concentrations in pore water upon large additions of DSi (Tuominen et al. 1998; Koski-Vähälä et al. 2001; Tallberg & Koski-Vahala 2001; Tallberg et al. 2008). Competition between phosphate and DSi for sorption sites may be environmentally relevant as calculations suggest that the deposition and dissolution of a large diatom bloom may result in high enough DSi concentrations to increase P release from sediments (Tallberg 1999; Tallberg & Koski-Vahala 2001). These results were corroborated in a sediment core incubation experiment where addition of diatoms increased P release (Tallberg et al. 2008).

The aims of this research were to investigate the mechanisms of retention and release of P and Si in Cootes' Paradise sediments. Cootes' Paradise has experienced many decades of high external P loading, which has resulted in the accumulation of legacy P in sediments, approximately 24% of which is Fe-bound (Parsons et al. 2017). Cootes' Paradise also experiences substantial internal P loading that contributes 22.7% of the total P inputs to the water column (Kelton & Chow-Fraser 2005). Conversely, little is known about Si dynamics and internal loading in Cootes' Paradise sediments and Si internal loading may influence the bioavailability of Si in the water column, which is an essential nutrient for diatom algae.

The objectives of this research were to determine if and to what extent internal loading of P and Si from Cootes' Paradise sediment is influenced by 1) oxic and anoxic conditions at the sediment-water interface, and 2) the relative concentrations of dissolved P and Si in pore waters, which may promote competition for sorption sites under oxic conditions. This was investigated through sediment core flow through reactor systems incubated under oxic and anoxic conditions and which received different combinations of nutrient (P, Si) additions. We hypothesized that 1) P and Si release from sediments would both increase under anoxic conditions due to reductive dissolution iron(III) oxide minerals and release of adsorbed and coprecipitated P and Si, and 2) under oxic conditions, addition of aqueous Si to sediment pore water would increase the release of P to the overlying water through competitive sorption on Fe(III) oxide minerals.

Competitive sorption of P and Si may reduce to the sorption capacity of Cootes' Paradise sediments towards P and contribute to greater internal P loading. This research will improve our understanding of the interactions of P and Si in sediments as well as the influence of anoxic conditions on sediment Si release.

2.2 Methods

2.2.1 Field site and sampling

Sediment cores were collected from West Pond (43°16'12.0" N 79°55'43.9" W) in Cootes' Paradise marsh (Figure 2.1) in September 2015 using a hand corer lined with a Plexiglas ring, 8 cm in length and 4.7 cm in inner

diameter (Figures 2.2a and 2b). Cootes' Paradise is a 2.5 km^2 severely degraded, hypereutrophic coastal wetland at the western end of Hamilton Harbour, Lake Ontario (Chow-Fraser et al. 1998). Cootes' Paradise has a history of high P loading from a nearby wastewater treatment plant that discharges into West Pond (Chow-Fraser et al. 1998). Cootes' Paradise also receives P inputs from urban runoff, combined sewer overflows, and several tributaries (Spencer Creek, Borer's Creek, Chedoke Creek, Ancanster Creek) (Hamilton Harbour RAP Technical Team 2010). Eutrophication has contributed to the loss of approximately 90% of the emergent vegetation in the marsh since the early 1900s, and Cootes' Paradise experiences extensive green filamentous algae growth in the summer (Figure 2.2c) (Chow-Fraser et al. 1998; Parsons et al. 2017).

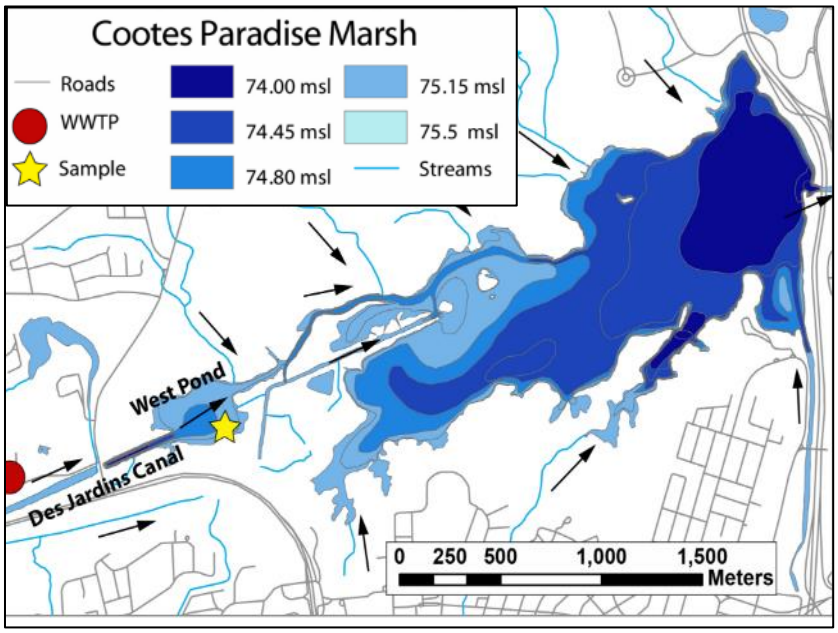

Figure 2.1. Map of Cootes' Paradise marsh showing the location of discharge from the WWTP and the sampling location (yellow star) in West Pond. Water depth is shown by blue colours (adapted from Parsons et al 2017).

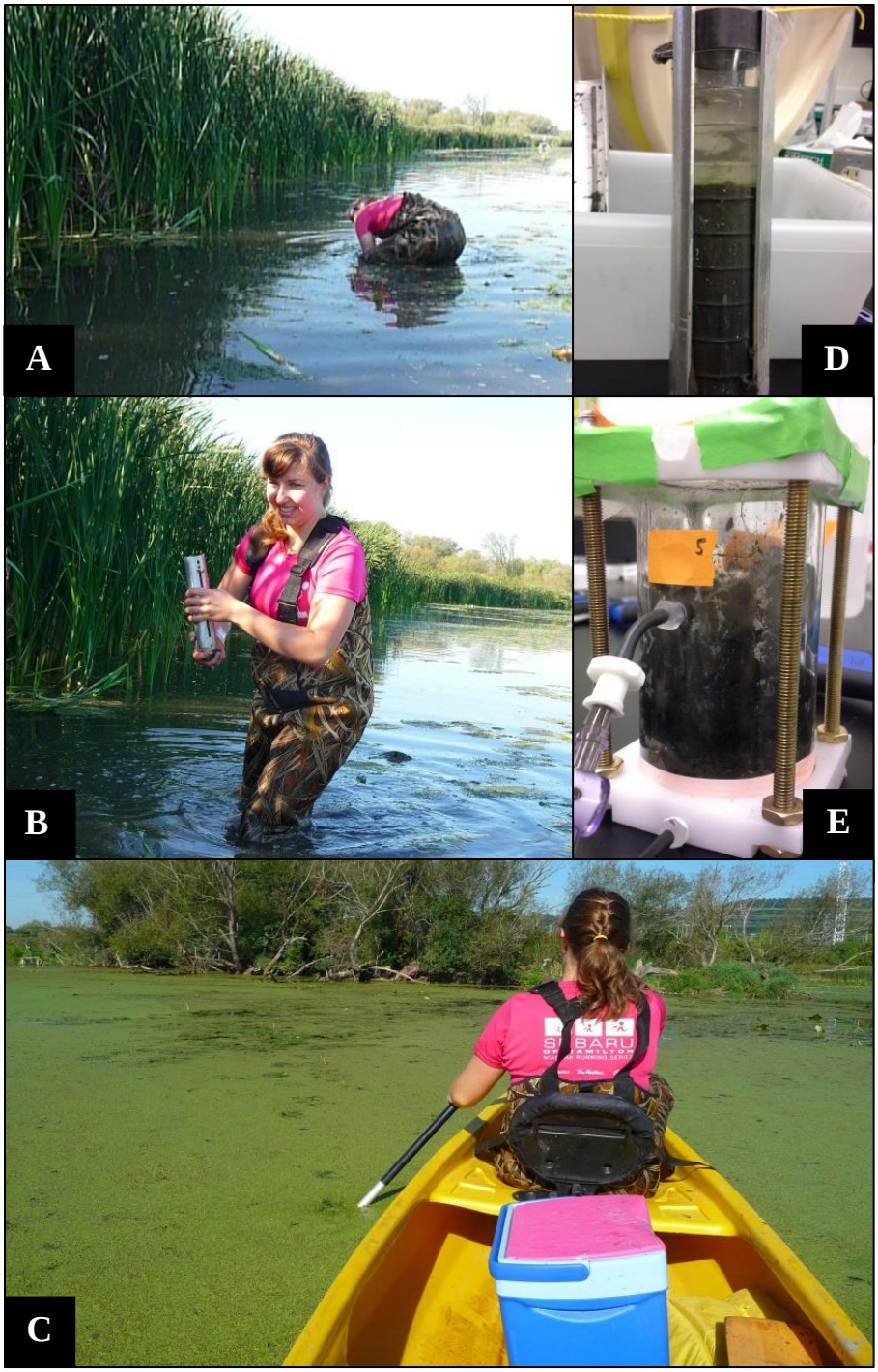

Figure 2.2. Photos of field sampling and sediment core flow through reactors. (A) Sediment cores were collected by crouching in the water and pushing the hand corer into the sediment. (B) A rubber stopper was inserted in the bottom to plug the hand corer and retrieve a sediment core. (C) There was extensive filamentous green algae growth in Cootes' Paradise marsh on the day of sampling. Sediment cores back to the laboratory in a cooler. (D) Sediment cores were collected without disturbing the sediment-water interface. (E) The lining of the hand corer with intact sediment served as the reactor vessel in the sediment core flow through reactors used in the experimental setup.

2.2.2 Experimental setup

The sediment core flow through reactor experiment consisted of 8 flow through reactors similar to the design of Pallud & Van Cappellen (2006) and Pallud et al. (2007). Each reactor contained a 5 cm long core of intact sediment in the Plexiglas ring in which the sediments were collected, which served as the reactor cell (Figures 2.2d, 2e and 2.3). Reactor cells were enclosed on either end by caps lined with o-rings to prevent leakage of gas and water and a 47 mm diameter 0.2 µm pore size nitrocellulose filter on the bottom cap to evenly distribute flow across the bottom of the core and to prevent blockage of the inflow port by sediment (Figure 2.3, o-rings and filters not shown). Threaded rods and nuts kept the top and bottom caps in place and a tight seal on the reactor cell (Figures 2.2e and 2.3). Flow-through reactor cells were kept in the dark by covering with aluminum foil in order to prevent phytoplankton growth.

Influent solution entered the reactor through the side of the bottom cap, which opened in the center (Figures 2.2e and 2.3). Effluent flowed out of the reactor at an exit port located 6 cm from the bottom of the reactor cell, creating a water column of approximately 1 cm above the sediment (Figures 2.2e and 2.3). Influent was delivered and effluent withdrawn at a rate of approximately 1 mL h^{-1} using peristaltic pumps. Two holes 1 cm in diameter were cut into the top cap to allow gas exchange between the atmosphere and the 2 cm of headspace of the reactor cell (Figure 2.3). The holes were covered with Parafilm that was punctured with small holes to prevent excessive loss of solution by evaporation (Figure 2.3). Four sediment core flow through reactors were incubated under oxic conditions on the lab bench, and 4 were incubated under anoxic conditions in an anaerobic chamber (98% N_2 2% H_2 atmosphere, <1 ppmv O_2, Coy laboratory products). Temperature was not controlled, and oxic reactors were incubated at approximately 22 ± 3°C and anoxic reactors at approximately 30 ± 2°C. This difference in temperature between the lab bench and the anaerobic chamber was not foreseen and the influence of temperature on the results is discussed.

The influent solution to each reactor consisted of a deoxygenated artificial pore water (APW) solution amended with different nutrient additions: a "control", a "P addition", a "Si addition" and a "P+Si addition" solution. The APW solution composition was based on pore water concentrations at 5 cm depth previously measured at the sampling site using peeper's (Table 2.1) (Hesslein 1976; Chris Parsons', unpublished data). The "control" APW solution contained no P or Si, the "P addition" APW solution contained 29 µmol L^{-1} P as KH_2PO_4, the "Si addition" APW solution contained 107 µmol L^{-1} Si as Na_2SiO_3, and the "P + Si addition" APW solution contained both 29 µmol L^{-1} P as KH_2PO_4 and 107 µmol L^{-1} Si as Na_2SiO_3 (Table 1). One of each of the 4 sediment core flow through reactors incubated under oxic and anoxic conditions received the "control", "P addition", "Si addition", and the "P + Si addition" solutions. The solutions were deoxygenated by vigorously sparging with N_2 gas for 2-3 hours and storing solutions in the anaerobic chamber overnight. The solutions were delivered to the sediment core flow through reactors through Viton tubing to prevent entry of oxygen. Except for the reactor cell, all parts coming into contact with the inflowing solutions were acid washed and/or sterilized by autoclaving as appropriate.

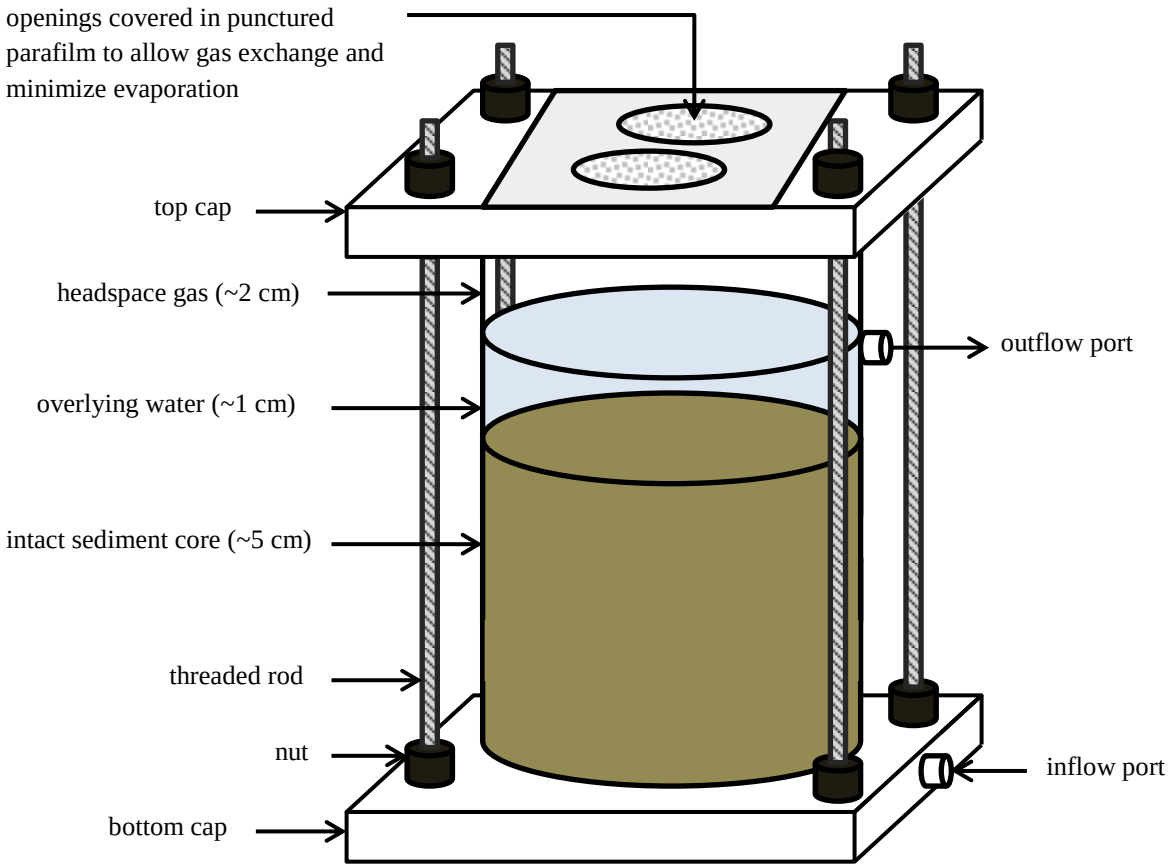

Figure 2.3. Sediment core flow through reactor setup.

2.2.3 Sediment core flow through experiment

Prior to the start of the incubation experiment, all 8 sediment core flow through reactors were flushed with the control APW solution at a rate of 1 mL h^{-1} on the lab bench under oxic conditions to ensure the saturation of pore space with solution. An APW solution amended with 130 µmol L^{-1} Br^-, a conservative tracer, was flushed through for approximately 8 days to investigate the transport properties of the sediment.

During the sediment core flow through experiment, the deoxygenated APW solutions were pumped through the flow-through reactors for approximately 16 days. Effluent from each reactor was continuously collected for varying time intervals, more frequently at the beginning of the experiment (3 times per day) and less frequently near the end (1-2 times per day). The sampling resolution was higher at the beginning of the experiment in order to

Table 2.1. Pore water concentrations measured by peepers at the sampling site in West Pond and the artificial pore water elemental concentrations for the nutrient treatment solutions. No Fe or Mn was added to the inflow solutions although they were present in the pore water.

Constituent	Concentration (µmol L^{-1})				
	Pore water (5 cm depth)	Artificial pore water solution			
		Control	P addition	Si addition	P+Si addition
Al^{3+}	0	0	0	0	0
Ca^{2+}	511	736	736	736	736
Mg^{2+}	270	378	378	378	378
Na^{+}	1261	1713	1713	1927	1927
K^{+}	88	69	102	69	102
Cl^{-}	4041	2535	2535	2535	2535
DIC-C (as HCO_3)	2230	1713	1713	1713	1713
DOC-C (as glucose)	358	489	489	489	489
SO_4	102	104	104	104	104
NH_4	771	1202	1202	1202	1202
Fe^{2+}	44	0	0	0	0
Mn^{4+}	7	0	0	0	0
P	44	0	29	0	29
Si	107	0	0	107	107

capture the initial changes in P and Si release expected to occur. The effluent was filtered through 0.45 µm polypropylene syringe filters for analysis of total dissolved P (TDP), Si (DSi), Mn (TDMn), Fe (TDFe), S (TDS), and soluble reactive P (SRP), and filtered through 0.2 µm supor (PES) Ion Chromatography certified syringe filters for analysis of Br^-, NO_2^-, NO_3^-, and SO_4^{2-}. Samples for analysis of TDP, DSi, TDMn, TDFe and TDS were acidified to 2% nitric acid and measured by Inductively Coupled Plasma-Optical Emission Spectrophotometry (ICP-OES, Thermo Scientific iCAP 6300). SRP was measured on unacidified filtered samples by a molybdenum blue method (Murphy & Riley 1962) on a UV-Visible Spectrophotometer (UV-Vis) (Thermo Evolution 260). Anions were measured by Ion Chromatography (IC) (Dionex ICS-5000). Limits of detection, limits of quantification, and precision of analytical methods are listed in Table 2.2.

Upon completion of the experiment, sediments in flow-through reactors were frozen at -80°C and sliced into 3 sections (0-1 cm, 1-3 cm, and 3-5 cm) using a bandsaw. Ascorbate extractions were performed in the anaerobic chamber on the top section (0-1 cm) of thawed and homogenized wet sediment according to Hyacinthe & Van Cappellen (2004). Ascorbate has been shown to extract highly reactive solid phase Fe, such as ferrihydrite (Kostka & Luther III 1994). Approximately 0.5 g of wet sediment was mixed with 12.5 mL of the ascorbate solution and shaken for 24 hours at 22 ± 3°C. The extraction vessels were centrifuged at high speed (5000 rpm or approximately 2500 x g) for 15 minutes and the supernatant removed, filtered to 0.45 µm pore size using polypropylene syringe filters, diluted to 2% nitric acid and analysed for DSi, TDP, TDMn and TDFe by ICP-OES.

Table 2.2. Limits of detection (LOD), limits of quantification (LOQ), and precision of analytical methods.

Analytical Method	Element	LOD (µmol L^{-1})	LOQ (µmol L^{-1})	Precision (%)
ICP-OES	Fe	0.007	0.02	20
	P	0.08	0.25	7
	Mn	0.04	0.01	-
	S	0.06	0.28	-
	Si	0.04	0.13	4
IC	Br	1.2	6.0	-
	NO_2^-	2.1	10.5	-
	NO_3^-	1.5	7.5	10
	SO_4^{-2}	0.8	4.1	10
SRP	P	0.5	1.4	10

2.2.4 TDP, SRP, and DSi steady-state fluxes and total release

Steady-state (SS) fluxes (µmol m^{-2} h^{-1}) of TDP, SRP, and DSi were calculated according to Equation 2.1:

$$SS\ Flux\ = \frac{C_{ss} * Q}{SA} \quad \text{Eq. 2.1}$$

where C_{ss} is the steady state concentration (µmol L^{-1}), Q is the flow rate (L h^{-1}), and SA is the surface area of the sediment core (m^{-2}). For oxic reactors, concentrations of TDP, SRP, and DSi were fairly consistent throughout the experiment and so C_{ss} was calculated as the mean concentration over the 16 days. For anoxic reactors, segmented linear regression of concentration and time was conducted using the SegReg free software program (www.waterlog.info/segreg.htm) and the breakpoint (time) between increasing and plateauing concentrations was identified. For TDP, SRP, and DSi in all reactors, except the "P+Si addition" reactor for SRP, the slope of the line after the breakpoint was 0, indicating a constant flux of TDP, SRP, and DSi had been reached. The mean concentration of TDP, SRP, and DSi after the breakpoint was used as the C_{ss}. There was no breakpoint for SRP concentrations in the "P+Si addition" reactor and so the C_{ss} was calculated from the mean concentration of the last 6 samples, which by visual inspection appeared to be the plateau.

Total release of TDP and DSi over the entire experiment in unites of µmoles was calculated according to Equation 2.2:

$$Total\ \mu moles\ released = \sum_{i=1}^{29} C * Q * t_i \quad \text{Eq. 2.2}$$

where *i* is the sample number (i.e. 1 through 29), C is the concentration of TDP or DSi measured in the *i*th sample (µmoles L^{-1}), Q is the flow rate (L h^{-1}), and t is the time interval over which the *i*th sample was collected (h).

2.3 Results

2.3.1 Transport properties

Figure 2.4 shows the Br^- breakthrough curves for oxic and anoxic reactors where C is the concentration of Br^- in the effluent, C_0 is the initial concentration of Br^- in the influent, and C/C_0 is relative Br^- concentration. Pore volumes were calculated according to Equation 2.3:

$$p = \frac{Q*t}{ø*L*A} \quad \text{Eq. 2.3}$$

where p is the number of pore volumes of fluid passed through a medium in time, Q is the flow rate ($cm^3\ h^{-1}$), t is time (h), ø is porosity, L is the length of the sediment core (cm), and A is the cross-sectional area of the sediment core (cm^2). Porosity was calculated according to Equation 2.4:

$$ø = 1 - \frac{\rho_{bulk}}{\rho_{particle}} \quad \text{Eq. 2.4}$$

where ρ_{bulk} is the bulk density of the sediment calculated as the dry sediment weight (wet sediment weight divided by the moisture content plus 1) divided by the saturated sediment volume, and $p_{particle}$ is the particle density assumed to be 2.65 g cm^{-3}.

The Br^- breakthrough curves were similar for all reactors, where breakthrough occurred almost immediately (Figure 2.4). C/C_0 reached 0.9 by 1 pore volume, and 1 by approximately 1.4 pore volumes. The similarity of Br^- breakthrough curves indicates that reactors were comparable in terms of physical transport prior to the start of the sediment core flow through experiment.

2.3.2 Oxic reactors effluent concentrations

In oxic reactors, concentrations of NO_2^- were generally below the detection limit (2.1 µmol L^{-1}), but reached up to approximately 40 µmol L^{-1} in a few samples (Figure 2.5). No large differences in NO_2^- concentrations were observed between nutrient treatments (Figure 2.5). Concentrations of NO_3^- generally increased over time (Figure 2.5). The "Si addition" reactor had the highest mean NO_3^- concentration (109.40 µmol L^{-1}) and the "control" reactor the lowest (44.87 µmol L^{-1}). NO_2^- and NO_3^- concentrations were well below the inflow concentration of NH_4^+ (1202 µmol L^{-1}), however NH_4^+ was not measured in the effluent (Figure 2.5).

TDMn and TDFe concentrations were low in all oxic reactors, often near or below detection limits (0.04 µmol Mn L^{-1}; 0.007 µmol Fe L^{-1}) (Figure 2.6). TDMn concentrations were generally in the range of 0.1-5 µmol L^{-1}, but increased to 10-18 µmol L^{-1} in the "control", "P addition" and "Si addition" reactors between 10 and 12 days (Figure 2.6). TDFe concentrations were generally in the range of 0.1-1 µmol L^{-1} with some spikes in concentration up to about 8 µmol L^{-1} (Figure 2.6).

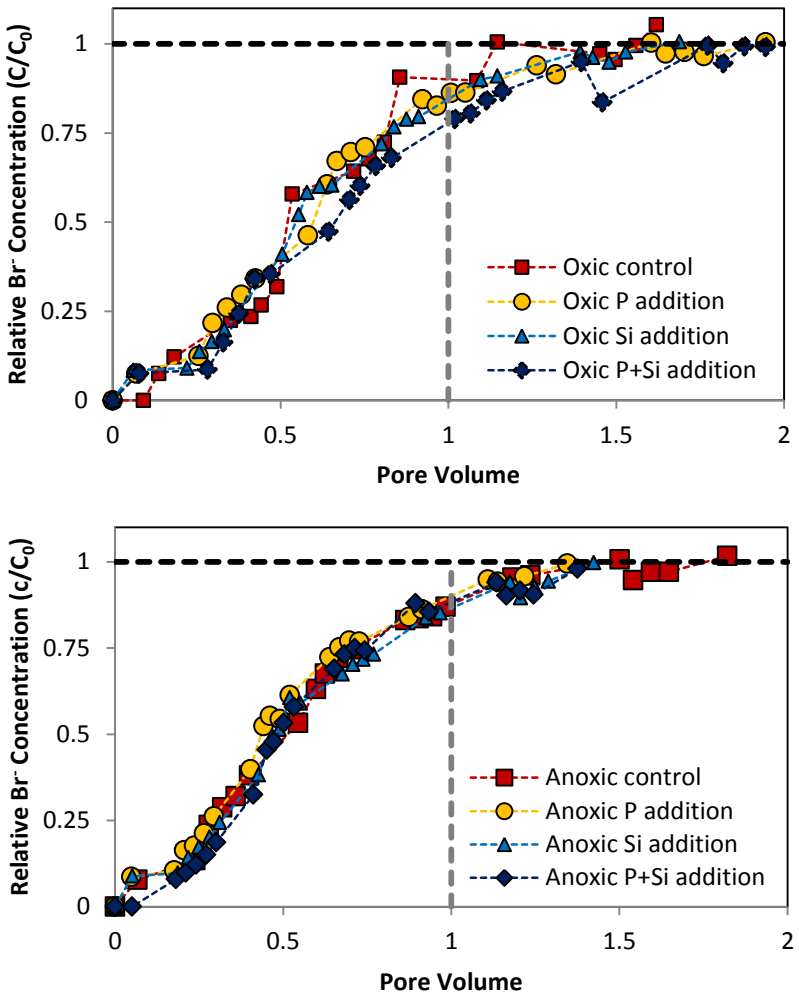

Figure 2.4. Br- breakthrough curves for oxic and anoxic flow-through reactors measured prior to the incubation experiment under oxic conditions where C is the concentration of Br- in the effluent, C0 is the initial concentration of Br- in the influent, and C/C0 is relative Br- concentration. Relative Br- concentrations of 1 were reached by approximately 1.4 pore volumes for all reactors.

TDS and SO_4^{2-} concentrations were similar in oxic reactors and exceeded that of the influent SO_4^{2-} concentration (Figure 2.7). SO_4^{2-} concentrations were highest in the "Si addition" reactor, followed by the "control", the "P+Si addition", and the "P addition" reactors, which had mean concentrations of 800.79 µmol L^{-1}, 717.64 µmol L^{-1}, 401.93 µmol L^{-1}, and 205.58 µmol L^{-1} respectively (Figure 2.7).

TDP concentrations remained low in the oxic "control", "P addition" and "P+Si addition" reactors, generally ranging between 2-10 µmol L^{-1} (Figure 2.8). TDP concentrations in the "Si addition" reactor were low and in a similar range as the other nutrient treatments in the first 8 days of the experiment, then increased up to 30 µmol L^{-1} in the last 8 days of the experiment (Figure 2.8). The effluent concentrations in the "P addition" and "P+Si addition" reactors were lower than that of the influent, while that of the "control" and "Si addition" reactors were higher (Figure 2.8). SRP concentrations generally followed the same trend as TDP, with SRP accounting for 17-50%

of TDP in the "control", 59-98% of TDP for the "P addition", 35-90% of TDP for the "Si addition" and 23-73% for the "P+Si addition" reactors (Figure 2.8).

DSi concentrations in the oxic reactors were fairly constant and varied approximately 10-15% from the mean over the duration of the experiment (Figure 2.9). The "P addition" reactor had the highest mean DSi concentration followed by the "Si addition", the "P+Si addition", and the "control" reactors, which had mean concentrations of 279.64 µmol L^{-1}, 250.93 µmol L^{-1}, 245.71 µmol L^{-1}, and 229.99 µmol L^{-1} respectively (Figure 2.9). In all reactors, DSi concentrations in the effluent were higher than the influent by at least 2 times (Figure 2.9).

2.3.3 Anoxic reactors effluent concentrations

NO_2^- concentrations were generally below the detection limit in anoxic reactors, but had large spikes in concentration of up to 400 µmol L^{-1} in a few samples (Figure 2.5). NO_3^- concentrations were initially around 8-30 µmol L^{-1} and decreased to values in the range of 1-10 µmol L^{-1} within the first day (Figure 2.5). As no NO_3^- was in the inflow solution, the initially present NO_3^- was likely produced before the experiment when sediment flow through reactors were outside the anaerobic chamber. NO_3^- concentrations remained low for the rest of the experiment, with all treatments having mean concentrations in the range of 6-7 µmol L^{-1} (Figure 2.5). NO_2^- and NO_3^- concentrations were below the inflow concentration of NH_4^+ (Figure 2.5).

TDMn concentrations in the effluent peaked at about 1 day then decreased to around 5-10 µmol L^{-1} and remained low (Figure 2.6). The "P+Si addition" reactor had the highest peak concentration of 100.49 µmol L^{-1}, followed by the "control" (48.87 µmol L^{-1}), the "Si addition" (44.62 µmol L^{-1}), and the "P addition" reactors (34.03 µmol L^{-1}) (Figure 2.6).

TDFe concentrations followed a similar trend as TDMn but peaked around 2-3 days when TDMn concentrations started declining (Figure 2.6). The "P+Si addition" reactor reached the highest peak TDFe concentration of 139.9 µmol L^{-1}, followed by the "P addition" (99.32 µmol L^{-1}), the "control" (69.89 µmol L^{-1}), and the "Si addition" (64.06 µmol L^{-1}) reactors (Figure 2.6). While TDFe concentrations decreased after the peak, concentrations remained fairly high in the range of 20-60 µmol L^{-1} for all nutrient treatments (Figure 2.5).

TDS and SO_4^{2-} concentrations in anoxic reactors were initially similar (Figure 2.7). Both TDS and SO_4^{2-} concentrations decreased to below that of the influent within the first day of the experiment, but SO_4^{2-} concentrations fell below that of TDS (Figure 2.7). SO_4^{2-} concentrations decreased to below 20 µmol L^{-1} with many samples below the detection limit (0.8 µmol L^{-1}), but TDS concentrations decreased to only 20-30 µmol L^{-1} (Figure 2.7). Apart from the initial concentrations, there were no large differences in TDS and SO_4^{2-} concentrations between nutrient treatments (Figure 2.7).

TDP and SRP concentrations increased at the same time as TDFe and continued increasing until around 10-11 days when concentrations plateaued (Figures 2.6 and 2.8). The "P+Si addition" reactor reached the highest plateau TDP concentration of 166 µmol L^{-1}, followed by the "Si addition" (139 µmol L^{-1}), the "control" (126 µmol L^{-1}), and the "P addition" (117 µmol L^{-1}) reactors (Figure 2.8). SRP reached concentrations of 147 µmol L^{-1} for the "P+Si addition" reactor, 114 µmol L^{-1} for the "Si addition" reactor, 109 µmol L^{-1} for the "control" reactor, and 102 µmol L^{-1} for the "P addition" reactor (Figure 2.8). On average SRP concentrations accounted for 80-85% of TDP for

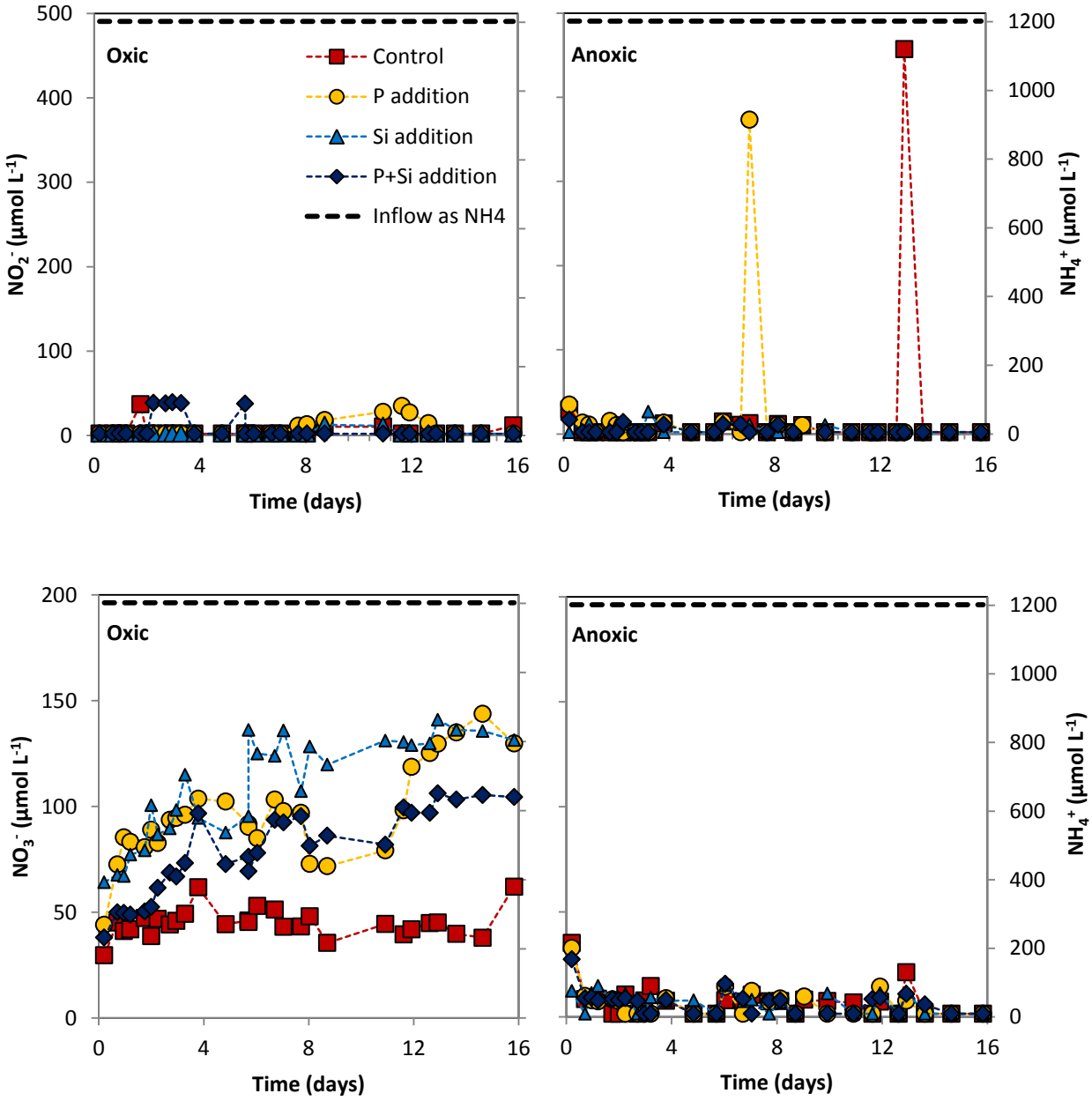

Figure 2.5. Concentrations of NO_2^- and NO_3^- in the effluent of oxic and anoxic sediment core flow through reactors over the course of the experiment. The influent concentration of NH_4^+ is shown by the dashed line (1202 µmol L^{-1}). NH_4^+ was not measured in the outflow.

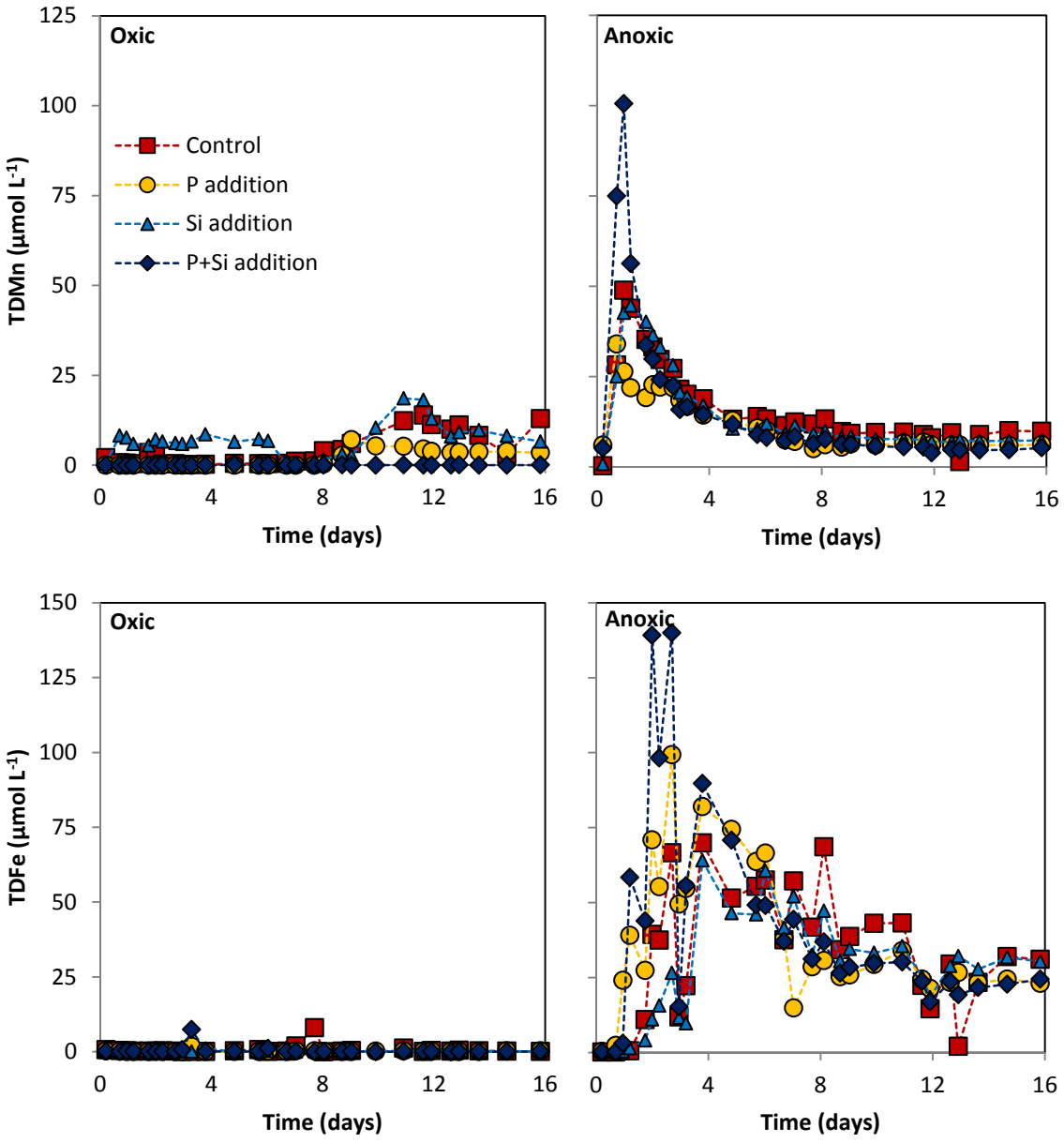

Figure 2.6. Concentrations of total dissolved Mn (TDMN) and total dissolved Fe (TDFe) in the effluent of oxic and anoxic sediment core flow through reactors over the course of the experiment. The influent solutions contained no Mn or Fe.

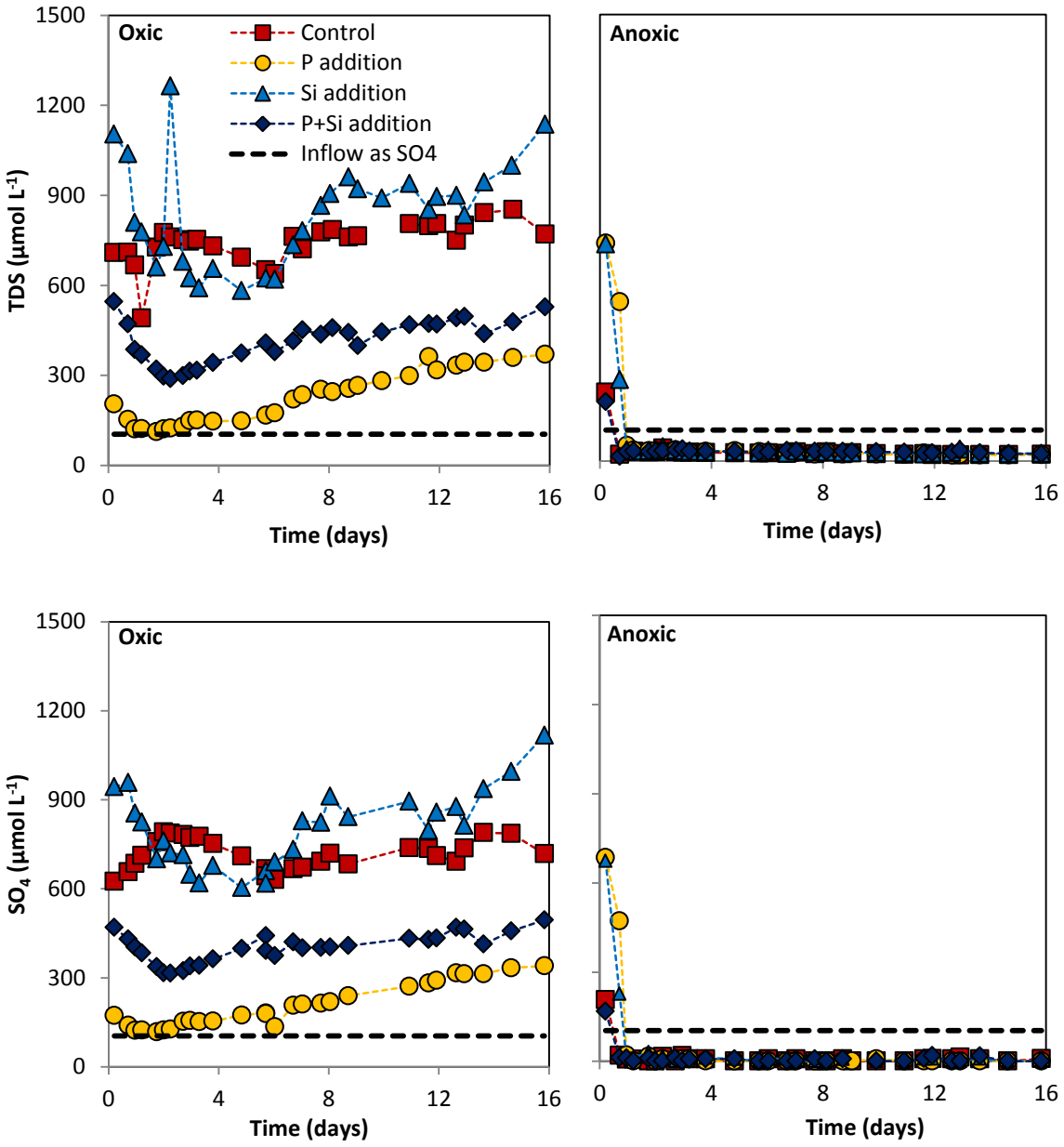

Figure 2.7. Concentrations of total dissolved S (TDS) and SO_4^{2-} in the effluent of oxic and anoxic sediment core flow through reactors over the course of the experiment. The influent concentration of SO_4^{2-} (104 µmol L^{-1}) is shown with the dashed black line.

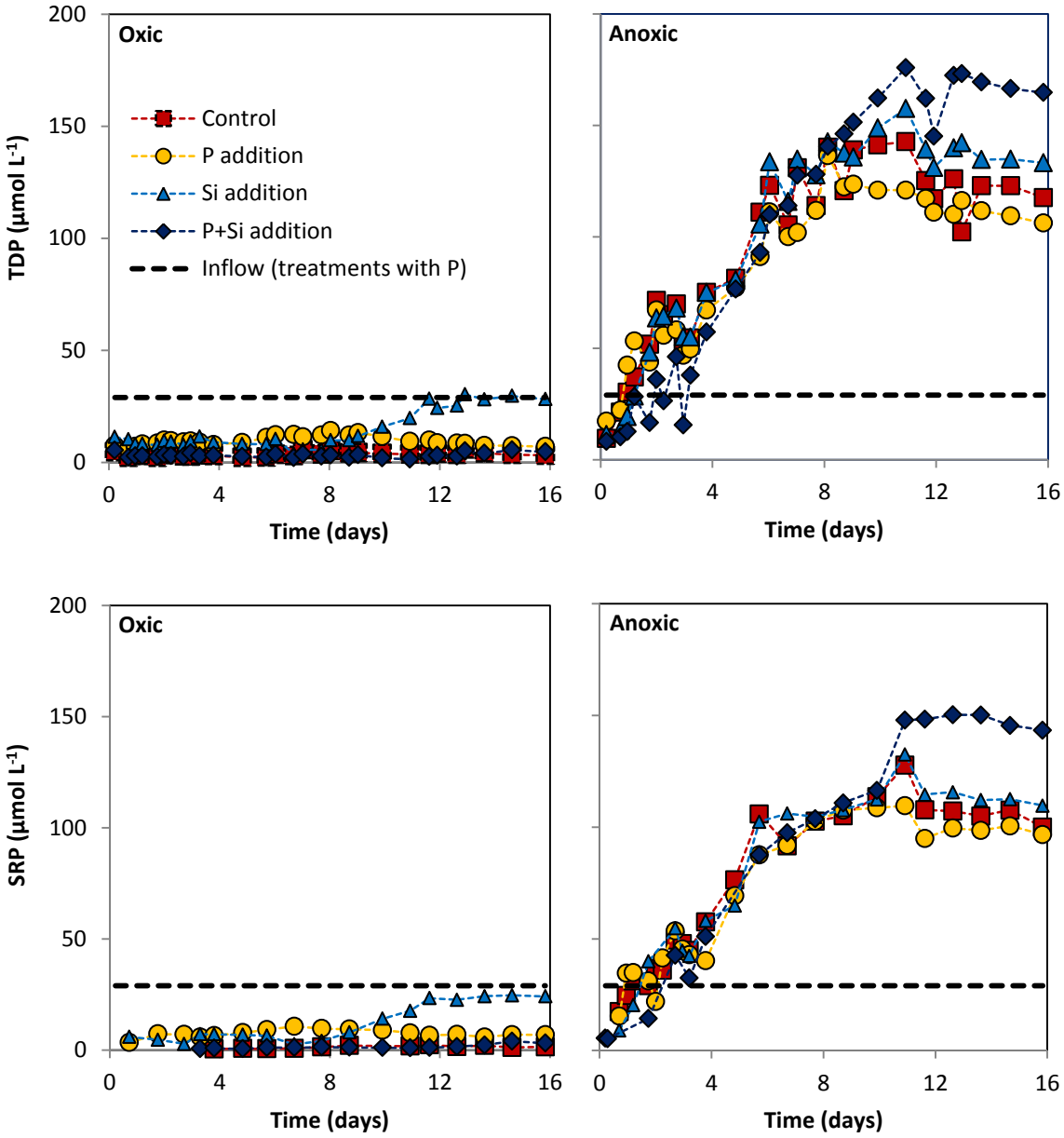

Figure 2.8. Concentrations of total dissolved P (TDP) and soluble reactive P (SRP) in the effluent of oxic and anoxic sediment core flow through reactors over the course of the experiment. The influent concentration of dissolved P for the "P addition" and "P+Si addition" reactors is shown with the dashed line. The "control" and "Si addition" reactors did not have P in the influent solution.

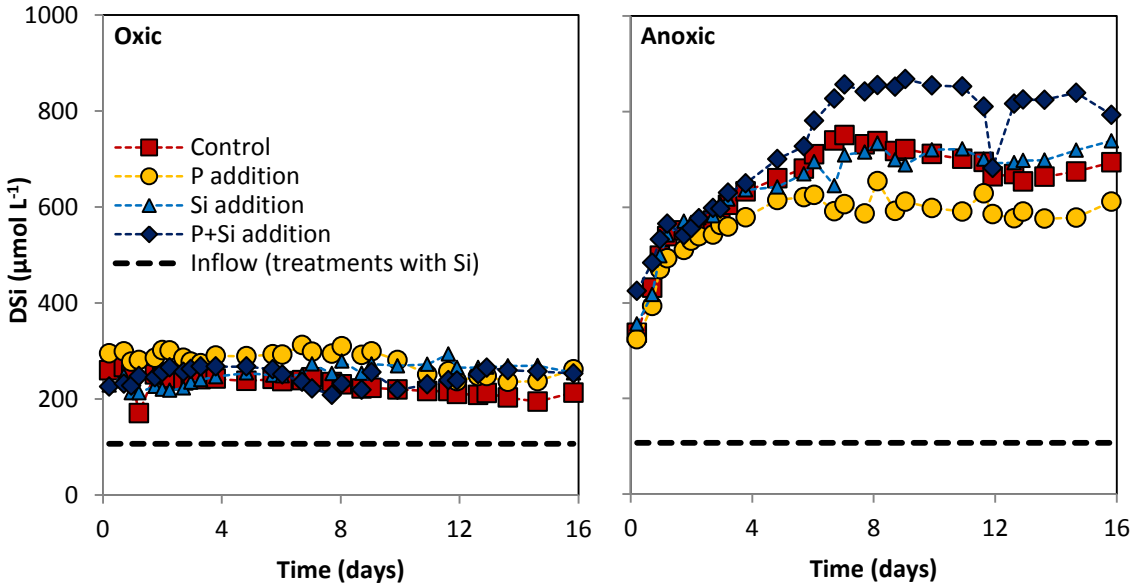

Figure 2.9. Concentrations of total dissolved Si (DSi) in the effluent of oxic and anoxic sediment core flow through reactors over the course of the experiment. The influent concentration of DSi for the "Si addition" and "P+Si addition" reactors is shown with the dashed line. The "control" and "P addition" reactors did not have DSi in the influent solution.

all nutrient treatments. For all reactors, the TDP and SRP concentrations of the effluent were initially less than that of the influent, but surpassed that of the influent within 1-3 days (Figure 2.8).

DSi concentrations increased in the first day of the experiment at the same time that TDMn concentrations increased and continued increasing at the same time as TDFe (Figures 2.6 and 2.9). DSi concentrations plateaued around 8 days (Figure 2.9). All nutrient treatments followed a similar trend but reached different plateau concentrations of approximately 699 µmol L^{-1} for the "control" and "Si addition" reactors, approximately 601 µmol L^{-1} for the "P addition" reactor, and approximately 826 µmol L^{-1} for the "P+Si addition" reactor (Figure 2.9). DSi concentrations in the "P+Si addition" reactor suddenly decreased from 810 µmol L^{-1} to 682 µmol L^{-1} and back up to 816 µmol L^{-1} at 11-12 days, and it is unknown what caused this sudden and short-lived decrease in concentration (Figure 2.9). In all reactors, DSi concentrations in the effluent were higher than the influent by at least 3 times (Figure 2.9).

2.3.4 Oxic and anoxic reactor effluent Si:P, Fe:P and Fe:Si ratios

Aqueous Si:P ratios of the effluent from oxic reactors were high and fluctuated over a large range throughout the experiment, while the Si:P ratios of the effluent from anoxic reactors were low and consistent (Figure 2.10). Oxic Si:P ratios ranged between 8.8 and 168.2 between the different nutrient treatments with mean Si:P ratios of 85.9 for the "P+Si addition" reactor, 69.0 for the "control" reactor, 30.3 for the "P addition" reactor and 23.9 for the "Si addition" (Figure 2.10). In anoxic reactors, Si:P ratios were initially between 18 and 50, and decreased in all treatments to around 5-6 by 8 days into the experiment (Figure 2.10). The anoxic "P+Si addition" reactor had a

mean Si:TDP ratio of 14.3, the anoxic "control" reactor a mean of 8.9, the anoxic "Si addition" reactor a mean of 9.4, and the anoxic "P addition" reactor a mean of 7.8 (Figure 2.10).

In the anoxic "control", "P addition", and "Si addition" reactors, aqueous Fe:P effluent ratios increased from 0 at the beginning of the experiment to around 1-1.7 at approximately 4 days, then decreased and remained around 0.1-0.2 from day 8 to day 16 of the experiment (Figure 2.10). The anoxic "P+Si addition" reactor Fe:P ratios increased from 0 to almost 4 at 2 days into the experiment, then decreased to around 0.1-0.2 in a similar pattern to the other reactors.

Anoxic reactor aqueous Fe:Si effluent ratios increased from 0 to 0.1-0.2 in the first 2-4 days of the experiment, then decreased to around 0.03 in the last 8 days of the experiment (Figure 2.10). The "P+Si addition" reactor reached the highest Fe:Si ratio of 0.25 at 2 days (Figure 2.10).

2.3.5 TDP, SRP and DSi steady-state fluxes and total release

Oxic and anoxic steady-state fluxes of TDP, SRP and DSi are shown in Table 2.3. Oxic steady-state TDP fluxes ranged from 1.9 to 6.9 μmol m^{-2} h^{-1} and increased in the order of "P+Si addition" < "control" < "P addition" < "Si addition" (Table 2.3). The mean of all oxic TDP fluxes was 4.1 μmol m^{-2} h^{-1}. Anoxic steady-state TDP fluxes were markedly higher than oxic fluxes (Table 2.3). Anoxic TDP fluxes increased in the order of "P addition" < "Si addition" < "control" < "P+Si addition" and ranged from 66 to 80 μmol m^{-2} h^{-1} (Table 2.3).

Oxic steady-state SRP fluxes were slightly lower than TDP fluxes but showed similar trends (Table 2.3). Oxic steady-state SRP fluxes were in the range of 0.8-6 μmol m^{-2} h^{-1} and increased in the order of "control" < "P+Si addition" < "P addition" < "Si addition" (Table 2.3). The mean SRP flux from all oxic reactors was 3.0 μmol m^{-2} h^{-1} (Table 2.3). Anoxic steady-state SRP fluxes ranged from 57 to 72 μmol m^{-2} h^{-1} and increased in the order of "Si addition" < "P addition" < "control" < "P+Si addition" with a mean flux of 63 μmol m^{-2} h^{-1} (Table 2.3).

Oxic steady-state DSi fluxes increased in the order of "Si addition" < "control" < "P+Si addition" < "P addition" reactors with fluxes ranging from 124 to 164 μmol m^{-2} h^{-1} (Table 2.3). The mean flux of all oxic reactors was 141 μmol m^{-2} h^{-1}. Anoxic steady-state DSi fluxes increased in the order of "P addition" < "Si addition" < "P+Si addition" < "control" with fluxes ranging from 341 to 435 μmol m^{-2} h^{-1} and the mean of all anoxic fluxes was 381 μmol m^{-2} h^{-1} (Table 2.3). Anoxic steady-state DSi fluxes were higher than oxic fluxes by 2-3 times (Table 2.3).

Total release of DSi and TDP over the experiment is shown in Table 2.3. Total release of SRP was not calculated as SRP was not measured on every sample. Total release of DSi from oxic reactors ranged from 85-106 μmoles with a mean of 248 μmoles, and in anoxic reactors ranged from 216-280 μmoles with a mean of 248 μmoles (Table 2.3). Oxic and anoxic reactor total TDP release ranged from 1.2-5.1 μmoles and 35-43 μmoles respectively, with means of 2.8 μmoles for oxic reactors and 40 μmoles for anoxic reactors (Table 2.3).

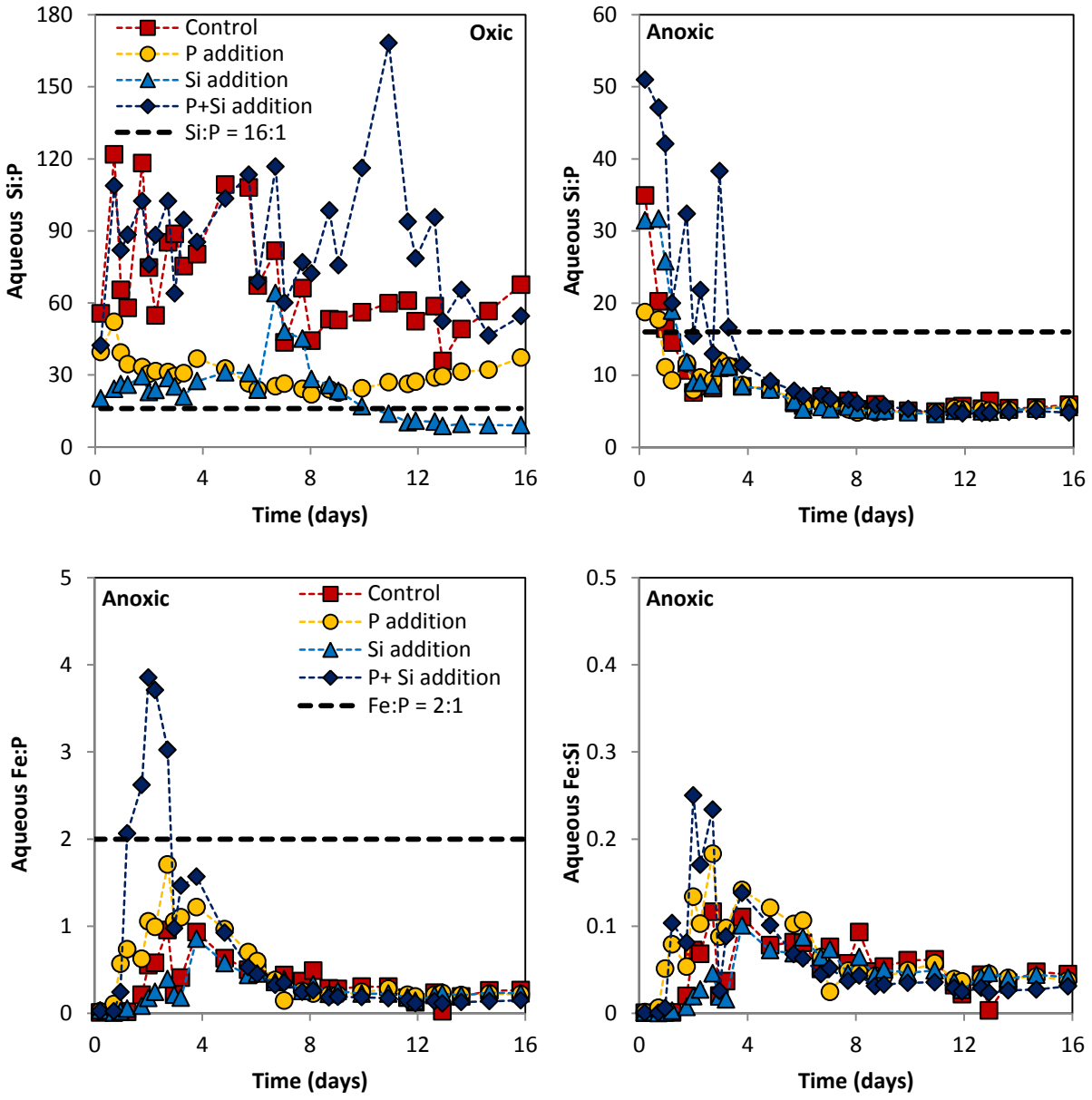

Figure 2.10. Aqueous Si:P ratios from the effluent of oxic and anoxic reactors, and aqueous Fe:P and Fe:Si ratios from the effluent of anoxic reactors over the course of the experiment. Note the different scales on the y-axis. Si:P ratios are shown in relation to the Redfield-Brzezinski ratio of Si:P = 16:1 delineating P limitation (Si:P > 16:1) and Si limitation (Si:P < 16:1) of diatom growth (Redfield 1958; Brzezinski 1985). Fe:P ratios are shown in relation to the theoretical maximum stoichiometric molar ratio of P incorporation into ferric oxides of Fe:P = 2:1 (Thibault et al. 2009).

Table 2.3. Oxic and anoxic steady-state fluxes of dissolved Si (DSi), total dissolved P (TDP), and soluble reactive P (SRP) and total release of DSi and TDP over the experiment for each nutrient treatment and the mean of all oxic and all anoxic reactors. Due to the increased temperature at which anoxic reactors were incubated, estimated anoxic steady-state fluxes and total release at 22°C were calculated using a Q_{10} of 2.06 for TDP and SRP and 2.27 for DSi (Kelton & Chow-Fraser 2005; Kamatani 1982).

Element	Nutrient Treatment	Steady-state flux (µmol m^{-2} h^{-1})			Total release over 16 days (µmoles)		
		Oxic (22°C)	Anoxic (30°C)	Anoxic (22°C)*	Oxic (22°C)	Anoxic (30°C)	Anoxic (22°C)*
DSi	Control	130	435	226	85	246	128
	P addition	164	341	177	106	216	112
	Si addition	124	347	180	84	248	129
	P+Si addition	146	400	208	96	280	145
	Mean	**141**	**381**	**198**	**93**	**248**	**128**
TDP	Control	2.0	78	44	1.3	39	22
	P addition	5.6	66	37	3.7	35	20
	Si addition	6.9	69	39	5.1	41	23
	P+Si addition	1.9	80	45	1.2	43	24
	Mean	**4.1**	**73**	**41**	**2.8**	**40**	**22**
SRP	Control	0.8	68	38			
	P addition	4.4	58	33			
	Si addition	6.0	57	32			
	P+Si addition	0.9	72	40			
	Mean	**3.0**	**64**	**36**			

2.3.6 Ascorbate leachable Fe, Mn, P and Si concentrations in surface sediments

Ascorbate leachable Fe, Mn, P, and Si concentrations from the top 1 cm of sediment are shown in Table 2.4. Ascorbate leachable Fe concentrations were higher than ascorbate leachable Mn by approximately 17 times, indicating that reactive Fe phases are likely more important in Cootes' Paradise sediment than reactive Mn phases (Table 2.4). Reactive Fe concentrations ranged from 62.53 to 83.49 µmoles g^{-1} dry sed. in oxic reactors and 63.09 to 70.65 g^{-1} dry sed. in anoxic reactors (Table 2.4). Oxic and anoxic reactors had mean reactive Fe concentrations of 70.04 and 66.70 µmoles g^{-1} dry sed. respectively (Table 2.4). Reactive Mn concentrations ranged between 3.05 and 4.85 µmoles g^{-1} dry sed. in the oxic reactors and 4.37 and 5.72 µmoles g^{-1} dry sed. in the anoxic reactors, with mean concentrations of 3.99 µmoles g^{-1} dry sed. and 4.87 µmoles g^{-1} dry sed. for oxic and anoxic reactors respectively (Table 2.4).

Ascorbate leachable P concentrations from oxic reactors ranged from 12.22 to 23.40 µmoles g^{-1} dry sed. with the "control" reactor and the "P addition" reactors having the lowest and highest concentrations respectively (Table 2.4). The Fe:P ratios were similar for all reactors except were lower in the "P addition" reactor. Oxic reactors had a mean ascorbate leachable P concentration of 16.13 µmoles g^{-1} dry sed. (Table 2.4).

Table 2.4. Fe, Mn, P, and Si concentrations (µmoles g^{-1} dry sed.) and Si:P, Fe:P, and Fe:Si ratios of the ascorbate leachable fraction of the top 1 cm of sediment from nutrient treatments and the mean of all oxic and all anoxic reactors.

Element	Nutrient Addition	Reactive Fe-bound fraction (µmoles g^{-1} dry sed.)	
		Oxic	**Anoxic**
Fe	Control	62.53	70.65
	P addition	83.49	64.82
	Si addition	65.02	63.09
	P+Si addition	69.10	68.22
	Mean	**70.04**	**66.70**
Mn	Control	4.10	4.99
	P addition	3.94	4.37
	Si addition	3.05	4.39
	P+Si addition	4.85	5.72
	Mean	**3.99**	**4.87**
P	Control	12.22	24.03
	P addition	23.40	21.79
	Si addition	13.70	19.96
	P+Si addition	15.21	23.76
	Mean	**16.13**	**22.39**
Si	Control	12.53	17.79
	P addition	13.05	20.48
	Si addition	13.00	19.38
	P+Si addition	13.90	21.07
	Mean	**13.12**	**19.68**
Si:P	Control	1.03	0.74
	P addition	0.56	0.94
	Si addition	0.95	0.97
	P+Si addition	0.91	0.89
	Mean	**0.86**	**0.88**
Fe:P	Control	5.12	2.94
	P addition	3.57	2.97
	Si addition	4.75	3.16
	P+Si addition	4.54	2.87
	Mean	**4.50**	**2.99**
Fe:Si	Control	4.99	3.97
	P addition	6.40	3.17
	Si addition	5.00	3.26
	P+Si addition	4.97	3.24
	Mean	**5.34**	**3.41**

Anoxic reactors had ascorbate leachable P concentrations that ranged from19.96 to 24.03 µmoles g^{-1} dry sed., with a mean of 22.39 µmoles g^{-1} dry sed. and the "Si addition" and "control" having the lowest and highest concentrations (Table 2.4). Fe:P ratios were lower than in oxic reactors and were similar for all treatments (Table 2.4).

Oxic reactor ascorbate leachable Si concentrations ranged from 12.53 to 13.90 μmoles g^{-1} dry sed. with the "control" and "P+Si addition" reactors having the lowest and highest concentrations respectively (Table 2.4). However, all reactors except the "P addition" reactor had the similar Fe:Si ratios. The mean ascorbate leachable Si concentration for oxic reactors was 13.12 μmoles g^{-1} dry sed. (Table 2.4).

Anoxic reactor ascorbate leachable Si concentrations were higher and ranged from 17.79-21.07 μmoles g^{-1} dry sed., with a mean of 19.68 μmoles g^{-1} dry sed., and the "control" and "P+Si addition" having the lowest and highest concentrations (Table 4). Fe:Si ratios were lower than in oxic reactors, and were similar for the "P addition", "Si addition", and "P+Si addition" reactors.

The Si:P ratio of ascorbate leachable fractions of oxic and anoxic reactors ranged between 0.56 and 1.03 for oxic reactors and 0.74 and 0.97 for anoxic reactors with mean Si:P ratios of 0.86 and 0.88 for oxic and anoxic reactors respectively (Table 2.4).

2.4 Discussion

2.4.1 Oxic and anoxic conditions at the sediment-water interface

Achievement of oxic conditions at the sediment-water interface in oxic reactors was demonstrated by the production of NO_3^- and SO_4^{2-}, which requires oxygen. The low release of TDMn and TDFe at the experimental pH (7-8) indicates formation of insoluble Fe and Mn oxides and thus high redox potential (Figure 2.11). Fe and Mn both have soluble reduced forms and insoluble oxyhydroxides (Figure 2.11) (Davison 1993).

Achievement of anoxic conditions and decreasing redox potential at the sediment-water interface in anoxic reactors was demonstrated by the sequence of NO_3^- and SO_4^{2-} reduction followed by TDMn and TDFe release, indicating the utilization of alternative terminal electron acceptors after depletion of oxygen (Figure 2.12) (Froelich et al. 1979). SO_4^{2-} was likely reduced to H_2S (Holmer & Storkholm 2001), which is in agreement with the higher concentration of TDS compared to SO_4^{2-} in the anoxic reactors. The release of TDMn and TDFe suggests the reductive dissolution of Fe and Mn oxides, such as $Fe(OH)_3$, FeOOH, ferrihydrite, and MnO_2 to reduced soluble forms of Fe and Mn (Figure 2.11).

2.4.2 P release under oxic conditions

Cootes' Paradise sediments were a net sink of P under oxic conditions. Oxic TDP and SRP steady-state fluxes were low and within the range previously reported for Cootes' Paradise sediments (0.96 to 28.3 mg P m^{-2} day^{-1} or 1.29 to 38.07 μmoles m^{-2} h^{-1}) by Kelton & Chow-Fraser (2005). The "P addition" reactor retained approximately 67% (7.5 μmoles) of P in the influent solution, and the "P+Si addition" reactor approximately 90% (10.2 μmoles). This retention was likely through sorption to Fe(III) oxides. If we assume that all P retention occurred in the top cm of sediment, P retention in the "P addition" and "P+Si addition" reactors equates to 0.9 μmoles P g^{-1} dry sed. and 1.4 μmoles P g^{-1} dry sed. respectively. The ascorbate extraction recovered 12-23 μmoles g^{-1} dry sed. reactive Fe-bound P (Table 2.4), and thus these concentrations would more than account for the amount

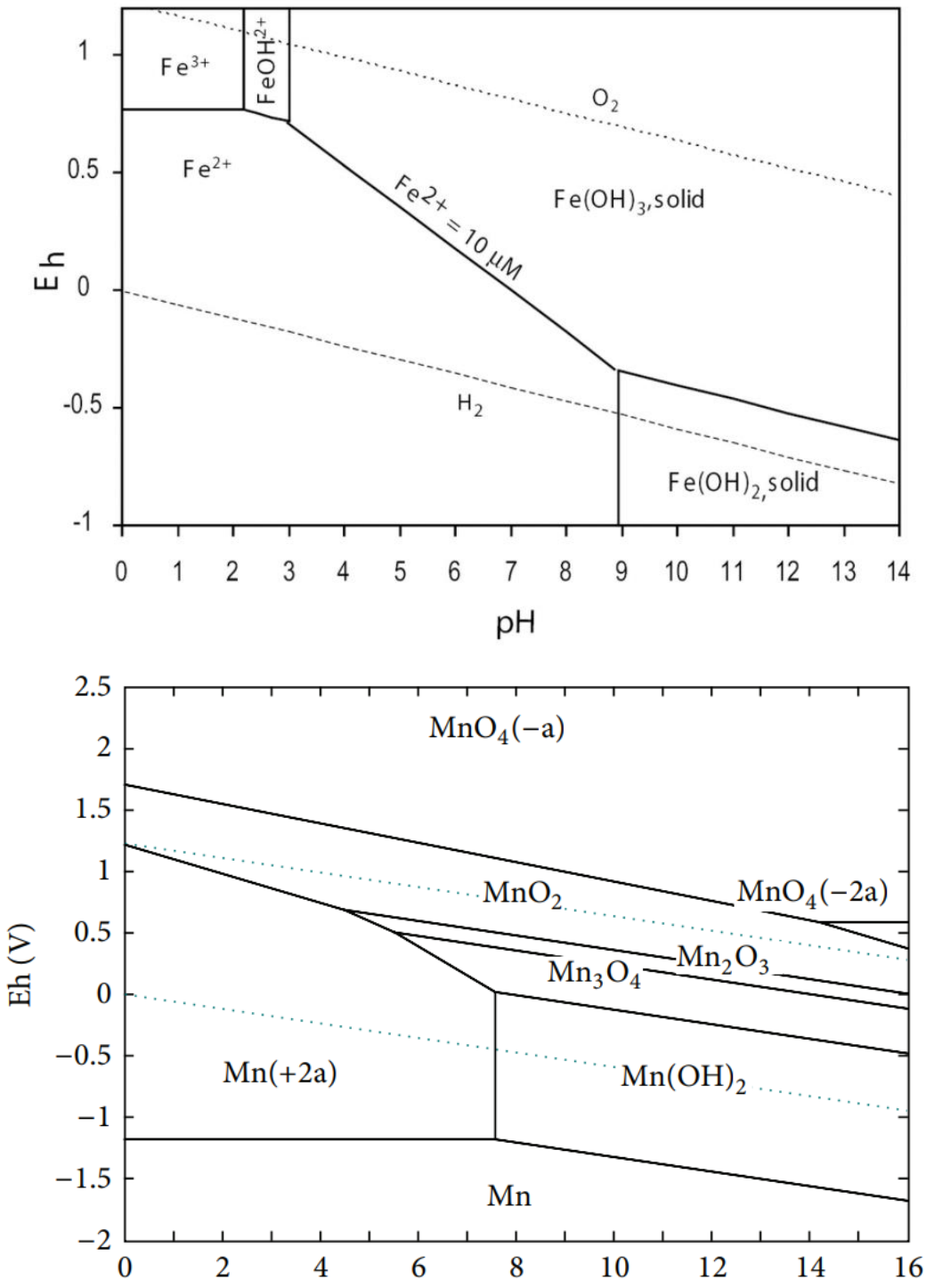

Figure. 2.11. Eh pH diagrams showing the speciation of Fe (top) and Mn (bottom) across a range of pH. Figures taken from Kappler & Straub (2005) Geomicrobiological cycling of iron. Reviews in Mineralogy and Geochemistry, 59(1):85-108; Freitas et al. (2013) Oxidative precipitation of manganese from acid mine drainage by potassium permanganate. Journal of Chemistry, 2013:8.

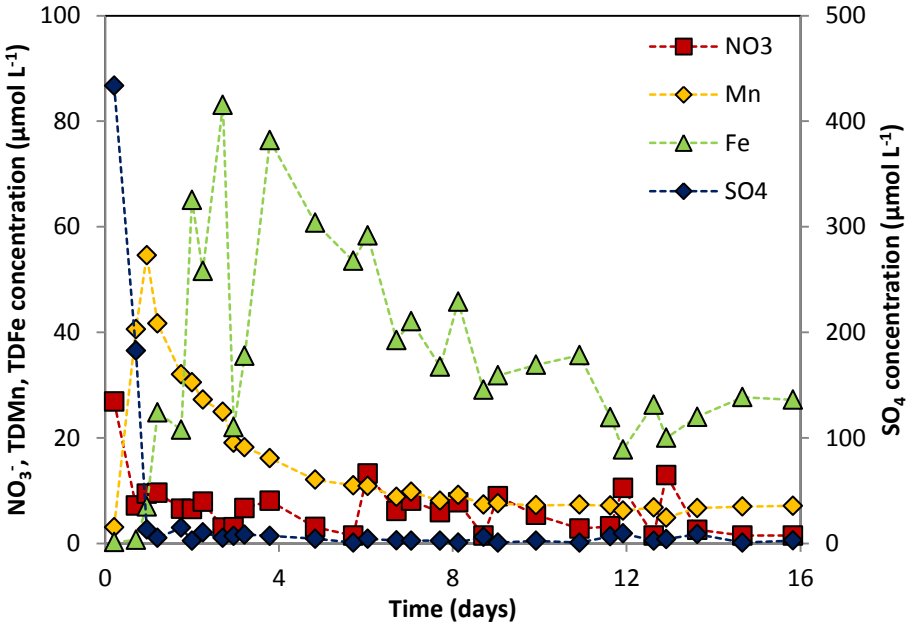

Figure 2.12. Average of anoxic reactors concentrations of NO_3^-, TDMn, TDFe, and SO_4^{2-} effluent concentrations showing the sequence of utilization of terminal electron acceptors.

of P retention observed. The solid phase Fe:P ratios ranged from 3.5-5 (Table 2.4). Considering the theoretical maximum molar ratio of phosphate incorporation in ferric oxides of Fe:P = 2:1 (Thibault et al. 2009), it seems reasonable that P retention was through sorption to reactive Fe(III) oxides as there was likely available sorption sites.

2.4.3 Si release under oxic conditions

Cootes' Paradise sediments were a net source of DSi under oxic conditions. Concentrations of 12-14 µmoles g^{-1} dry sed. reactive Fe-bound Si were recovered in the ascorbate leachable fraction, with Fe:Si ratios ranging from 5-6.5 (Table 2.4). This suggests that there was some sorption of Si to reactive Fe(III) oxides but that this sorption was not great enough relative to the pore water concentration of DSi to cause net retention as in the case of P. It is unknown what the source of DSi release under oxic conditions was, but the dissolution of BSi seem probable due to its higher reactivity compared to mineral silicates (DeMaster 1981). The concentration of BSi in sediment collected near the sampling site in Cootes' Paradise marsh was previously measured at approximately 142 µmoles g^{-1} dry sediment, which equates to approximately 5000-6000 µmoles BSi per sediment core (Shuhuan Li, unpublished data). The total DSi released from oxic reactors over the experiment ranged from 84-106 µmoles, and therefore the supply of BSi in sediment was likely more than enough to account for this DSi release.

2.4.4 P release under anoxic conditions

Cootes' Paradise sediments were a net source of P under anoxic conditions. Anoxic P fluxes were approximately 18 times that of oxic P fluxes (Table 2.3). It is unlikely that the increased P release was due solely to

the increased incubation temperature of anoxic reactors compared to the oxic reactors (Table 2.3). A Q_{10} of 2.06 was determined for anoxic P fluxes in Cootes' Paradise sediments (Kelton & Chow-Fraser 2005), and as such an approximately 8°C higher incubation temperature cannot account for all of the 18 fold increase in P release under anoxic conditions (Table 2.3). Thus, the source of P under anoxic conditions was likely release from reductive dissolution of reactive Fe(III) oxides. In anoxic reactors, TDP and SRP were released at the same time as TDFe, suggesting the same source (Figures 2.6 and 2.8). Ascorbate leachable reactive Fe concentrations were lower in the anoxic reactors (mean of 66.70 µmol g^{-1} dry sed.) compared to the oxic (mean of 70.04 µmol g^{-1} dry sed.) (Table 2.4), suggesting dissolution of reactive Fe under anoxic conditions. Again, considering the theoretical maximal Fe:P ratio of 2:1 (Thibault et al. 2009), the dissolution of approximately 3 µmol g^{-1} dry sed. of reactive Fe, which equates to approximately 20 µmol reactive Fe in the top cm of sediment, could have released approximately 10 µmoles P from the top cm of sediment. The anoxic reactors released a total of 35-43 µmoles P during the experiment (Table 2.3). Therefore about 25% of total released P could have been release from reductive dissolution of Fe(III) oxides in the top cm of sediment. The remaining P release could have been from reductive dissolution of Fe(III) oxides below the top cm of sediment formed during the time the reactors were exposed to oxygen prior to the start of the experiment (approximately 10 days). As well, P could have been released from other pools in the sediment such as the loosely sorbed P pool.

While there appeared to be concurrent release of P and Fe, aqueous Fe:P ratios in the effluent from anoxic reactors were not consistent but changed over the course of the experiment (Figure 2.10). Additionally, except for the "P+Si addition" reactor, aqueous Fe:P ratios were below the stoichiometric maximal Fe:P release of 2:1 (Figure 2.10). This may be explained the reduction of Fe(III) by H_2S produced through reduction of SO_4^{2-}, which produces Fe(II) and molecular S that can react to form FeS (Boström et al. 1988). Formation of FeS would remove both Fe^{2+} and S from pore water, leading to decreased TDFe concentrations and Fe:P ratios in the effluent. Precipitation of FeS would also explain the low TDS concentrations relative to the influent SO_4^{2-} concentration and thus potentially account for the missing sink of S (Figure 2.7). Low aqueous Fe:P ratios relative to the theoretical maximum were also found by Parsons et al. (2017) using Cootes' Paradise sediments, and formation of FeS was suggested as a potential reason for Fe^{2+} removal.

The concentration of Fe in the ascorbate leachable fraction in anoxic reactors decreased relative to the oxic, but a considerable concentration of reactive Fe was still extracted, and was therefore apparently undissolved, at the end of the experiment (Table 2.4). This is consistent with the observation of a thin lighter layer at the top of the anoxic sediments, indicative of ferric iron. The concentration of reactive Fe-bound P increased in anoxic reactors relative to oxic and this may have been due to resorption of P released deeper in the sediment core to as yet undissolved Fe(III) oxide minerals near the surface.

Retention and release of P from Fe(III) oxides is consistent with previous studies, which have found that Cootes' Paradise sediments contain substantial concentrations of Fe (313.69 µmol g^{-1} dry sed.) (Chris Parsons' unpublished data) and P (57 ± 4 µmol g^{-1} dry sed.), and approximately 24% of the total sediment P is Fe-bound (Na dithionite-extractable) (Parsons et al. 2017). In an experiment where Cootes' Paradise sediment was subjected to oscillating oxic and anoxic periods, the Fe-bound P pool was found to increase during oxic and decrease during

anoxic periods, and aqueous P concentrations to decrease during oxic and increase during anoxic periods, strongly suggesting retention and release of aqueous P by Fe oxide minerals (Parsons et al. 2017). The high concentrations of Fe recovered in the ascorbate leachable fractions from surface sediments suggests that Cootes' Paradise has a high capacity to both retain and release P (Table 2.4).

2.4.5 Si release under anoxic conditions

Sediments were a net source of DSi to the overlying water under oxic conditions, with anoxic Si fluxes being approximately 2.7 times that of oxic fluxes (Table 2.3). However, the increased temperature at which anoxic reactors were incubated may have contributed to the majority of the increased Si release under anoxic conditions. Assuming the source of DSi under oxic conditions was BSi predominantly in the form of diatoms, the 8°C higher incubation temperature of anoxic reactors probably increased BSi dissolution, which has been found to increase by a factor of 2.27 for each 10°C increase in temperature (Kamatani 1982). Using this Q_{10} relationship, estimated anoxic fluxes at 22°C were on average approximately 1.4 times, as opposed to 2.7 times, higher than oxic fluxes (Table 2.3). This suggests that approximately 60% of the DSi release from anoxic reactors may have been due to the effect of temperature alone.

The remaining DSi release under anoxic conditions may have been from reductive dissolution of Fe(III) oxides. Similar to P, there was concurrent release of DSi and TDFe from anoxic reactors and aqueous Fe:Si ratios showed a similar pattern to Fe:P ratios (Figures 2.6 and 2.9). However, aqueous Fe:Si ratios were about an order of magnitude lower (0.01-0.25) than Fe:P ratios (0.1-3.9) (Figure 2.10). These low Fe:Si ratios suggest that release of Si through reductive dissolution of reactive Fe(III) oxides was likely not the dominant source of Si under anoxic conditions. This somewhat agrees with sediment sequential extractions performed on sediments from other parts of the world where redox sensitive Si pools were smaller than BSi (Tallberg et al 2008, Tallberg et al 2012). In the Gulf of Finland, the labile and potentially reactive oxide-bound or adsorbed Si was estimated to be between 4 and 16 µmol g^{-1} dry sed. while the BSi was found to be 99 µmol g^{-1} dry sed. (Tallberg et al. 2008). Similarly, in the Bay of Brest BSi was found to be the largest potentially bioavailable Si pool (Tallberg et al. 2012). However, there is a lack of data on Si speciation in sediments for freshwater marsh environments.

Similar to P, reactive Fe-bound Si concentrations in anoxic reactors were higher than oxic, and could be due to the same reason i.e. resorption of DSi released to pore water deeper in the sediment to undissolved Fe(III) oxides near the surface (Table 2.4).

The relative contribution of temperature and redox to increased anoxic fluxes cannot be explicitly determined here and temperature controlled experiments are needed to confirm the effect of anoxia on DSi release. As well, the source of DSi under oxic and anoxic conditions cannot be confirmed. However, these results highlight the potential for substantial (40%) increase in DSi release from sediments under anoxic conditions, some of which may be due the reductive dissolution of Fe(III) oxides.

2.4.6 Competition between Si and P for sorption sites

The fluxes of DSi, TDP, and SRP between nutrient treatments did not give any clear evidence of the influence of Si and P on each nutrient's release. However, Si:P ratios slightly lower than 1, and lower Fe:P ratios compared to Fe:Si ratios in the ascorbate leachable fraction from oxic reactors indicate that P was preferentially sorbed to Fe(III) oxides over Si (Table 2.4). This resulted in the ability of P to decrease Si sorption but not the ability for Si to decrease P sorption. This is consistent with the fact that the additions of Si in the "Si addition" and "P+Si addition" treatments had little effect on the Fe:P ratio relative to the control, but that the addition of P in the "P addition" treatment decreased the Fe:P ratio to 3.5 and increased the Fe:Si ratio to 6.4 indicating that there was higher P sorption at the expense of Si (Table 2.4).

The ability of Si to compete with P for sorption sites changes with pH due to the pKa values of phosphoric and silicic acid and the charge on the Fe oxide mineral surface (Figure 2.13, Hartikainen et al. 1996; Brinkman 1993). Between pH 2 and 7, phosphate is predominantly in the form of H_2PO4^-, silicate is predominantly in the form of H_4SiO_4, and, using hematite as an example, the charge on the surface of the Fe oxide mineral is positive (Figure 2.13, Brinkman 1993). In this pH range, P is preferentially sorbed due to stronger attraction between the -1 charge on the phosphate and the positively charged mineral surface than the 0 charge on the silicate (Brinkman 1993). Between pH 7 and 12, phosphate and silicate dissociate to HPO_4^{2-} and $H_3SiO_4^-$ and the charge on the surface of hematite decreases (Figure 2.13, Brinkman 1993). The negative charge on the silicate ion improves adsorption to the Fe oxide surface, enabling Si to more effectively compete with P for sorption sites (Brinkman 1993). At pH greater than 12, phosphate and silicate dissociate to PO_4^{3-} and $H_2SiO_4^{2-}$ and the charge on the surface of hematite becomes negative (Figure 2.13, Brinkman 1993). Consequently, there is repulsion between phosphate and the mineral surface, and Si is preferentially sorbed (Brinkman 1993).

The ability of Si to compete with P for sorption sites is also influenced by Si concentration, with high Si concentrations having as great an effect on P desorption as increased pH (Koski-Vähälä et al. 2001). Koski-Vähälä et al. (2001) noted that there may be a threshold concentration of Si needed to get any effect on P sorption. However, Tallberg et al. (2008) found that pore water dissolved P concentrations increased even with relatively small additions of Si (1-2 mmol L^{-1} sediment), but the effect increased with increasing Si concentrations. So, this threshold Si concentration may be different between sediments. Therefore, the inability of Si to influence P sorption in the experiment may have been due to the pH and the pore water concentrations of Si being too low for this to occur.

As well, the act of flowing solution containing Si through the sediment cores as opposed to adding Si in a pulse may have also resulted in different effects than were observed in other experiments (Koski-Vähälä et al. 2001; Tallberg et al. 2008). Pulse additions may be more representative of the effects of a large diatom bloom, while slow flow of Si may be more representative typical conditions in areas of upwelling of Si-rich groundwater. Therefore, the influence of Si on P sorption may only become important in more extreme events such as the deposition of a large diatom bloom, whereas there may be no or less of an effect under typical "everyday" conditions.

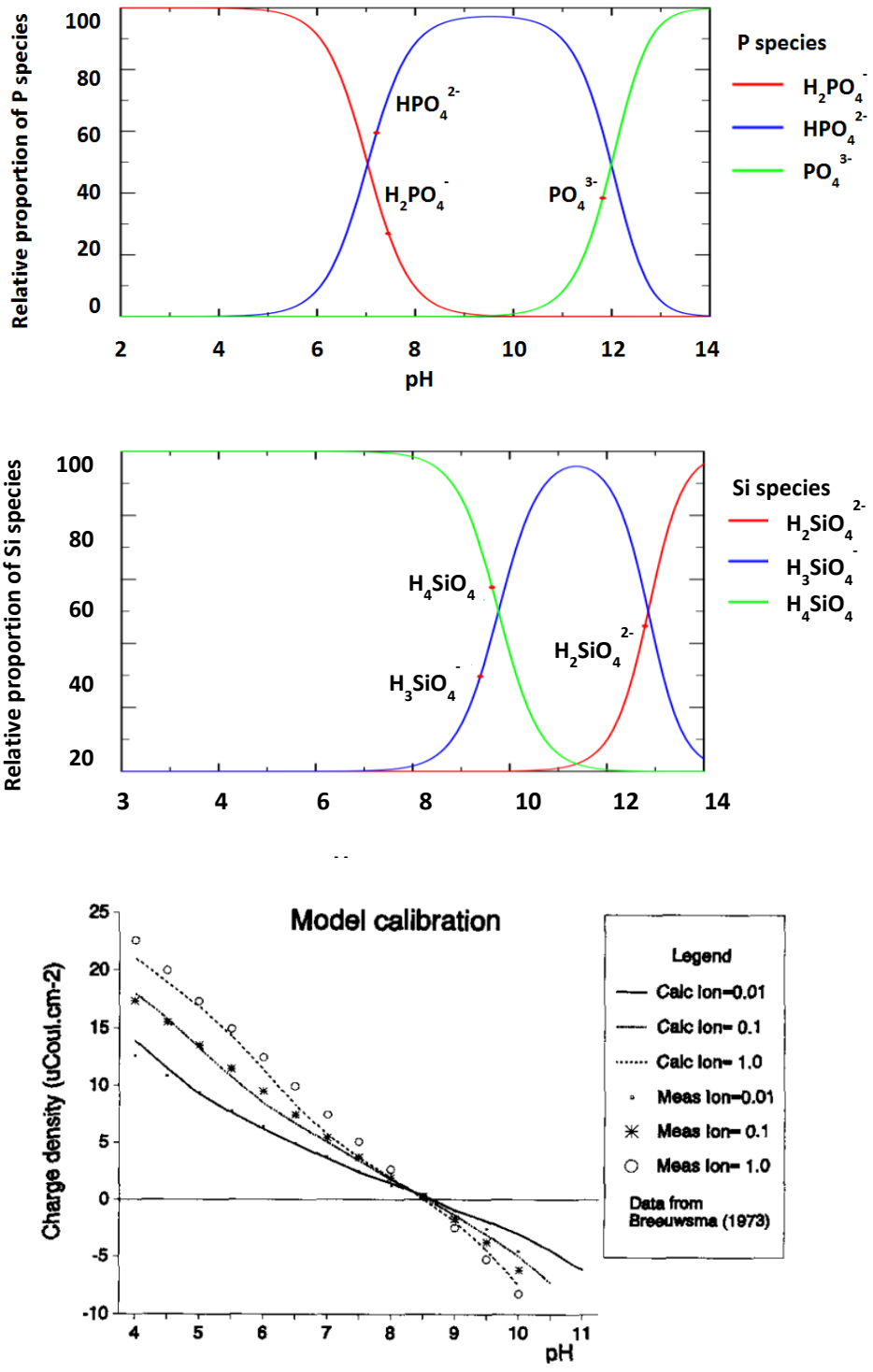

Figure 2.13. Speciation of phosphoric (top) and silicic acid (middle) and the charge density on the surface of hematite (bottom) across a range of pH. Phosphoric acid has pKa's at 7.1 and 12.7, and silicic acid has pKa's at 9.7 and 13.2. Speciation diagrams were made using PHREEQC and PHREEPLOT and the included thermodynamic database (Parkhurst and Appelo 1999; Kinniburgh and Cooper 2011). Bottom figure taken from Brinkman (1993) A double-layer model for ion adsorption onto metal oxides, applied to experimental data and to natural sediments of Lake Veluwe, the Netherlands. Hydrbiologia, 253:31-45.

2.4.7 Implication of internal loading of Si and P on water column Si:P ratio

Steady-state fluxes of TDP and SRP increased by approximately 18 times while Si increased by 2.7 times under anoxic conditions (Table 2.3). Thus, P fluxes increased more than Si fluxes under anoxic conditions. This resulted in a large decrease in the Si:TDP ratio of the effluent from well above 16:1 under oxic conditions to below 16:1 under anoxic conditions (Figure 2.10). The Si:P ratio of 16:1 represents the delineation between P limited and Si limited diatom growth based on the nutrient content of marine diatoms under non-nutrient limiting conditions (Redfield 1958; Brzezinski 1985). Si limited diatom growth (Si:P < 16:1) may promote the growth and dominance of non-siliceous phytoplankton such as flagellates or cyanobacteria, which can alter food web dynamics and may exacerbate the effects of eutrophication (Egge & Aksnes 1992; Peterson Holm & Armstrong 1981; Sommer & Stabel 1983; Sommer 1994; Moss et al. 1991; Officer & Ryther 1980; Sommer et al. 2002). If internal loading is a substantial source of nutrients relative to external nutrient loads, the Si:P ratio of sediment release may have implications for phytoplankton community composition through promoting either P limited or Si limited growth. Our results indicate that anoxic conditions at the sediment-water interface may release proportionally more P than Si and in turn may promote the growth of non-siliceous phytoplankton (Sommer et al. 2002; Sommer 1983; Sommer 1985; Peterson Holm & Armstrong 1981). Anoxic conditions could arise from a large phytoplankton bloom settling to the sediments due to depletion of oxygen through mineralization of organic matter by aerobic respiration (Froelich et al. 1979). Therefore, avoiding oxygen depletion in shallow eutrophic lakes where a significant portion of sediment P is associated with redox sensitive phase may be critical to remediation.

2.5 Conclusion

Cootes' Paradise sediment was a net sink of P and a net source of Si under oxic conditions, and a net source of both P and Si under anoxic conditions. Sediments retained 67-90% of influent P, which was likely through sorption to Fe(III) oxides. Fe:P ratios of the ascorbate leachable fraction were high relative to the theoretical maximum ratio of incorporation of P in ferric oxides indicating availability of sorption sites . The likely source of DSi under oxic conditions was dissolution of BSi. Recovery of Si in the ascorbate leachable fraction suggests that sorption of Si with Fe(III) oxides may have slightly reduced oxic DSi fluxes from the sediment. After accounting for the likely effects of temperature, anoxic TDP and DSi fluxes were approximately 8 times and 1.4 times larger than oxic fluxes respectively. Therefore, anoxic conditions had a disproportionate effect on P and Si release, with P release increasing substantially more than Si release. The reductive dissolution of Fe(III) oxide minerals and release of sorbed P and Si was likely responsible for the difference between oxic and anoxic fluxes.

Ratios of Si:P, Fe:P, and Fe:Si indicated preferential sorption of P over Si to Fe(III) oxides in the surficial sediment. This indicates that competition between P and Si for sorption sites resulted in P being the superior competitor, which had the effect of decreasing Si sorption and possibly increasing DSi fluxes from sediment. The inability of Si to outcompete P for sorption sites was likely related to the experimental pH and Si concentrations being too low to have an effect.

These results show that there may a significant effect of anoxia on sediment Si release, potentially increasing Si release by up to 40%. However, due to the disproportionate increase in P over Si under anoxic condtions, Si:TDP ratios of sediment release decreased from well above the 16:1 Redfield-Brzezinski ratio under oxic conditions to around 5-6 under anoxic conditions. Thus anoxic conditions at the sediment-water interface may promote the growth of non-siliceous phytoplankton through delivering a Si limited flux to the water column.

Chapter 3

Nutrient silicon cycling and limitation at the land-large lake interface: Case study of Hamilton Harbour (Ontario, Canada)

3.1 Introduction

The freshwater biogeochemical silicon (Si) cycle has historically been relatively understudied compared to those of the macronutrient elements phosphorus (P) and nitrogen (N). However, in recent years, it has been gaining increasing attention as an important link between the terrestrial and oceanic Si cycles (Street-Perrott and Barker 2009; Frings et al. 2014). Ortho-silicic acid (H_4SiO_4), the most bioavailable form of Si, is produced through chemical weathering of silicate minerals in the earth's crust (Harriss 1966). Silicon is an essential nutrient for many terrestrial and aquatic plants, including diatom algae, which are important primary producers in rivers, lakes, and oceans (Willen 1991; Treguer et al. 1995). Dissolved Si (DSi) assimilated by plants is precipitated as biogenic silica (BSi), a hydrated amorphous form of silica (Epstein 1994). Lakes and reservoirs are areas where significant amounts of nutrient Si are retained as a result of uptake by diatoms and other plants, followed by deposition and storage of BSi in sediments, thereby decreasing DSi export from land to the ocean (Frings et al. 2014; Harrison et al. 2012). Globally, it has been estimated that artificial reservoirs retain approximately 3% of DSi and 5.3% of the total reactive Si loading to rivers (Maavara et al., 2014), and up to 27% of the river DSi fluxes when lakes and reservoirs are combined (Frings et al. 2014).

Anthropogenic enrichment of rivers and lakes with P and N can enhance Si retention by relieving P or N limitation of the growth of siliceous algae resulting in increased production of BSi, ultimately leading to Si limitation in the downstream coastal area (Conley et al., 1993; Garnier et al., 2002; Garnier et al., 2010; Schelske and Stoermer, 1972; Seitzinger et al., 2010). Silicon limiting conditions favour the growth of non-siliceous phytoplankton, including flagellates and cyanobacteria, which can become dominant members of the plankton community (Egge & Aksnes, 1992; Peterson Holm and Armstrong, 1981; Sommer, 1983, 1994). A shift in the plankton community composition to non-siliceous algae can alter food quality and energy transfer to higher trophic levels with potentially negative implications for zooplankton and fish (Moss et al., 1991; Officer and Ryther, 1980; Sommer et al., 2002). Changing nutrient ratios, including a shift toward enhanced Si limitation, associated with anthropogenic eutrophication of freshwater and marine aquatic ecosystems are receiving increasing attention (Conley and Malone 1992; Danielsson et al. 2008; Glibert et al. 1995; Humborg et al. 2000; Justic et al. 1995; Justic et al. 1995; Li et al. 2007; Rocha et al. 2002; Turner et al. 1998; Viaroli et al. 2013; Maavara et al. 2015). However, despite the significant ecological consequences of Si limitation and the important influence of lakes and reservoirs on the riverine fluxes of reactive Si, relatively few studies have investigated how coastal freshwater ecosystems affect the exchanges of reactive Si at the land-large lake interface

This study aimed to enhance the quantitative understanding of Si limitation and reactive Si cycling in Hamilton Harbour, Ontario, Canada. Hamilton Harbour is a highly urbanized and human-impacted coastal freshwater ecosystem and is representative of what the future may hold for many other coastal urban centers. Hamilton Harbour is located along Lake Ontario, one of the lower Laurentian Great Lakes, and represents a transitional environment along the land-river-lake continuum. Continued loading of P and N from anthropogenic activities in the watershed of Hamilton Harbour and the relatively low representation of diatoms in the phytoplankton community suggest that Si may be limiting for diatom growth (Dermott et al. 2007; Munawar et al.

2017). Silicon limitation could in turn be contributing factor to the recurrence of harmful algal blooms in Hamilton Harbour (Hiriart-Baer et al. 2009).

The following hypotheses guided our work. 1) Hamilton Harbour is a net sink of reactive Si due to biological uptake of DSi and subsequent deposition and accumulation of BSi in sediments. 2) Diatom growth in Hamilton Harbour is Si limited due to high demand of DSi under the prevailing eutrophic conditions. To test these hypotheses, a mass balance model of DSi and reactive particulate Si (RPSi) for Hamilton Harbour was constructed. This involved identifying and quantifying reactive Si inflows and outflows, and internal Si cycling processes through field sampling, laboratory incubation experiments, and published literature. To determine if Si was stoichiometrically limiting to diatom growth, water samples from Hamilton Harbour were collected and analysed for DSi and total dissolved P (TDP) and molar dissolved Si:P ratios calculated across the spring, summer and fall of 2016.

3.2 Methods

3.2.1 Study site

Hamilton Harbour (Ontario, Canada, 43°17'17.3"N 79°50'03.7"W) is a 21.5 km^2 embayment at the western end of Lake Ontario (Figure 3.1) that is heavily impacted by anthropogenic activity (Barica 1989). Hamilton Harbour has mean and maximum depths of 13 m and 23 m, respectively. The cities of Burlington and Hamilton border the north and south shores of the harbour, which are inhabited by approximately 747,000 people (Statistics Canada 2017). Major sources of nutrients to Hamilton Harbour are three tributaries that drain urban and agricultural land (Long et al., 2014), a channel connecting Hamilton Harbour to Cootes' Paradise Marsh, a highly eutrophic coastal wetland (Chow-Fraser et al. 1998), plus direct effluent discharges from two wastewater treatment plants (WWTPs) and 18 combined sewer overflows (CSOs). Water from the harbour is also used to cool a large steel mill on the southern shore. Hamilton Harbour is connected to Lake Ontario by the man made Burlington Ship Canal (BSC) (820 m long, 88 m wide, 9.5 m deep), which creates a complex two-way hydraulic exchange between Hamilton Harbour and Lake Ontario driven by differences in water level (year round) and density (during summer stratification) (Ling et al. 1993; Barica 1989; Klapwijk and Snodgrass 1985).

Hamilton Harbour and the adjoining Cootes' Paradise Marsh were designated as one of 43 Great Lakes Areas of Concern by the International Joint Commission in 1987 due to severely degraded water quality and environmental health (International Joint Commission United States and Canada 1987; Hiriart-Baer et al. 2009; Hiriart-Baer et al. 2016). A Remedial Action Plan was established to protect environmental quality and restore the impaired beneficial uses including those resulting from "eutrophication or undesirable algae" (Hiriart-Baer et al. 2016). Nutrient abatement strategies have focused primarily on reducing P and N loads and have led to some improvements in water quality (Hiriart-Baer et al. 2016). However, algal blooms, including those of cyanobacteria, continue to be a problem (Hiriart-Baer et al. 2009; Munawar et al. 2017).

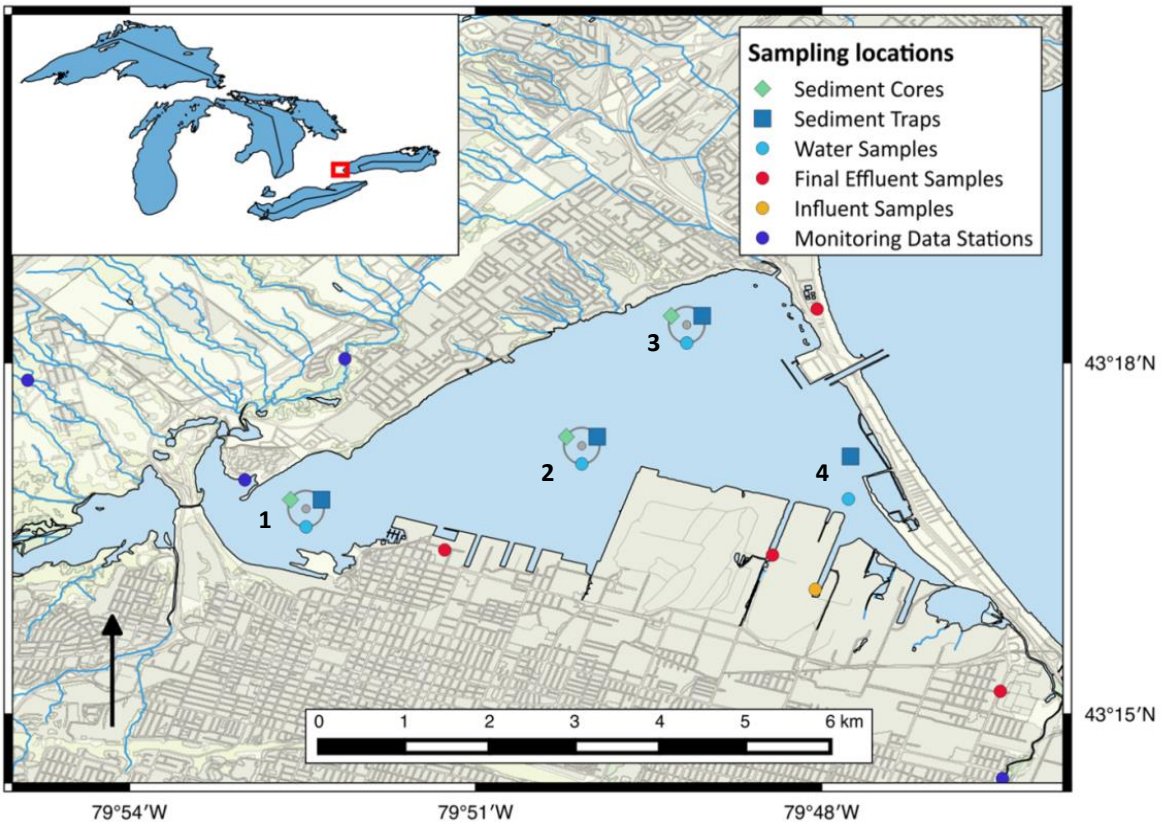

Figure 3.1. Map of Hamilton Harbour, Ontario, Canada with the locations that water, suspended sediment, and sediment cores were collected throughout 2015 and 2016 as well as the locations of monitoring data stations from which data was used.

3.2.2 Water budget

Hamilton Harbour's water budget was calculated according to Equation 3.1 assuming that inflows and outflows balance each other on a monthly time scale. Water inflows considered in the budget are discharge from the three tributaries (T), the channel connecting Cootes' Paradise Marsh to Hamilton Harbour (CP), the two WWTPs (WWTP), the 18 CSOs (CSO), the steel mill (SMD), plus precipitation (P), groundwater discharge (G), and inflow from Lake Ontario (LO). Water outflows included evaporation (E), steel mill intake (SMI), and outflow from Hamilton Harbour to Lake Ontario (HH):

$$T + CP + WWTP + CSO + SMD + P + G + LO = E + SMI + HH \quad \text{Eq. 3.1}$$

Sources of information used to calculate the water budget are described in Table 3.1. Outflow from Hamilton Harbour to Lake Ontario was calculated as the residual term in Equation 3.1. Precipitation and evaporation data

Table 3.1. Sources of discharge data used to constrain the hydrologic budget. WWTP = wastewater treatment plants, CSOs = combined sewer overflows.

Water Source	Data Source/Reference	Temporal Resolution
Grindstone Cr.	WSC Hydrometric St. 02HB012	1998-2015 daily mean discharge
Redhill Cr.	WSC Hydrometric St. 02HA014	1998-2015 daily mean discharge
Indian Cr.	WSC Hydrometric St. 02HA014; Long et al (2014)	1998-2015 daily mean discharge
Cootes' Paradise	WSC Hydrometric St. 02HB007; Long et al (2014)	1998-2015 daily mean discharge
WWTPs	Region of Halton, City of Hamilton	1998-2015 monthly mean discharge
CSOs	City of Hamilton	2015 annual discharge
Steel Mill	ArcelorMittal-Dofasco Steel Mill	2014-2016 monthly mean daily discharge
Precipitation	1981-2010 Canadian Climate Normals, Hamilton Royal Botanical Gardens Weather St.	1981-2010 monthly mean
Evaporation	1981-2010 Canadian Climate Normals, Hamilton Royal Botanical Gardens Weather St.	1981-2010 monthly mean daily
Groundwater	Harvey et al. (2000)	1997 annual discharge
Lake Ontario	Hamblin & He (2003)	Unstratified (Feb. 1989) and stratified (July 1996) exchange estimates
Hamilton Harbour	Mass balance	Monthly

collected by a weather station located at the western end of Hamilton Harbour (Figure 3.1) were extrapolated to the entire surface area of Hamilton Harbour.

3.2.3 Sampling and analytical methods

A regular field sampling program was undertaken between April and November 2016; it involved collection of water, suspended sediment, and bottom sediment samples from multiple sites and depths across Hamilton Harbour, as well as water samples from the two WWTPs, the steel mill intake and surface water discharge points and the CSOs (Figure 3.1, Table 3.2). Water samples from Hamilton Harbour were collected on a bi-weekly basis at 1 m below the surface (epilimnion) and 1 m above the sediment-water interface (hypolimnion) using Niskin bottles (General Oceanics). Suspended sediments were collected on a monthly basis with sediment traps based on the design of Marvin et al. (2004). Sediment cores were collected using box corers. Details of sample collection from other sites and other sources of reactive Si data are described in Table 3.2.

All water samples were collected in 1 L amber high-density polyethylene bottles and refrigerated at 4°C in the dark until analysis. Approximately 30 mL of the 1 L sample was filtered through 0.45 µm pore size polypropylene syringe filters for analysis of total dissolved Si (DSi), total dissolved P (TDP) and soluble reactive Si (SRSi). Samples for analysis of DSi and TDP were acidified with 2% nitric acid and analysed using Inductively

Table 3.2. Sources of reactive silicon concentration data for external sources and sinks used in mass balance model. Dissolved silicon (DSi), reactive particulate silicon (RPSi), and total reactive silicon (TRSi) = DSi + RPSi, PGMN = Provincial Groundwater Monitoring Network, GLSP = Great Lakes Surveillance Program, WSC = Water Survey of Canada

Source	Data Reference	Reactive Si Measured	Temporal Resolution
Grindstone Cr.	Unpublished data from Long et al. (2014)	TRSi	87 24-hr level weighted samples from baseflow and storm/melt events Jul. 2010 – May 2012
Redhill Cr.	Unpublished data from Long et al. (2014)	TRSi	87 24-hr level weighted samples from baseflow and storm/melt events Jul. 2010 – May 2012
Indian Cr.	Unpublished data from Long et al. (2014)	TRSi	87 24-hr level weighted samples from baseflow and storm/melt events Jul. 2010 – May 2012
Cootes' Paradise	Unpublished data from Long et al. (2014)	TRSi	87 24-hr level weighted samples from baseflow and storm/melt events Jul. 2010 – May 2012
WWTP	Sample collection (this study)	DSi, RPSi	Weekly 24-hr composite (WWTP 1), monthly grab samples (WWTP 2) Nov. 2015 – Nov. 2016
CSO	Sample collection (this study)	DSi	9 grab samples, Mar. – Oct. 2016
Steel Mill	Sample collection (this study)	DSi, RPSi	Weekly 24-hr composite samples Nov. 2015 – Nov. 2016
Precipitation	Chan & Kuntz (1982), bulk precipitation	TRSi	Monthly averaged over 1975-1978 (uncontaminated)
Groundwater	PGMN wells W0000002-1 and W0000338-1	DSi	Annual or bi-annual water samples 2003-2013
Lake Ontario	GLSP PSN 1 and Fisheries and Oceans	DSi	Biweekly, monthly, or annual grab samples spanning 2006-2016
Hamilton Harbour	Sample collection (this study)	DSi, RPSi	Biweekly grab samples Apr. – Nov. 2016

Coupled Plasma-Optical Emission Spectrophotometry (ICP-OES, Thermo Scientific iCAP 6300) with detection limits of 0.05 µmol Si L^{-1} and 0.1 µmol P L^{-1}, quantification limits of 0.15 µmol Si L^{-1} and 0.35 µmol P L^{-1}, and precision better than 15% for both Si and P (low concentrations). SRSi was measured by the molybdenum blue method (Environmental Protection Agency 1978) on a UV-Visible Spectrophotometer (Thermo Evolution 260) with a detection limit of 0.6 µmol Si L^{-1}, a quantification limit of 1.8 µmol Si L^{-1}, and precision better than 10%.

The remaining volume of each water sample was vacuum filtered and suspended particulate matter collected on 0.45 µm pore size nylon membrane filters (Whatman 47 mm type WNYL). Filters were air dried and particulate matter (approximately 5-25 mg) extracted for RPSi by placing filters in 100 mL of 0.5 M NaOH for 3 hours in a water bath at 85°C following a modified alkaline extraction method (DeMaster, 1981; Koning et al.,

1997; Koning et al., 2002). One mL of extractant was subsampled every 30 min, filtered through 0.45 µm pore size nylon membrane syringe filters, acidified to 2% nitric acid and measured for DSi by ICP-OES. Freeze-dried and lightly ground suspended sediments and bottom sediments were extracted for RPSi following the same method. The y-intercept of the regression line of DSi concentration versus time then yielded the RPSi content of the sample. To calculate RPSi concentrations, the RPSi content (as wt% Si) was multiplied by the total suspended solid matter density (TSS), which was calculated as the mass of suspended particulate matter collected per volume filtered. To evaluate the extraction efficiency, material used in an inter-laboratory comparison of BSi extraction techniques was extracted and measured Si contents (as wt% SiO_2) were within one standard deviation of reported values (Conley, 1998). The extracted RPSi includes BSi, silicate ions loosely bound to organic and inorganic particulate matter, and additional amorphous and poorly crystalline silicate mineral phases (Conley, 1998; Tallberg et al., 2009).

3.2.4 Sediment core incubations

Sediment core incubation experiments were carried out in order to estimate the internal loading fluxes of DSi from sediments to the water column. Sediment cores were collected in July and October 2016 from multiple sites across Hamilton Harbour (Figure 3.1) using a box corer. The sediments were subsampled onboard by inserting plastic core tubes (7.5 cm in diameter, 60 cm long) into the box corer. Bottom water was also collected at each site at 1 m above the sediment-water interface using Niskin bottles (General Oceanics). Incubation experiments began within 24 hours of sediment core collection using a similar setup as Beutel (2006) and Cowan and Boynton (1996) (Figure 3.2). Bottom water was carefully poured into the core tubes to create an overlying water column of approximately 1 – 1.2 L in volume (Figure 3.2). The effects of bottom water oxygenation and temperature on the internal loading DSi flux were tested in two separate incubation experiments. In the first, sediment cores were incubated at 22±2°C while the overlying water column was bubbled with either air or N_2 gas. In the second, sediment cores were incubated at a range of temperatures (3°C, 16°C, 19°C, and 22°C) while the water column was bubbled with air (Figure 3.2). In both experiments, sediment cores were incubated for approximately 72 hours. The overlying water was sampled 2-4 times per day through ports installed in the top cap of the core tubes and analysed for DSi and SRSi (see analytical methods above) (Figure 3.2). After completion of the incubation experiments sediment cores were frozen and sectioned into 1 or 2 cm intervals for RPSi extraction.

3.2.5 Reactive Si budget

The conceptual model of the reactive Si cycle in Hamilton Harbour is shown in Figure 3.3. Hamilton Harbour was divided into 4 reactive Si reservoirs: 1) water column DSi, 2) water column RPSi, 3) sediment DSi, and 4) sediment RPSi (Figure 3.3). The temporal resolution of the model was one month. On this monthly time scale, the water column was assumed to be well mixed and spatially homogenous. The fluxes affecting the reactive Si reservoirs are then: 1) exchange fluxes with land-based sources and sinks, which include the tributaries, Cootes'

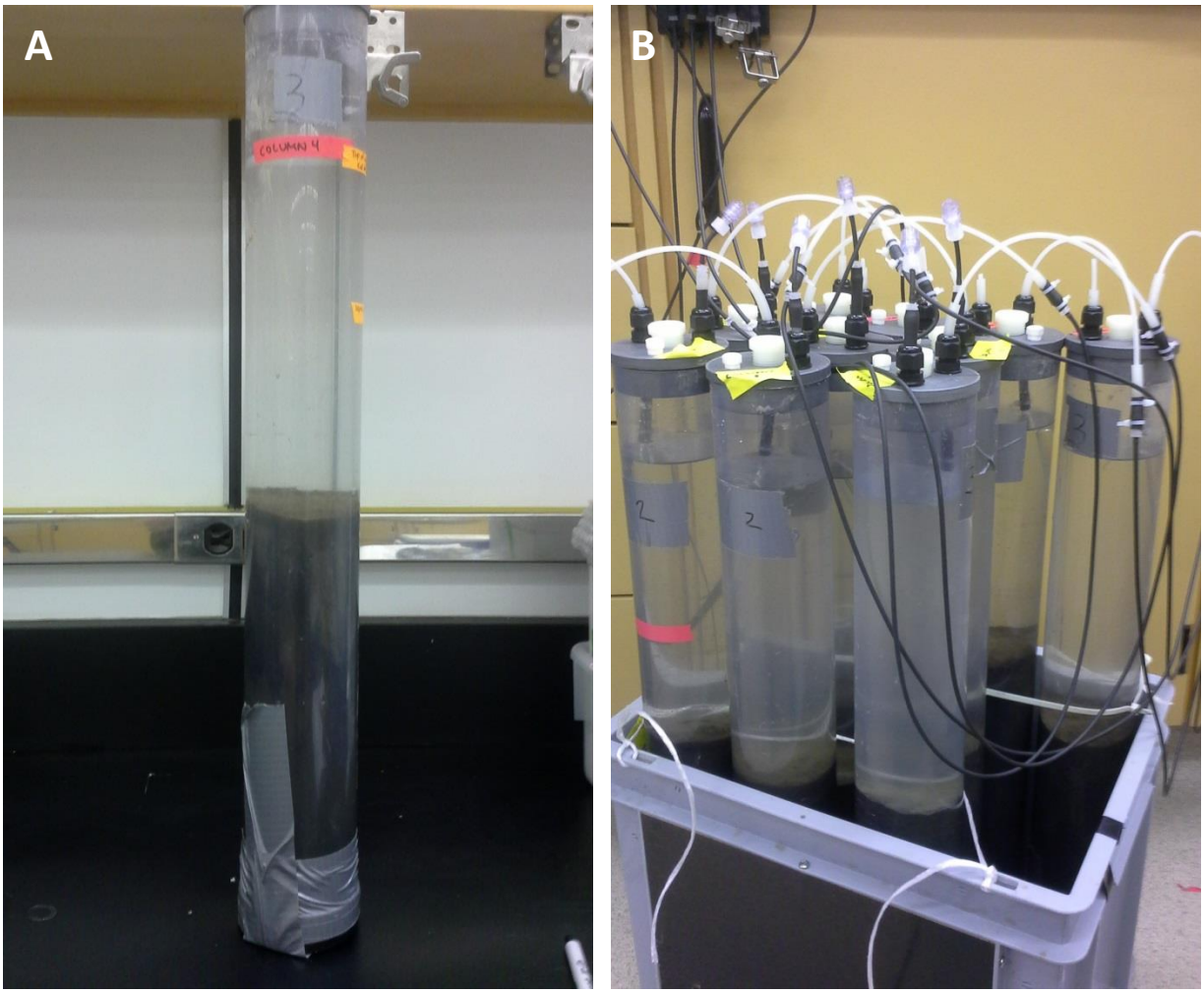

Figure 3.2. Sediment core design and experimental set-up during the sediment incubation experiments. Sediment cores were capped at the top and bottom and contained 25-30 cm of intact sediment overlain by water collected from 1 m above the sediment-water interface (A). Sediment columns were bubbled with gas to mix the water column and keep it oxygenated or deoxygenated as desired (B). Samples of the water column were taken through ports in the top cap throughout the incubation period (B).

Paradise, WWTPs, CSOs, steel mill (intake and discharge), precipitation and groundwater, 2) internal Si cycling fluxes, which include uptake and dissolution in the water column, sedimentation, resuspension, and internal loading, and 3) exchange fluxes with Lake Ontario, that is, inflow from the lake and outflow from Hamilton Harbour.

The DSi and RPSi mass balances were calculated on a monthly basis from May to November 2016 according to Equations 3.2 and 3.3, where ΔM_{DSi} and ΔM_{RPSi} are the monthly change in mass of DSi and RPSi in the water column, respectively, and the F terms correspond to the numbered fluxes in Figure 3.3:

$$\Delta M_{DSi} = F_1 + F_2 + F_3 + F_4 + F_5 + F_6 + F_7 + F_{16} + F_{19} - F_{13} - F_{19} \quad \text{Eq. 3.2}$$

$$\Delta M_{RPSi} = F_8 + F_9 + F_{10} + F_{11} + F_{12} + F_{13} + F_{15} + F_{20} - F_{14} - F_{21} \quad \text{Eq. 3.3}$$

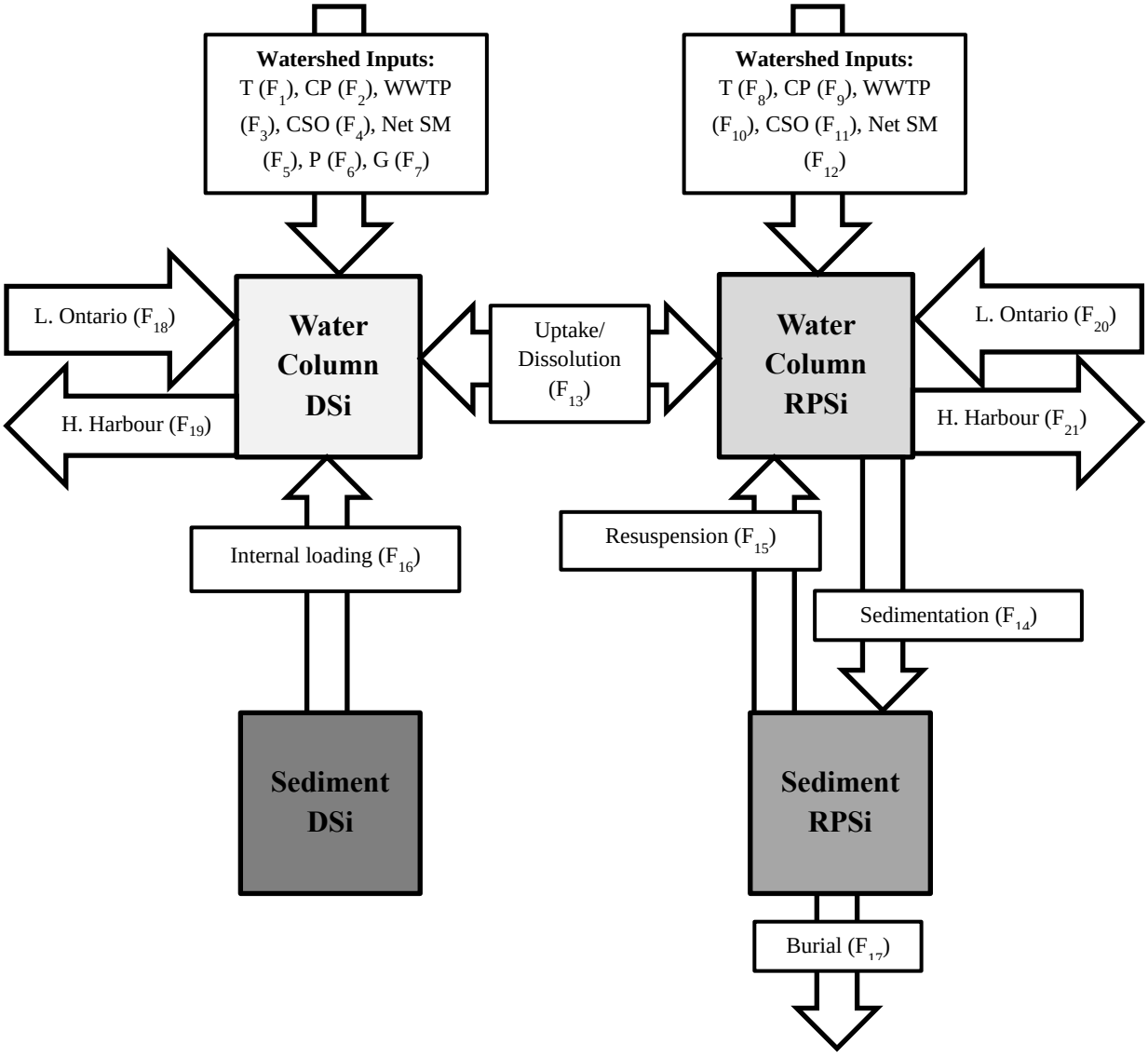

Figure 3.3. Conceptual model of reactive silicon cycling in Hamilton Harbour. Boxes represent reservoirs and arrows fluxes of reactive Si to and from reservoirs. DSi = dissolved Si, RPSi = reactive particulate Si, T = tributaries, CP = Cootes' Paradise marsh, WWTP = wastewater treatment plants, CSO = combined sewer overflows, Net SM = net steel mill flux (intake – discharge), P = precipitation, G = groundwater, L. Ontario = Lake Ontario, H. Harbour = Hamilton Harbour.

Monthly mean watershed (F_1 to F_{12}) and harbour-lake exchange (F_{18} to F_{21}) fluxes of DSi and RPSi (expressed in units of moles day^{-1}) were calculated by multiplying monthly mean concentrations of DSi or RPSi (moles m^{-3}) by monthly mean water flows (m^3 day^{-1}) from each source. Mean fluxes for the entire May to November period were calculated by summing all monthly fluxes and dividing by 214 days.

Total reactive Si concentrations from the 3 tributaries, and outflow from Cootes' Paradise Marsh were measured on water samples collected from storm or melt events and baseflow conditions between July 2010 and May 2012 (Long et al., 2014 unpublished data). For tributaries and Cootes' Paradise, monthly mean total reactive Si concentrations were calculated according to Equation 3.4 where $C_{monthly\ avg}$ is the monthly average concentration of

total reactive Si; $C_{storm,melt}$ and $C_{baseflow}$ are the average concentrations of total reactive Si in samples collected during storm/melt events and baseflow in each month respectively; *events* is the number of days per month on which a storm/melt event occurred; *baseflow* is the number of days in the given month that no storm/melt event occurred and as such was assumed to be baseflow conditions:

$$C_{monthly\ avg} = \left(\frac{C_{storm,melt} * events}{days\ in\ month}\right) + \left(\frac{C_{baseflow} * baseflow}{days\ in\ month}\right) \quad \text{Eq. 3.4}$$

In order to separate total reactive Si into DSi and RPSi, DSi was assumed to be 84% and RPSi 16% of the monthly total reactive silicates concentration according to the global average for rivers (Conley 1997).

For other sources, RPSi concentrations were calculated according to Equation 3.5, where *TSS* is the total suspended solids, *wt%RPSi* is the proportion of RPSi in suspended matter determined by the RPSi extraction, and 28.085 is the molar weight of Si (g):

$$C_{RPSi} = \frac{TSS * wt\%RPSi}{28.085} \quad \text{Eq. 3.5}$$

For sources where water samples were collected and analysed for RPSi, TSS was calculated from the weight (g) of suspended matter collected on the filter divided by the volume of water filtered (m^3). TSS concentrations for Lake Ontario were obtained from Ling et al., (1993), and TSS for CSO from the Hamilton Harbour RAP Technical Team (2010). Lake Ontario RPSi concentrations were not available and as such were calculated assuming 5% of TSS by weight was RPSi based on the average percent weight RPSi measured in Hamilton Harbour water samples. Limited sample volumes from CSOs prevented analysis of RPSi. As such, RPSi concentrations were calculated using the percent weight of RPSi measured in samples collected from WWTP 2.

The internal loading fluxes of DSi from sediments (F_{16}) were estimated from the sediment incubation experiments. The DSi flux from each sediment core was calculated from the linear regression of DSi concentration measured in the water column versus time (Figure 3.4). No significant differences in DSi fluxes were found between oxic and anoxic water column treatments, but significant differences were found at different temperatures (at the α = 0.05 level in a t-test), resulting in the following flux-temperature relationship (Equation 3.6, Figure 3.5):

$$Log(mmol\ DSi\ m^{-2}d^{-1}) = 0.0433T - 0.2617 \qquad r^2 = 0.97,\ p < 0.001 \quad \text{Eq. 3.6}$$

where temperature (T) is in °C. Net uptake of DSi in the water column (F_{13}) was calculated as the residual term in Equation 3.2. Sedimentation (F_{14}) was calculated from the sedimentation rate measured by sediment traps multiplied by the RPSi content of the suspended sediments determined in the alkaline extractions. Resuspension (F_{17}) was calculated as the residual term in Equation 3.3. The burial flux (F_{17}) was calculated according to Equation 3.7:

$$F_{17} = F_{14} - F_{15} - F_{16} \quad \text{Eq. 3.7}$$

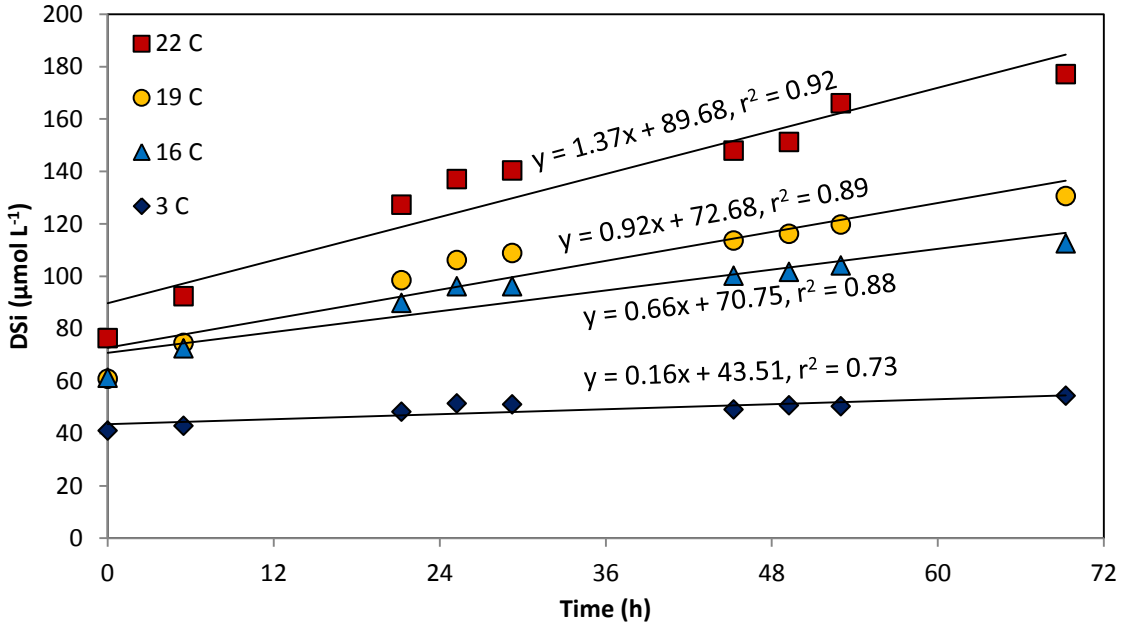

Figure 3.4. Graph of DSi concentration vs time for cores taken from Hamilton Harbour 258 incubated at 4 different temperatures. The slope of the regression line is the DSi flux (µmol L^{-1} h^{-1}). Fluxes were then converted to units of mmol m^{-2} day^{-1} by multiplying by the volume of the water column (L), dividing by the surface area of the core (m^2), and making units conversions to give fluxes in mmol m^{-2} day^{-1}.

Note that negative values of F_{17} occur when sediment RPSi dissolution exceeds net sedimentation of RPSi. In this case, the dissolution of previously deposited RPSi sustains an internal loading flux of DSi that is greater than the (net) supply flux of RPSi from the water column.

3.3 Results

3.3.1 Water budget

The annual hydrologic budget for Hamilton Harbour averaged over the time period 1998-2015 is shown in Figure 3.6 and monthly water fluxes are given in Appendix 1 Table 1. Water fluxes used in the calculation of the monthly reactive Si budget are given in Table 3.3. Between May and November, water exchanges between Hamilton Harbour and Lake Ontario dominate the water budget. Exchanges with Lake Ontario account for 75% of the total water inflow and 87% of the total outflow. Intake and discharge of water by the steel mill is the second largest water inflow and outflow, but results in no net loss or gain of water as the fluxes are equal. Discharge from WWTPs is the third largest water inflow, contributing 6.8% of the total water input to Hamilton Harbour between May and November. Tributaries, Cootes' Paradise Marsh, CSOs, precipitation, groundwater and evaporation all contribute less than 2.5% each to the total water inflows or outflows, and thus are relatively minor components of the overall water budget.

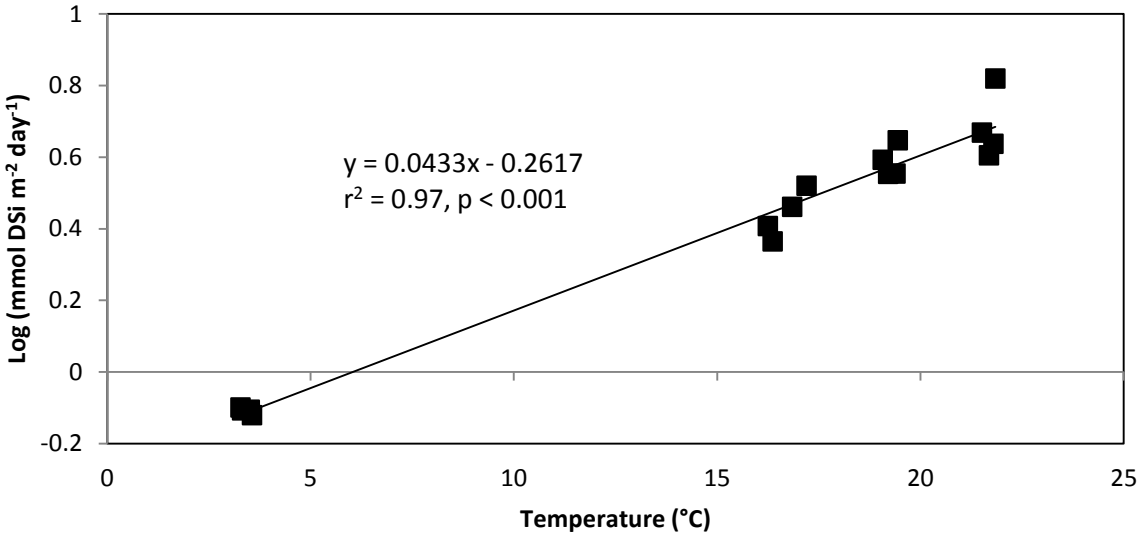

Figure 3.5. The regression of the log of the DSi flux from all 16 cores versus incubation temperature gave a significant positive correlation where DSi flux increased with increasing temperature. The equation of the regression line was used to estimate internal loading DSi fluxes at measured hypolimnetic water temperatures between May to November 2016.

3.3.2 Reactive Si concentrations

The concentrations of DSi, SRSi, TDP and RPSi measured in water and suspended sediment samples collected at 4 sites across Hamilton Harbour between April and November 2016 are listed in Appendix 1 Tables 2 through 5; concentrations of DSi, SRSi, TDP and RPSi measured in water samples collected from the two WWTPs and from the steel mill intake and discharge points between November 2015 and November 2016 can be found in Appendix 1 Tables 7 through 12. Water column concentrations of DSi and RPSi varied significantly between April and November 2016 (Figure 3.7). DSi concentrations in the epilimnion and hypolimnion were lowest in spring, in the ranges 1.8-2.3 µmol L^{-1} and 1.8-4.7 µmol L^{-1}, respectively, and highest in the fall in the ranges 20.1-22.6 µmol L^{-1} and 22.9-26.1 µmol L^{-1}, respectively (Figure 3.7). Hypolimnetic DSi tended to be slightly higher than epilimnetic DSi, hence justifying treating the water column as a homogeneous reservoir (Figure 3.7). The water column concentrations of DSi began increasing at the end of May in both the epilimnion and hypolimnion (Figure 3.7). However, while the increase in hypolimnetic DSi concentration remained fairly steady, the epilimnion DSi concentration exhibited dips around June-July and again in September (Figure 3.7). The concentrations of RPSi generally showed an opposite trend to DSi (Figure 3.7). Eplimnetic and hypolimnetic RPSi concentrations were highest in the spring, in the ranges 4.3-13.5 µmol L^{-1} and 6.8-11.4 µmol L^{-1}, respectively, and lower in summer and fall, in the ranges 1.3-7.1 µmol L^{-1} and 2.0-6.2 µmol L^{-1}, respectively (Figure 3.7).

The seasonal trends of water column TDP deviated from that of DSi (Figure 3.8). Concentrations of TDP in the epilimnion were relatively high in the spring, in the range 1.0-1.3 µmol L^{-1}, decreased throughout the summer to minimum concentrations around 0.3-0.4 µmol L^{-1} in mid-August to mid-September, and increased again to

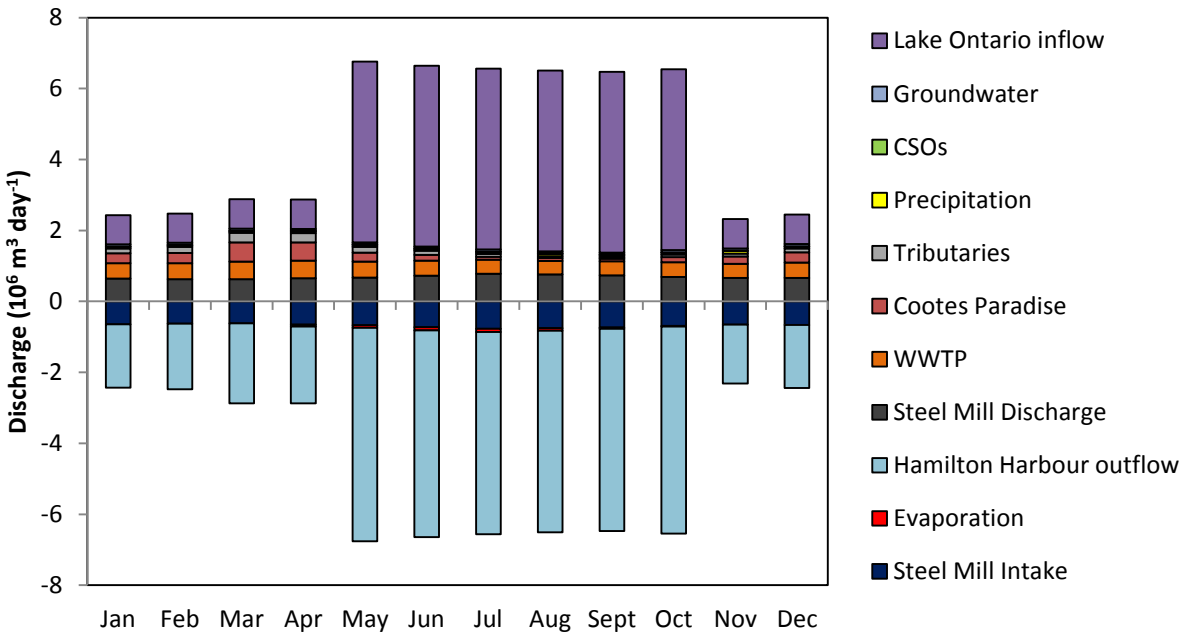

Figure 3.6. Annual hydrologic budget for Hamilton Harbour averaged over the time period 1998-2015. Positive discharge indicates water input and negative discharge indicates water export from the Hamilton Harbour water column.

concentrations in the range 1.3-1.7 µmol L^{-1} in the fall (Figure 3.8). Hypolimnetic TDP concentrations were relatively constant throughout the spring and early summer in the range of 0.8-1.0 µmol L^{-1}, increased through August and into September reaching 2.1 µmol L^{-1}, and decreased through the fall to 1.3 µmol L^{-1} in November (Figure 3.8).

Molar Si:P (= DSi:TDP) ratios in the epilimnion were lowest in the spring, in the range 1.4-2.3, peaked in August and September reaching 28 and 27, respectively, and dropped to values of 10.7-17.4 in the fall (Figure 3.9). Hypolimnetic Si:P ratios were also lowest in the spring, in the range 2.2-4.9, peaked in late July reaching 20.6, decreased to 10.8 in September, and rose again to 17.7 in November (Figure 3.9).

3.3.3 Reactive Si budget

Mean DSi and RPSi fluxes averaged across the entire May to November period are listed in Table 3.3, while the DSi and RPSi fluxes for the individual months can be found in Appendix 1 Tables 13 and 14. Sources and estimates of uncertainty associated with water flows, reactive Si concentrations and reactive Si fluxes are presented in Appendix 2 Tables 1 through 4.

From May to November 2016, the largest DSi influx to Hamilton Harbour from the watershed was the WWTPs, followed in decreasing order of importance by groundwater, Cootes' Paradise Marsh, the tributaries, the net flux from the steel mill, CSOs, and precipitation (Table 3.3). Together these watershed sources amounted to 51 x 10^3 moles day^{-1} of DSi and 4.4 x 10^3 moles day^{-1} of RPSi. WWTPs contributed 25 x 10^3 moles day^{-1}, or 49% of the

Table 3.3. Mean May to November 2016 discharge and fluxes of DSi and RPSi to and from Hamilton Harbour ± uncertainty. WWTP = wastewater treatment plants, CSO = combined sewer overflows. Net uptake is a sink for DSi and a source for RPSi. A positive value of net uptake indicates net assimilation of DSi to RPSi, and negative value for net uptake indicates net dissolution of RPSi to DSi. DSi sources are tributaries, Cootes' Paradise, WWTPs, CSOs, steel mill discharge, groundwater, precipitation, net dissolution, internal loading, and Lake Ontario (L. Ontario) inflow. DSi sinks are net uptake, steel mill withdrawal and Hamilton Harbour (H. H.) outflow. RPSi sources are tributaries, Cootes' Paradise, WWTPs, CSOs, steel mill discharge, net uptake, resuspension, and Lake Ontario (L. Ontario) inflow. RPSi sinks are net dissolution, steel mill withdrawal, sedimentation, burial and Hamilton Harbour (H. H.) outflow. Total sources and sinks of DSi and RPSi were not equal resulting in accumulation of DSi and depletion of RPSi in the water column.

Sources/Sinks	**Mean May to November Discharge (10^3 m^3 day^{-1})**	**Mean May to November Flux (10^3 moles day^{-1})**	
		DSi	**RPSi**
Watershed Fluxes			
Tributaries (F_1,F_8)	86.4 ± 13.5	5.5 ± 1.4	1.1 ± 0.5
Cootes' Paradise (F_2,F_9)	145.4 ± 36.5	8.3 ± 2.9	1.6 ± 0.6
WWTP (F_3,F_{10})	408.2 ± 4.1	24.7 ± 5.2	1.0 ± 0.2
CSO (F_4,F_{11})	13.2 ± 2.6	0.9 ± 0.9	0.3 ± 0.2
Net steel mill flux (F_5, F_{12})	0	0.7	0.4
Precipitation (F_6)	57.7 ± 9.8	0.2 ± 0.2	
Groundwater (F_7)	58.1 ± 29.1	10.6 ± 7.4	
Evaporation	54.2 ± 21.7		
Total Watershed Inputs		50.9	4.4
Internal Si Cycling			
Net uptake (F_{13})		38.0 ± 14.2	38.0 ± 14.2
Sedimentation (F_{14})			972.6 ± 301.5
Resuspension (F_{15})			929.8 ± 288.2
Internal loading (F_{16})		40.9 ± 16.3	
Burial (F_{17})			1.9
Harbour-Lake Exchange			
L. Ontario inflow (F_{18},F_{20})	4499.3 ± 510.7	38.7 ± 14.1	8.9 ± 4.2
H.H. outflow (F_{19},F_{21})	5214.1 ± 842.9	67.3 ± 24.3	19.6 ± 7.3
Net Transfer		-28.6	-10.7
Total External Inputs		89.6	13.3
Total External Outputs		67.3	19.6
Total Sources	5985.2 ± 713.9	140.9	983.9
Total Sinks	5985.4 ± 972.2	115.7	995.0
Water column accumulation/depletion		25.2	-11.1

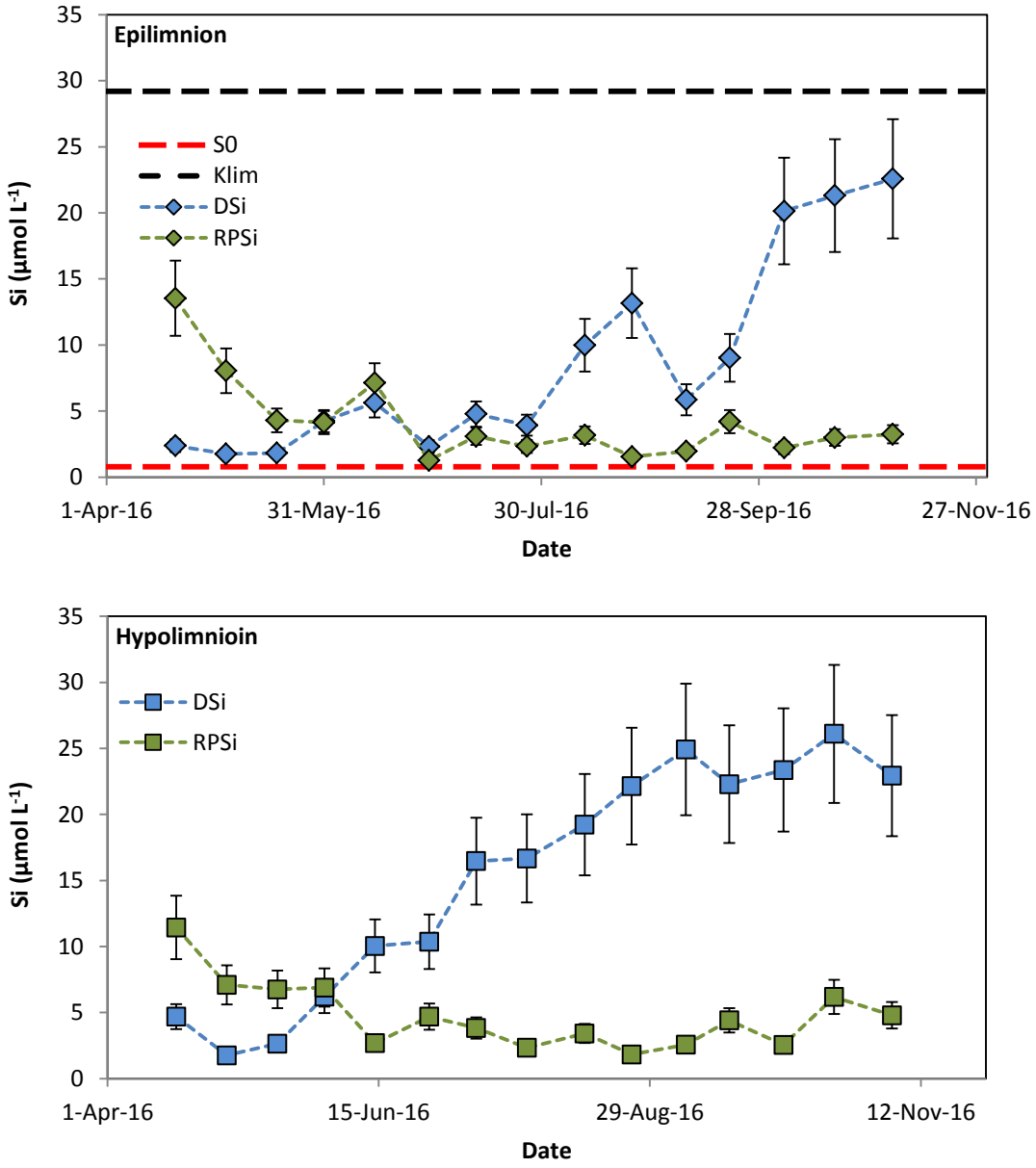

Figure 3.7. DSi and RPSi concentrations in measured in water samples collected from Hamilton Harbour from 1 m below the surface (epilimnion) and from 1 m above the sediment-water interface (hypolimnion) between April and November 2016. Error bars represent uncertainty associated with sample storage and analysis. Epilimnion DSi and RPSi concentrations are shown in relation to the S_0 and the K_{lim} DSi concentrations for the diatom *Asterionella formosa* (Tilman and Kilham, 1976). Below the K_{lim} concentration, diatom growth is controlled by Si availability and below the S_0 concentration no diatom growth occurs (Finenko and Krupatkina, 1974; Tilman and Kilham, 1976).

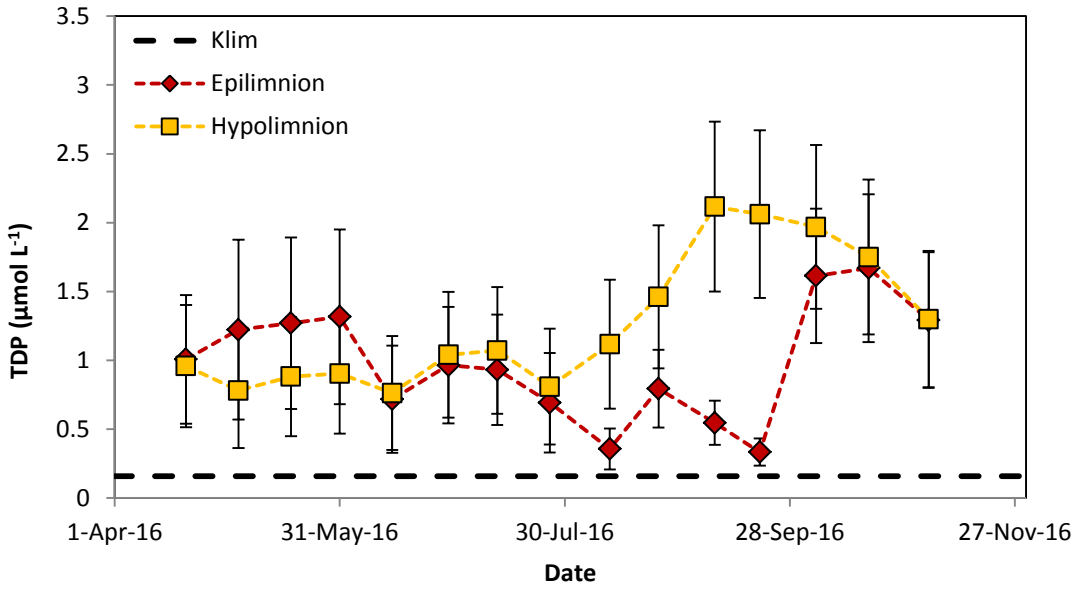

Figure 3.8. TDP concentrations in measured in water samples collected from Hamilton Harbour from 1 m below the surface (epilimnion) and from 1 m above the sediment-water interface (hypolimnion) between April and November 2016. Error bars represent uncertainty associated with sample collection, storage, and analysis. Epilimnion TDP concentrations are shown in relation to the K_{lim} P concentration for the diatom *Asterionella formosa*, below which diatom growth is controlled by P availability (Finenko and Krupatkina-Akinina, 1974; Tilman and Kilham, 1976).

total watershed DSi input (Table 3.3). Groundwater, Cootes' Paradise Marsh and tributaries contributed 21, 16 and 11% of the total DSi input from watershed sources, respectively (Table 3.3). The DSi flux discharging from the steel mill was slightly higher than that of the intake resulting in a net contribution of 0.7 x 10^3 moles day^{-1} Si (Table 3.3). DSi fluxes from the steel mill (net), CSOs, and precipitation were all minor DSi sources and relatively unimportant in the overall budget (Table 3.3). RPSi fluxes from the watershed were relatively minor compared to DSi fluxes and ranged from 0.3 x 10^3 moles day^{-1} to 1.6 x 10^3 moles day^{-1}, with the steel mill contributing a net flux of 0.4 x 10^3 moles day^{-1} (Table 3.3).

Exchanges with Lake Ontario constituted the largest external input and output of reactive Si for Hamilton Harbour. The input of DSi from Lake Ontario was estimated at 39 x 10^3 moles day^{-1} of DSi, that is, 43% of the total external DSi input, and 8.9 x 10^3 moles day^{-1} of RPSi, or 67% of the total external RPSi input (Table 3.3). Outflow from Hamilton Harbour to Lake Ontario removed 67 x 10^3 moles day^{-1} of DSi and 20 x 10^3 moles day^{-1} of RPSi. The net transfer of reactive Si from Hamilton Harbour to Lake Ontario thus consisted of 29 x 10^3 moles day^{-1} of DSi and 11 x 10^3 moles day^{-1} of RPSi (Table 3.3).

Only net DSi uptake fluxes are calculated, because the dissolution of RPSi in the water column could not be independently estimated. Uptake is a source of RPSi in the water column and dissolution a sink. Therefore, positive net uptake fluxes indicate that gross uptake exceeded gross dissolution, and vice versa. Negative net uptake will be referred to as net dissolution. Net uptake utilized approximately 42% of the total external DSi input to

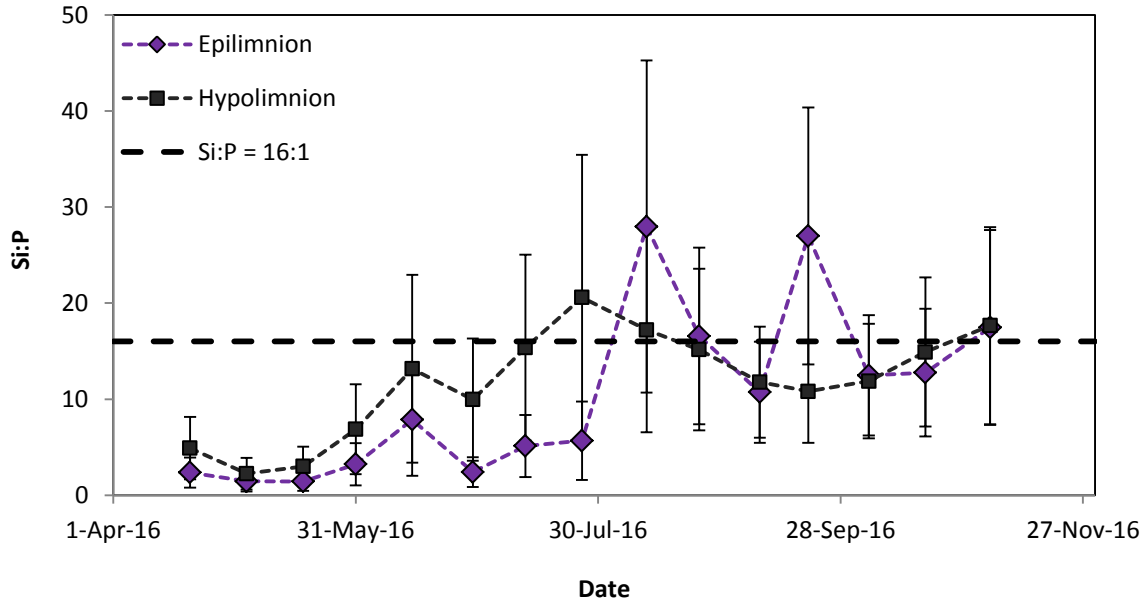

Figure 3.9. Si:P ratios calculated from DSi and TDP concentrations measured in water samples collected from Hamilton Harbour from 1 m below the surface (epilimnion) and from 1 m above the sediment-water interface (hypolimnion) between April and November 2016. Error bars represent uncertainty associated with sample collection, storage, and analysis for both Si and TDP. Si:P ratios are shown in relation to the idealized Redfield-Brzezinski ratios of nutrient uptake for marine diatoms (Redfield 1958; Brzezinski 1985).

Hamilton Harbour and transformed 38 x 10^3 moles day^{-1} of DSi to RPSi (Table 3.3). Net uptake was highest in May (146 x 10^3 moles day^{-1}) and decreased through June (69 x 10^3 moles day^{-1}) and July (38 x 10^3 moles day^{-1}) (Figure 3.10). Net dissolution was 38 x 10^3 moles day^{-1} in August and 60 x 10^3 moles day^{-1} in October (Figure 3.10). Net uptake was 42 x 10^3 moles day^{-1} in September and 71 x 10^3 moles day^{-1} in November (Figure 3.10).

Monthly gross sedimentation rates from the 4 sites across Hamilton Harbour are given in Appendix 1 Table 6. Average sedimentation and resuspension fluxes between May and November amounted to 973 x 10^3 moles day^{-1} and 930 x 10^3 moles day^{-1}, respectively (Table 3.3), indicating intense exchanges between the water column and bottom sediments. Net sedimentation, that is, sedimentation minus resuspension, therefore amounted to 43 x 10^3 moles day^{-1} RPSi (Table 3.3). Net sedimentation was highest in May (181 x 10^3 moles Si day^{-1}) and decreased through June (82 x 10^3 moles Si day^{-1}) and July (43 x 10^3 moles Si day^{-1}) (Figure 3.10). Net sedimentation was negative in August (-36 x 10^3 moles Si day^{-1}) and October (-67 x 10^3 moles Si day^{-1}) as resuspension exceeded sedimentation (Figure 3.10). Net sedimentation increased again to 29 x 10^3 moles Si day^{-1} in September and 69 x 10^3 moles Si day^{-1} in November (Figure 3.10).

The estimated internal loading of DSi from sediments was 41 x 10^3 moles day^{-1}, compared to the total external DSi input to Hamilton Harbour of 90 x 10^3 moles day^{-1} (Table 3.3). Internal loading was lowest in May (31 x 10^3 moles Si day^{-1}) and increased throughout the summer to a maximum in October (49 x 10^3 moles Si day^{-1}) (Figure 3.10). Internal loading decreased in November returning to a similar value as in May (Figure 3.10). Internal loading returned approximately 96% of net RPSi sedimentation back to the water column as DSi, while the

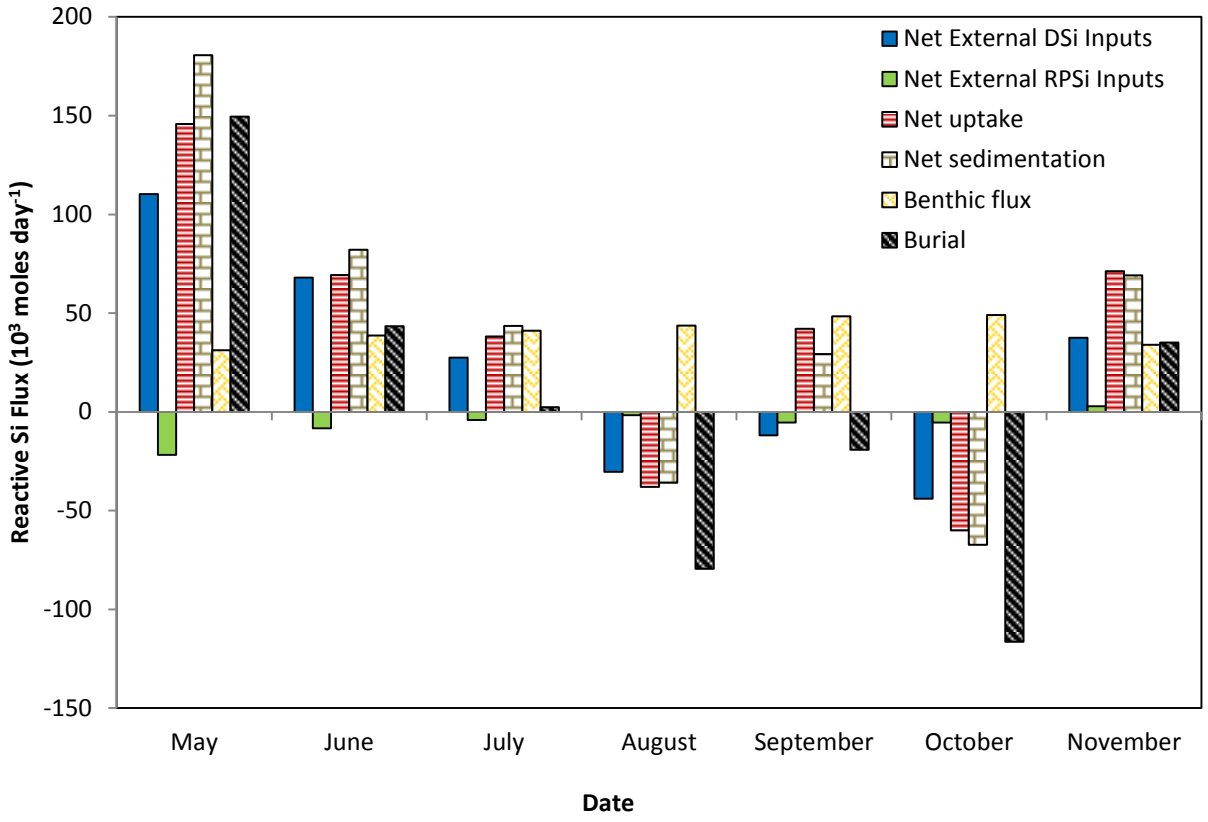

Figure 3.10. Monthly net external DSi and RPSi inputs and internal cycling fluxes. Net external DSi and RPSi inputs were calculated as the sum of watershed fluxes and inflow from Lake Ontario minus Hamilton Harbour outflow. Positive net external inputs indicate Hamilton Harbour was a net sink of DSi or RPSi, and negative net external inputs indicate Hamilton Harbour was a net source of DSi or RPSi. Net sedimentation was calculated as sedimentation minus resuspension. Positive values of net uptake indicate net uptake of DSi and negative values net dissolution of RPSi.

remaining 4% (1.9 x 10^3 moles day^{-1}) was buried (Table 3.3). Burial was greatest in May (150 x 10^3 moles day^{-1}) and decreased until July (Figure 3.10). In August and October negative burial fluxes were calculated, indicating that the internal loading of DSi from the sediments was being sustained by the dissolution from previously deposited RPSi (Figure 3.10). In September the burial flux was again positive (Figure 3.10).

3.3.4 Hamilton Harbour: Net source or sink of reactive Si?

Net external DSi and RPSi inputs to Hamilton Harbour were calculated as the sum of the external inputs from the watershed and Lake Ontario, minus the outputs associated with outflow to Lake Ontario. In May, June, July, and November, the external inputs of DSi exceeded the outputs, indicating that during these months Hamilton Harbour was a net DSi sink (positive net external DSi inputs on Figure 3.10). In August, September and October, the combined external DSi inputs were smaller than the output of DSi to Lake Ontario (negative net external DSi inputs on Figure 3.10) and, thus, Hamilton Harbour was a net DSi source. For RPSi, the external inputs were smaller than

the corresponding RPSi outputs to Lake Ontario in all months, except November (Figure 3.10). Integrated over the entire May to November period, Hamilton Harbour retained 4.8 x 10^6 moles DSi (25% of total DSi inputs) and 3.4 x 10^6 moles total reactive Si (DSi + RPSi) (16% of total reactive Si inputs). Over the same time period, the net export of RPSi to Lake Ontario was 1.4 x 10^6 moles.

3.4 Discussion

3.4.1 Watershed Si fluxes

Of the watershed reactive Si fluxes, WWTPs, Cootes' Paradise, groundwater, and tributaries were the largest, and CSOs, the net steel mill flux, and precipitation were relatively unimportant (Table 3.3). The DSi flux from WWTP effluent was the second largest external source of DSi and was more than double that of groundwater and all 3 tributaries (Table 3.3). This is similar to that found at the Deer Island Treatment Plant where the flux of DSi was greater than that of the 3 adjacent rivers combined (Maguire & Fulweiler 2017). Si in WWTP effluent comes from sewage, groundwater, and surface runoff (Maguire & Fulweiler 2016). Sources of DSi in sewage include laundry and dishwasher detergents as well as consumption of food (Sferratore et al., 2006). Detergents contain soluble silicates known as waterglass (Van Dokkum et al., 2004). WWTPs do not appear to remove DSi during the treatment process (Maguire & Fulweiler 2017).

Between November 2015 and November 2016, the annual average concentrations of DSi in WWTP effluent were 70.6 µmol L^{-1} from WWTP 1 and 72.3 µmol L^{-1} from WWTP 2, with an average Si:P ratio of 34.1 from WWTP 1 and 16.5 from WWTP 2. This DSi concentration is lower than the Deer Island Treatment Plant in the U.S. and the Acheres Wastewater Treatment Plant in France, where DSi concentrations in the range 138-177 µmol L^{-1} were measured (Maguire & Fulweiler, 2016, 2017; Sferratore et al. 2006). The annual average Si:P ratio of effluent from the Deer Island Treatment Plant was 37.2, which is similar to that found here (Maguire & Fulweiler 2017). However Si:P ratios in that study were calculated using dissolved inorganic P (DIP) and thus are not directly comparable to the Si:P ratios reported here calculated using TDP.

Few studies have measured DSi and RPSi concentrations in WWTP effluent and this source is just beginning to be recognized as a potentially important anthropogenic effect on the global Si cycle (Sferratore et al. 2006; Maguire & Fulweiler 2016; Maguire & Fulweiler 2017). Wastewater is likely to become an even more important source of Si in the future as volumes of wastewater discharging from concentrated areas are predicted to increase with population growth (Carey & Migliaccio, 2009 and references therein). However, the effects that WWTP effluent may have on the concentrations and ratios of nutrients in the receiving water bodies is unclear.

Compared to rivers, WWTPs discharge a substantially higher volume of water that has higher Si and P concentrations and lower Si:P ratios (Maguire & Fulweiler 2017; Carey & Migliaccio 2009). Thus, WWTP effluent may exert a much greater influence on the chemical composition of the receiving water body than tributaries, and relatively low Si:P ratios in WWTP effluent may cause a shift towards Si limitation. However, this effect was not observed in Massachusetts Bay where plumes of DSi, dissolved inorganic N, and DIP were found to extend 2.7 km, 10.1 km, and 3.8 km away from the effluent discharge site of the Deer Island Treatment Plant, but no differences in

Si:P or Si:N ratios were observed outside of the immediate area above the WWTP diffuser (Maguire & Fulweiler 2017). As well, since the opening of the effluent diffusers in 2000, there have been no significant changes to phytoplankton biomass or composition in Massachusetts Bay despite nutrient loading from the WWTP (Maguire & Fulweiler 2017). In Hamilton Harbour, the impact of WWTP effluent on DSi and TDP concentrations and ratios in the water column may be minimal due to the flushing and "short circuiting" action of exchange with Lake Ontario that prevents substantial migration of effluent plumes into the harbour (Barica 1989). Therefore, while there is potential for WWTP effluent to be an important factor influencing Si:P ratios and phytoplankton community composition in a receiving water body, this may only occur under certain conditions. The impact of WWTP effluent may be extremely isolated and is likely influenced by the size, circulation patterns, and water exchanges of a given water body (Maguire & Fulweiler 2017).

3.4.2 Si cycling within Hamilton Harbour water column and sediments

The timing of peak uptake rates in the spring (146 x 10^3 moles day^{-1} in April and 69 x 10^3 moles day^{-1} in May) and fall (42 x 10^3 moles day^{-1} in September) coincide with the spring and fall diatom blooms that regularly occur in Hamilton Harbour (Figure 3.10) (Dermott et al. 2007; Munawar et al. 2017). Extrapolating the May to November average net uptake rate of 38 x 10^3 moles day^{-1} (Table 3.3) to the entire year, diatoms assimilated approximately 0.6 moles Si m^{-2} yr^{-1} on per area basis. This value is likely an underestimate of gross uptake as concurrent dissolution of RPSi in the water column may have supported higher uptake. Nriagu (1978) estimated that approximately 90% of the BSi pool in the water column dissolved before reaching the sediments in Lake Ontario. If this were the case in Hamilton Harbour, gross uptake may have been as much as 6 moles Si m^{-2} yr^{-1} or 380 x 10^3 moles day^{-1}. Therefore, an estimate of gross DSi uptake in Hamilton Harbour is in the range of 0.6-6 moles Si m^{-2} yr^{-1}. The low end of this range is similar to that found in oligotrophic Lake Superior (0.3-0.6 moles Si m^{-2} yr^{-1}) and the mean for the global ocean (0.6-0.8 moles Si m^{-2} yr^{-1}), and is lower than that found for mesotrophic to eutrophic Lake Michigan (1.4-1.8 moles Si m^{-2} yr^{-1}) (Nelson et al., 1995; Parker et al., 1977; Schelske, 1985). The upper end of the range is lower than the global mean uptake for coastal upwelling areas (8.3 moles Si m^{-2} yr^{-1}) (Nelson et al., 1995). Thus, estimated uptake rates in Hamilton Harbour match reasonably well to a range of environments despite being extremely eutrophic, which may be due to Si limitation in the water column limiting uptake rates.

DSi internal loading was calculated from sediment core incubation experiments, which is a widely used technique (Beutel, 2006; Conley et al., 1997; Conley et al., 1988; Cowan & Boynton, 1996; Denis & Grenz, 2003; Heinen & McManus, 2004; Lehrter et al., 2012; Spears et al., 2008; Srithongouthai et al., 2003). The internal loading DSi flux was calculated as a function of temperature, which strongly influences BSi dissolution and sediment Si release rates (Gibson et al., 2000; Kamatani, 1982; Srithongouthai et al., 2003). The fluxes obtained were within the range of published values for other freshwater lakes and marine coastal areas using similar methods (Conley et al., 1997; Cowan & Boynton, 1996; Denis & Grenz, 2003; Heinen & McManus, 2004; Lehrter et al., 2012; Srithongouthai et al., 2003).

Internal loading recycles Si deposited to sediments back to the water column and is therefore ultimately dependent on external nutrient loads. Internal loading of DSi from sediment was the largest DSi flux into the water

column of Hamilton Harbour and is likely important for sustaining diatom growth. Internal recycling of Si through dissolution of particulate Si in the water column and internal loading of Si from sediments have been found to be a substantial Si source important for sustaining diatom growth across a wide variety of freshwater lakes and marine coastal areas across many continents and oceans (Cornwell & Banahan, 1992; Johnson & Eisenreich, 1978; Nriagu, 1978; Schelske et al., 1983; Schelske, 1985; Schelske et al., 1986; Miretzky & Cirelli, 2004; Bailey-Watts, 1976; Gibson et al., 2000; Bootsma et al., 2003; Degobbis et al., 1990; Savchuk, 2002; Singh et al., 2015; D'Elia et al., 1983). In Chesapeake Bay, the sediment Si flux exceeded the total riverine input by a factor of at least 5 (D'Elia et al. 1983), which is similar to the present work where internal loading was approximately 7 times larger than tributary inputs. Internal loading can exceed tributary inputs because tributaries are not always the main external source of Si. In Hamilton Harbour, Si inputs from exchange with Lake Ontario, WWTP effluent, and inflow from Cootes' Paradise were all larger than that contributed by tributaries.

Approximately 96% of gross sedimentation was resuspended in the water column (Table 3.3). High resuspension fluxes in Hamilton Harbour are enabled by wind-induced mixing and exchange with Lake Ontario that create vertical instability, and lead to high suspended matter concentrations (Barica, 1989; Haffner et al., 1983). Similarly high resuspension fluxes have been found in Lake Erie, where resuspended sediments constituted between 76% and 90% of the catch in the bottom sediment trap (Bloesch 1982), and in nearshore Lake Ontario, where resuspension was about 85% of total sedimentation (Rosa 1985). The mean net sedimentation rate between May and November was approximately 0.04 g cm^{-2} $year^{-1}$, which is comparable to rates reported for Hamilton Harbour by Mayer & Johnson (1994) (0.038-0.097 g cm^{-2} $year^{-1}$) and Rukavina & Versteeg (1996) (0.067-0.222 g cm^{-2} $year^{-1}$).

Net uptake and net sedimentation fluxes were of similar magnitudes and followed similar trends between May and November, indicating that the diatom frustules that did not dissolve in the water column sank to the sediments (Figure 3.10). However, due to the high recycling efficiency at the sediment-water interface, relatively little RPSi, approximately 1.6 % of total reactive Si inputs or 0.03 moles m^{-2} yr^{-1}, was permanently buried in the sediments.

3.4.3 Harbour-lake exchange

The overall net effect of exchange between Hamilton Harbour and Lake Ontario over the period May to November 2016 was removal of DSi and RPSi from Hamilton Harbour. The flux of Si from Hamilton Harbour to Lake Ontario was almost double that of inflow from Lake Ontario, making Hamilton Harbour an overall net source of reactive Si to Lake Ontario (Table 3.3). The impact of Lake Ontario on Hamilton Harbour is thought to be largely beneficial through providing oxygen to the hypolimnion and diluting concentrations of pollutants and nutrients (Barica 1989). However, this also acts to dilute concentrations of Si which are already in low supply. In contrast, the impact of Hamilton Harbour on Lake Ontario has received little attention. As a net source of Si, Hamilton Harbour may be contributing to the observed increase in spring surface water Si concentrations in offshore areas of Lake Ontario since the 1990s (Dove 2009).

3.4.4 Hamilton Harbour: Net source or sink of reactive Si?

Hamilton Harbour retained approximately 25% of external DSi inputs, thereby acting as a net sink of DSi and decreasing the flux of DSi from the watershed to Lake Ontario. This retention is within the range of estimated global DSi retention by lakes and reservoirs (21-27%) (Frings et al. 2014). However, Hamilton Harbour was a net source of RPSi relative to external inputs. The DSi:RPSi ratio of watershed reactive Si inputs to Hamilton Harbour was 11.6 while the DSi:RPSi ratio of outflow to Lake Ontario was 3.5. Thus, some of the DSi retained was in fact exported as RPSi and the total reactive Si retention in Hamilton Harbour was 16%. This highlights the importance of considering both DSi and RPSi reactive forms in Si budgets as retention of DSi does not necessarily equate to retention of total reactive Si.

While Hamilton Harbour was an overall net sink of reactive Si between May and November, Hamilton Harbour was a source of reactive Si in some months (i.e. August, September, and October). The fate of Si in Hamilton Harbour was largely influenced by the amount of uptake of DSi and subsequent sedimentation of RPSi. In the spring when uptake was high, DSi was assimilated and retained in Hamilton Harbour as RPSi. In the summer, when uptake was low or net dissolution was occurring, DSi was not assimilated or retained. Consequently, more DSi was exported to Lake Ontario. Therefore, the internal cycling of Si largely dictates the fate of Si in the water column and whether it will be retained or exported downstream.

Nriagu (1978) calculated a DSi mass balance budget for Lake Ontario where total DSi inflow was estimated to be 12.32×10^7 kg yr^{-1} and total outflow 5.83×10^7 kg yr^{-1}. From this, net retention of DSi in Lake Ontario is estimated to be 6.49×10^7 kg yr^{-1}. Using the surface area of Lake Ontario (18,960 km^2), this converts to a per area average DSi retention of 5.7×10^4 moles km^{-2} yr^{-1}. The per area average DSi retention in Hamilton Harbour between May and November 2016 is calculated to be approximately 38×10^4 moles km^{-2} yr^{-1}. Therefore, retention of DSi in Hamilton Harbour is approximately 6-7 times higher than the per area average for all of Lake Ontario, indicating that Si retention may be focused in nearshore areas. This is likely due to the higher nutrient inputs received by the nearshore zone stimulating biological activity, DSi uptake and RPSi burial. This is in agreement with our current understanding of Si cycling in marine coastal zones, which act as nutrient sinks and hot spots for biogeochemical cycling (Laruelle et al. 2009; Mackenzie et al. 2000; Jickells 1998).

3.4.5 Si limited diatom growth in Hamilton Harbour

The relative and absolute concentrations of DSi and TDP in the water column of Hamilton Harbour indicate stoichiometric and possible physiological Si limitation of diatom growth. Epilimnetic and hypolimnetic Si:P ratios were below the idealized Redfield-Brzezinski ratio of 16:1 throughout most April to November 2016 (Figure 3.9). Si:P ratios were particularly low in the spring and early summer when the highest diatom uptake of DSi was predicted (Figures 3.9 and 3.10). The Si:P ratio of 16:1 is based on the typical nutrient composition of marine diatoms under non-limiting nutrient conditions (Brzezinski 1985; Redfield 1958). However, this may not accurately

represent the nutrient requirements of freshwater diatoms as Si content has been found to vary between marine and freshwater species(Conley & Kilham 1989).

Stoichiometric Si limitation does not necessarily imply physiological limitation as DSi may still be replete in the water column. However, physiological limitation of diatom growth was indicated by severely depleted epilimnetic DSi concentrations in the spring and early summer of 2016. In Figure 3.7, Hamilton Harbour epilimnetic DSi concentrations are shown in relation to the K_{lim} and S_0 DSi concentrations for the diatom *Asterionella formosa* (Tilman & Kilham 1976), which is a consistent member of the diatom community in Hamilton Harbour (Dermott et al. 2007; Munawar et al. 2017). The K_{lim} concentration is the concentration at which the rate of cell division is 90% of maximal and therefore the division rate is limited by Si bioavailability below this concentration (Finenko and Krupatkina-Akinina 1974; Tilman & Kilham 1976). The S_0 concentration is the minimum DSi concentration needed for growth and therefore growth is inhibited below this concentration (Tilman and Kilham 1976). Epilimnetic DSi concentrations were consistently below the K_{lim} concentration of 29.2 µmol L^{-1} DSi from April to November and approached the S_0 concentration of 0.78 µmol L^{-1} DSi in the spring (Figure 3.7). This suggests that diatom growth was regulated by DSi bioavailability and that low DSi concentrations may have terminated the spring bloom. Si limitation of diatom growth also agrees with the observation of relatively low Si uptake rates considering the eutrophic status of Hamilton Harbour. However, it should be noted that other factors such as turbulence, light, temperature and zooplankton grazing may also have influenced diatom growth (Willen 1991). Hamilton Harbour has an unusually high abundance of zooplankton compared to other eutrophic embayment's, which this is likely due to high primary productivity particularly of edible and nutritious phytoplankton including some species of flagellates, green algae, and diatoms (Bowen and Currie 2017).

In addition, TDP concentrations were consistently above the K_{lim} concentration of P for *A. formosa* between April and November suggesting that diatom growth was not regulated by P bioavailability (Figure 3.8). Diatom growth did not deplete TDP concentrations in the spring and TDP concentrations remained detectable and above the K_{lim} concentration even in the late summer when peak biomass in Hamilton Harbour typically occurs (Figure 3.8) (Dermott et al. 2007; Munawar et al. 2017). Thus, P was likely available in excess to diatoms and potentially all phytoplankton in 2016.

The main strategy to decrease algal blooms in Hamilton Harbour is to decrease P concentrations, which is based on the assumption that total phytoplankton growth is P limited (Hiriart-Baer et al., 2009). However, our data suggest that diatom growth was Si limited and that P is in such excess that the growth of non-siliceous phytoplankton may not have been limited by P. Analysis of two decades of water quality trends revealed that P limitation of phytoplankton growth only occurs when other factors, such as light availability and high growth rates supported by elevated temperatures, cause P demand to be greater than supply (Hiriart-Baer et al. 2009). Otherwise, P is sufficient in the water column and does not control growth rates, which is in agreement with our finding (Hiriart-Baer et al. 2009).

The Si and P K_{lim} and Si S_0 concentrations of *A. formosa* may not be directly applicable to the entire diatom community as the concentrations vary between diatom species (Tilman and Kilham 1976; Kilham 1975; Willen 1991). However, S_0 is generally in the range of 1-6.6 µmol DSi L^{-1} for freshwater and marine diatoms

(Willen 1991 and references therein), and growth inhibiting concentrations determined under culture conditions are generally lower than concentrations that would inhibit growth in nature (Kilham 1975; Tilman and Kilham 1976). Therefore, it is reasonable that the DSi concentrations measured here were physiologically limiting and potentially inhibiting to spring diatom growth in Hamilton Harbour.

3.4.6 Implications of Si limitation in nearshore zones of lakes and oceans

Areas of freshwater and marine aquatic environments may be moving towards Si limitation as changes to nutrient stoichiometry and shifts in phytoplankton community composition towards non-siliceous species have been observed in numerous rivers, lakes, reservoirs, and areas of the coastal and open ocean (Conley and Malone, 1992; Danielsson et al., 2008; Glibert et al., 1995; Humborg et al., 2000; Justic et al., 1995; Justic et al., 1995; Kling et al., 2011; Li et al., 2007; Rocha et al., 2002; Turner et al., 2003; Viaroli et al., 2013). Phytoplankton communities dominated by flagellates or cyanobacteria can lead to changes in food web structure and less efficient energy transfer to higher trophic levels (Moss et al. 1991; Officer and Ryther 1980; Sommer et al. 2002). Si limitation may also lead to higher incidence of toxic diatom blooms. Parsons et al. (2002) found the relative abundance of toxic *Pseudo-nitzchia* species in sediment cores taken from the Gulf of Mexico near the Mississippi River plume were positively correlated to Mississippi River nitrate fluxes and negatively correlated to the Mississippi River Si:N ratios. This indicates that *Pseudo-nitzchia* species may be stimulated more than other diatom species under high N and low Si conditions, leading to harmful diatom blooms (Parsons et al. 2002). Further, the negative effects of Si limitation may be exacerbated with warming temperatures and acidification as is expected to occur in the future due to climate change (Calbet et al. 2014).

Nearshore zones of lakes and the ocean can act as nutrient sinks of Si (Laruelle et al. 2009; Mackenzie et al. 2000; Strayer and Findlay 2010). Severe DSi depletion in nearshore zones due to Si limitation may result in negative consequences at the local scale and may cause or enhance Si limitation downstream through decreased DSi exports. Thus, nearshore zones of lakes experiencing eutrophication may be critical areas to focus remediation efforts as the effects of Si limitation may cascade and magnify further downstream.

Recovery from Si limitation appears possible upon reduction of P concentrations and increasing the Si:P ratio (Barbiero et al. 2002; Gaedke & Schweizer 1993; Krivtsov et al. 2000). Upon P reductions in Lake Michigan and Lake Constance, increases in diatoms and DSi concentrations were observed (Barbiero et al., 2002; Gaedke and Schweizer, 1993). A different approach to combating Si limitation and eutrophication could be to enhance P uptake by diatoms in the spring through addition of Si, which would reduce the P available for non-siliceous algae in the summer (Krivtsov et al., 2000). In a modelling exercise assuming Si limitation of diatoms in spring and P limitation of cyanobacteria in the summer, Krivtsov et al. (2000) found that increasing winter Si concentrations led to a larger spring diatom bloom and a lower summer cyanobacteria bloom. This was because increased Si availability enabled higher diatom growth and greater assimilation of P from the water column, leaving less P available for cyanobacteria growth in the summer (Krivtsov et al., 2000). This inverse relationship between the sizes of diatom and cyanobacteria blooms was observed in the Saidenback reservoir where P limited diatom growth resulted in depletion of water column P and a small or absent cyanobacteria bloom, and Si limited diatom growth

was unable to deplete water column P, resulting in a smaller diatom and a larger cyanobacteria bloom (Horn and Uhlmann 1995). This pattern was qualitatively observed in Hamilton Harbour where relatively high spring diatom biomass in 2002 was followed by relatively low summer cyanobacteria and total phytoplankton biomass, and relatively low spring diatom biomass in 2006 was followed by relatively high summer cyanobacteria and total phytoplankton biomass (Munawar et al. 2017). Through manipulating this inverse relationship, augmenting water bodies with Si may be able to shift peak phytoplankton biomass from the summer to the spring and thereby limit or eliminate the growth of potentially harmful algal species (Krivtsov et al. 2000).

However, the addition of Si as a remediation strategy may have several negative consequences. Greater diatom growth in the spring will deliver a larger supply of organic matter to the sediments, which may increase biological oxygen demand and drive anoxic conditions at the sediment-water interface. This may result in a release of P bound to iron oxides in the sediment, which may counteract the benefits of P drawdown in the water column. In addition, Krivtsov et al. (2000) note that increased Si in the water column may lead to release of phosphate bound to Al through competitive binding of Si. Therefore, P removal by means of Si addition is likely to be most effective in lakes that have relatively low levels of Al-bound phosphates (Krivtsov et al., 2000). Thus, while Si addition remains an interesting and potentially effective remediation strategy, it may only be beneficial under certain conditions.

3.4.7 Model limitations and considerations

The assumption of complete mixing of all reactive Si inputs and the water column was made for simplification but is likely unrepresentative of the environmental conditions. Hamilton Harbour thermally stratifies between May and October, which prevents complete mixing of water at the surface and at depth (Hamblin & He 2003). Reactive Si inputs likely have a greater influence in the vicinity of their discharge points rather than the whole of Hamilton Harbour (Barica 1989; Maguire and Fulweiler 2017). As well, exchange with Lake Ontario may prevent mixing of reactive Si inputs that enter near the BSC such as discharge from WWTP (Barica 1989). This occurs through a “short-circuiting” action as water from these sources are removed from the harbour before it gets completely mixed (Barica 1989).

Further, lack of data and inability to collect samples during the winter months prevented the establishment of a full annual Si budget. Si biogeochemistry in lakes over the winter period is a time we know relatively little about yet studies have shown that diatoms can continue to grow over winter in the North American Great Lakes (Burns et al., 1978). Therefore, future endeavors should plan to incorporate winter sampling in order to get the full picture of Si cycling over the year and capture winter and early spring diatom growth.

Finally, it should be noted that measurement of TDP in the water column of Hamilton Harbour likely overestimated the immediately bioavailable P to phytoplankton (Bostrom et al. 1988). TDP includes both SRP and dissolved organic P (DOP). SRP is the most directly available P source for phytoplankton (Bostrom et al. 1988). However, some DOP fractions may also be bioavailable (Bostrom et al. 1988; Qin et al. 2015). In bioassay experiments, algae grown for 14 days with DOP from the effluent of two wastewater treatment plants indicated that approximately 75% of DOP was potentially bioavailable (Qin et al. 2015). Therefore, while SRP indicates the minimum immediately bioavailable P, TDP may be more representative of the potentially bioavailable P (Bostrom

et al. 1988; Qin et al. 2015). Further, particulate P was not measured but may also contribute bioavailable P through desorption, dissolution and degradation of particulate matter (Bostrom et al. 1988).

3.5 Conclusion

A reactive Si budget was established for Hamilton Harbour between May and November 2016. The budget showed that internal loading of DSi from sediments, exchange with Lake Ontario, and WWTPs were the largest DSi fluxes to the Hamilton Harbour water column, which is in contrast to the widely held assumption that watershed sources such as tributaries and groundwater are the major contributions of reactive Si to lakes. Hamilton Harbour was a net sink of reactive Si over May to November 2016, but became a net source of reactive Si during periods of limited/no diatom growth showing that biological assimilation was a large control on the fate of reactive Si. RPSi was efficiently recycled at the sediment-water interface leading to low burial rates of only 1.6 % of total reactive Si inputs. This research showed that diatom growth in Hamilton Harbour is stoichiometrically and likely physiologically Si limited, which is in contradiction to the assumption of P limitation. Si limitation may be exacerbating the negative effects of eutrophication in Hamilton Harbour and other coastal freshwater and marine areas by shifting phytoplankton community composition in favour of non-siliceous algae.

Chapter 4

General Conclusions and Recommendations

4.1 Summary of key findings

This thesis examined the biogeochemical cycling of Si in a human impacted nearshore environment, using the Hamilton Harbour Area of Concern as a case study. In Chapter 2, mechanisms of internal loading of P and Si from Cootes' Paradise sediments were tested through sediment core flow through systems under oxic and anoxic conditions and with different nutrient (P, Si) additions. This study demonstrated that both P and Si are associated with reactive iron (Fe) phases in sediments but that P and Si behave differently under oxic and anoxic conditions. There was net retention of P under oxic conditions and net release under anoxic conditions, with anoxic P release being approximately 8 times that of oxic P release. P retention and release appeared to be dominated by sorption to Fe(III) oxides under oxic conditions and release from Fe(III) oxides under anoxic conditions due to reductive dissolution. However, there was net release of Si under both oxic and anoxic conditions, and anoxic release of Si increased by only 1.4 times. Thus, other potentially bioavailable Si pools in sediment, which are ostensibly not redox sensitive such as BSi, may have been a greater contribution to DSi release from sediments than retention and release from Fe(III) oxides. The different mechanisms governing release of P and Si lead to high Si:P ratios of release under oxic and low Si:P ratios of release under anoxic conditions relative to the nutrient requirements for diatom growth (Redfield 1958; Brzezinski 1985). This is the first laboratory study to compare the release of P and Si from intact sediment cores under oxic and anoxic conditions, and show decoupling of P and Si cycles. P was found to outcompete Si sorption sites, which is consistent with our knowledge of the effects of Si concentration and pH on competitive sorption, with Si only being able to outcompete P at high concentrations and high pH (>9) (Brinkman 1993; Koski-Vähälä et al. 2001; Tallberg et al. 2008). In areas where sediments are a major source of nutrients to the water column, nutrient stoichiometry of internal loading may drive nutrient dynamics in the water column through promoting P limitation or Si limitation of diatom growth. Understanding the behaviour of the cycling of Si and P in sediments under variable redox conditions may be critical to the development of effective remediation strategies and determining how nutrient cycling in sediments may change due to eutrophication induced hypoxia (Rabalais et al. 2010).

In Chapter 3, the biogeochemical cycling of reactive Si in Hamilton Harbour was explored through the development of a reactive Si mass balance budget. The results demonstrated that Hamilton Harbour was a net sink of reactive Si between May and November 2016, retaining 16% of total reactive Si inputs from external sources. The retention of Si was strongly controlled by biological uptake of DSi and recycling of BSi at the sediment water interface, with lower retention occurring in months with lower DSi uptake or higher recycling rates. This finding is in agreement with studies demonstrating net retention of Si in freshwater lakes and reservoirs and in marine coastal zones (Frings et al. 2014; Maavara et al. 2014; Taylor Maavara et al. 2015; Laruelle et al. 2009). This study also demonstrated that Si was stoichiometrically and likely physiologically limiting to diatom growth with respect to P in Hamilton Harbour, which is in contrast to the assumption of P limited phytoplankton growth (Hiriart-Baer et al. 2009). This is in agreement with studies showing Si limitation of coastal nearshore zones following nutrient enrichment, but is one of the first studies to show Si limitation in the nearshore zone of a large lake (Schelske & Stoermer 1971; Schelske & Stoermer 1972; Schelske et al. 1986; Conley & Malone 1992; Chauvaud et al. 2000; D

Justic et al. 1995; Dubravko Justic et al. 1995; Rocha et al. 2002; Gobler et al. 2006; Danielsson et al. 2008; Garnier et al. 2002; Peeters et al. 1991).

4.2 Research limitations

In chapter 2, the increased temperature inside the anaerobic chamber relative to the lab bench resulted in anoxic reactors being incubated at approximately 30°C and the oxic at approximately 22°C. Temperature can alter nutrient fluxes across the sediment-water interface and therefore incubation temperature was a confounding variable in the study design (Kamatani 1982; Srithongouthai et al. 2003; Kelton & Chow-Fraser 2005; Zhou et al. 2016; Duan & Kaushal 2013). Anoxic reactors were incubated inside the anaerobic chamber to ensure anoxic conditions at the sediment-water interface and of the outflow solutions being collected, which would have been difficult to achieve and maintain on the lab bench. While N_2 gas could have been used to make the sediment-water interface anoxic, there did not seem a feasible way to prevent oxidation of the outflow solutions being continuously collected. Oxidation of the outflowing solutions likely would have drastically altered the results through oxidation and precipitation of Fe(III) and potentially coprecipitation and/or adsorption of other dissolves constituents with Fe(III). The achievement of oxic and anoxic conditions at the sediment-water interface was critical to answering our research questions and therefore was prioritized. The extent of the temperature differential between the interior and exterior of the chamber was only discovered during the course of the experiment. Given the sensitivity of nutrient fluxes to temperature, future experiments should ensure temperature control and consistency between treatments. This could be achieved through the use of an environmental chamber or perhaps a water bath.

A second limitation encountered in the sediment core flow through experiment was a lack of replicate sediment cores in order to assess the reproducibility of the results and if differences between nutrient treatments were significant or simply natural variability in elemental composition, microbial activity and benthic bioturbation potentially causing differences in solute transport (Andersson et al. 1988). The study design involved 8 different nutrient treatments. Set-up, maintenance, sample collection and sample analysis in a timely fashion from 8 flow-through reactors was challenging for 1 person. Having more than 8 reactors would have required substantial additional human resources. However, if this experiment were to be repeated, replicate samples should be incorporated. This could be achieved through collaboration between several people to work on the experiment planned ahead of time in order to maximize the data that comes out of it.

In chapter 3, a lack of DSi and BSi data from November 2015 through March 2016 prevented the establishment of an annual reactive Si budget, and winter Si dynamics are a missing piece of the story. Collaboration with Environment and Climate Change Canada enabled sample collection from Hamilton Harbour between April and November 2016, for which we are grateful as sample collection would not have been feasible without their assistance. Winter sampling is not a routine practice for Environment and Climate Change Canada due to safety concerns and as such, no samples were collected during the winter months. Further, there are no historical Si data from these months available to estimate DSi and BSi concentrations or suspended sediment deposition. Consequently, the reactive Si budget had to be restricted to May to November 2016. However, the winter Si budget may be an important period of the year as phytoplankton growth can persist over the winter (Burns et al. 1978;

Pernica et al. 2017). Therefore, in the future, efforts to collect samples over winter should be made. This would likely require planning with an organization such as Environment and Climate Change Canada well in advance, but may be subject to funds available and weather conditions. Thus, winter sampling will likely continue to be a challenge, but little is known about Si cycling during this time of year, and therefore effort should be made to include these months if possible.

Year to year variability of DSi and BSi fluxes were unable to be evaluated in the Hamilton Harbour reactive Si budget due to a lack of data and the time restrictions of a Master of Science degree (2 years). DSi is not frequently measured in monitoring programs or by WWTP or industry, and RPSi has rarely been measured in mass balance studies. Therefore, the 1 year data set established here is the first for the Hamilton Harbour region, and one of the few globally to include both DSi and RPSi species. Due to the amount of laboratory work necessary to analyse samples for DSi and RPSi, sample collection could not be extended past November 2016. However, routine monitoring, for example once per month, of freshwater bodies including rivers, wetlands, and lakes, and measurement of both DSi and RPSi would greatly increase our ability to evaluate the temporal variability of Si cycling in nearshore areas such as Hamilton Harbour. As well, the establishment of a longer time series of data would enable evaluation of trends and changes in Si cycling over time, which is an important aspect of remediation.

4.3 Recommendations for future research and concluding remarks

The effect of anoxia on release of Si from sediment is still an underdeveloped area of research that warrants further investigation. While anoxic conditions have been shown in increase P internal loading in a many sedimentary environments (Orihel et al. 2017), the effect of anoxia on Si release from sediments is still not well established (Siipola et al. 2016; Lehtimäki et al. 2016). There are several potentially bioavailable pools of Si in sediment that may be mobilized under different environmental conditions, and therefore the relative importance of each bioavailable Si pool may change under different environmental conditions (Kamatani 1982; Loucaides et al. 2008b; Lehtimäki et al. 2016; Siipola et al. 2016). Research is needed on how environmental variables such as temperature, redox, pH and ionic strength influence the release of Si from redox sensitive phases, and the relative importance of release of Fe-bound Si compared to BSi at different temperatures, redox, pH and ionic strength conditions. This knowledge may be important for understanding how nutrient cycling in sediments may change with increasing temperatures due to climate change (Zhou et al. 2016; Duan & Kaushal 2013) and increasing hypoxic areas (Rabalais et al. 2010).

Studies investigating competitive sorption between P and Si have had mixed results and suggest that Si may only have a significant impact on P release under high concentrations and/or high pH (Koski-Vähälä et al. 2001; Tallberg et al. 2008). Future studies could investigate if there are threshold Si concentrations or pH at which point the system tips to Si being the better competitor for sorption sites. Studies in clean systems using pure mineral phases are needed to better understand the mechanisms of competitive sorption between P and Si. As well, experiments determining whether competition between P and Si for sorption sites is likely to affect P and Si internal loading in an environmentally relevant setup are needed. Further, as efforts to reduce external nutrient loads

continue, the influence of internal loading of legacy P and Si under oxic and anoxic conditions on water column phytoplankton community composition would also be interesting and relevant to investigate.

Si limitation may be occurring in other eutrophic areas of the Laurentian Great Lakes or other large lakes. Si limitation may enhance Si retention due to excess P and may therefore even further reduce Si delivery downstream or offshore relative to the degree of natural retention in these areas. Thus, the effects of Si limitation on Si retention and export in eutrophic areas should be investigated. Further, Si addition as a remediation strategy should be tested in longer term (months) laboratory, mesocosm, and whole lake experiments to see how Si addition effects phytoplankton community composition, seasonal succession, deposition of organic matter in the sediments, and oxygenation of the sediment-water interface over time.

In northern temperate lakes, winter may be an important time of year for Si cycling and should be further investigated. Little is known about Si cycling during the winter months but some studies have found diatom growth to persist through the winter (Burns et al. 1978) and Si limitation may shift diatom growth towards the winter (Stoermer 1993). Winter diatom growth may lead to greater RPSi burial due to low water temperatures and therefore lower RPSi dissolution and recycling rates at the sediment-water interface.

This research has demonstrated that freshwater nearshore zones such as coastal wetlands and embayment's are important areas of nutrient cycling that can alter nutrient fluxes from the watershed to the open lake. Sediments may act as a source or a sink of Si and P under different redox conditions, which can potentially drive diatom dominated or non-diatom dominated phytoplankton growth and nutrient dynamics in the water column. Human activities exert enormous pressure on nearshore zones through nutrient loading, which can alter the Si biogeochemical cycle. Eutrophication can lead to Si limitation of diatom growth, which may enhance the proliferation of harmful algal blooms. Further, Si limitation in the nearshore may enhance Si retention, decreasing Si exports offshore and downstream, which may potentially affect nutrient cycling in the coastal ocean. Understanding Si cycling and the interactions between Si and other nutrient cycles in human impacted nearshore zones is valuable knowledge that may ultimately help protect ecosystem health and the valuable ecosystem services that nearshore zones provide (Sierszen et al. 2012; Strayer & Findlay 2010).

Bibliography

Andersson, G., Graneli, W. & Stenson, J., 1988. The influence of animals on phosphorus cycling in lake ecosystems. *Hydrobiologia*, 170, pp.267–284.

Aoki, Y., Hoshino, M. & Matsubara, T., 2007. Silica and testate amoebae in a soil under pine-oak forest. *Geoderma*, 142(1–2), pp.29–35.

Bailey-Watts, A.E., 1976. Planktonic diatoms and some diatom-silica relations in a shallow eutrophic Scottish loch. *Freshwater Biology*, 6, pp.69–80.

Barbiero, R.P. et al., 2002. Evidence of recovery from phosphorus enrichment in Lake Michigan. *Canadian Journal of Fisheries and Aquatic Sciences*, 59, pp.1639–1647.

Barica, J., 1989. Unique limnological phenomena affecting water quality of Hamilton Harbour, Lake Ontario. *Journal of Great Lakes Research*, 15(3), pp.519–530.

Bates, S.S. & Trainer, V.L., 2006. The ecology of harmful diatoms. In E. Graneli & J. T. Turner, eds. *Ecology of Harmful Algae*. Berlin: Springer-Verlag, pp. 81–88.

Beutel, M.W., 2006. Inhibition of ammonia release from anoxic profundal sediments in lakes using hypolimnetic oxygenation. *Ecological Engineering*, 28, pp.271–279.

Bloesch, J., 1982. Inshore-offshore sedimentation differences resulting from resuspension in the Eastern basin of Lake Erie. *Canadian Journal of Fisheries and Aquatic Sciences*, 39, pp.748–759.

Blomqvist, S., Gunnars, A. & Elmgren, R., 2004. Why the limiting nutrient differs between temperate coastal seas and freshwater lakes: A matter of salt. *Limnology and Oceanography*, 49(6), pp.2236–2241.

Bootsma, H.A. et al., 2003. Inputs, outputs, and internal cycling of silica in a large, tropical lake. *Journal of Great Lakes Research*, 29(Supplement 2), pp.121–138.

Boström, B. et al., 1988. Exchange of phosphorus across the sediment-water interface. *Hydrobiologia*, 170(1), pp.229–244.

Bostrom, B., Persson, G. & Broberg, B., 1988. Bioavailability of different phosphorus forms in freshwater systems. *Hydrobiologia*, 170, pp.133–155.

Bowen, K.L. & Currie, W.J.S., 2017. Elevated zooplankton production in a eutrophic Lake Ontario embayment : Hamilton Harbour 2002-2014. *Aquatic Ecosystem Health & Management*.

Boyce, F.M. et al., 1990. Evaluation of sediment traps in Lake St. Clair, Lake Ontario, and Hamilton Harbour. *Journal of Great Lakes Research*, 16(3), pp.366–379.

Brinkman, A.G., 1993. A double-layer model for ion adsorption onto metal oxides, applied to experimental data and to natural sediments of Lake Veluwe, the Netherlands. *Hydrobiologia*, 253, pp.31–45.

Brzezinski, M., 1985. The Si:C:N ratio of marine diatoms: Interspecific variability and the effect of some environmental variables. *Journal of Phycology*, 21, pp.347–357.

Burns, N.M., Rosa, F. & Gedeon, A., 1978. Lake Erie in mid-winter. *Journal of Great Lakes Research*, 4(2), pp.134–141.

Calbet, A. et al., 2014. Future climate scenarios for a coastal productive planktonic food web resulting in microplankton phenology changes and decreased trophic transfer efficiency. *Plos One*, 9(4).

Carey, J.C. & Fulweiler, R.W., 2012. Human activities directly alter watershed dissolved silica fluxes.

Biogeochemistry, 111, pp.125–138.

Carey, R.O. & Migliaccio, K.W., 2009. Contribution of wastewater treatment plant effluents to nutrient dynamics in aquatic systems: A review. *Environmental Management*, 44, pp.205–217.

Chan, C.H. & Kuntz, K.W., 1982. Lake Ontario atmospheric deposition. *Water, Air, and Soil Pollution*, 18, pp.83–99.

Chauvaud, L. et al., 2000. Long-term variation of the Bay of Brest ecosystem: Benthic-pelagic coupling revisited. *Marine Ecology Progress Series*, 200, pp.35–48.

Chow-Fraser, P. et al., 1998. Long-term response of the biotic community to fluctuating water levels and changes in water quality in Cootes Paradise Marsh, a degraded coastal wetland of Lake Ontario. *Wetlands Ecology and Management*, 6, pp.19–42.

City of Hamilton, 2011. *City of Hamilton Wastewater Treatment Facilities 2011 Annual Report*,

City of Hamilton, 2017. *Hamilton combined sewer overflow reporting (2016) final report*,

Clark, J.F. et al., 1992. Geochemistry and loading history of phosphate and silicate in the Hudson estuary. *Estuarine, Coastal and Shelf Science*, 34, pp.213–233.

Conley, D.J., 1998. An interlaboratory comparison for the measurement of biogenic silica in sediments. *Marine Chemistry*, 63, pp.39–48.

Conley, D.J. et al., 2008. Deforestation causes increased dissolved silicate losses in the Hubbard Brook Experimental Forest. *Global Change Biology*, 14, pp.2548–2554.

Conley, D.J., 1997. Riverine contribution of biogenic silica to the oceanic silica budget. *Limnology and Oceanography*, 42(4), pp.774–777.

Conley, D.J. et al., 1997. Sediment-water nutrient fluxes in the Gulf of Finland, Baltic Sea. *Estuarine, Coastal and Shelf Science*, 45, pp.591–598.

Conley, D.J., 2002. Terrestrial ecosystems and the global biogeochemical silica cycle. *Global Biogeochemical Cycles*, 16(4), pp.68-1-68–8.

Conley, D.J. & Kilham, S.S., 1989. Differences in silica content between marine and freshwater diatoms. *Limnology and Oceanography*, 34(1), pp.205–213.

Conley, D.J. & Malone, T.C., 1992. Annual cycle of dissolved silicate in Chesapeake Bay: Implications for the production and fate of phytoplankton biomass. *Marine Ecology Progress Series*, 81, pp.121–128.

Conley, D.J., Quigley, M.A. & Schelske, C.L., 1988. Silica and phosphorus flux from sediments: Importance of internal recycling in Lake Michigan. *Canadian Journal of Fisheries and Aquatic Sciences*, 45, pp.1030–1035.

Conley, D.J., Schelske, C.L. & Stoermer, E.F., 1993. Modification of the biogeochemical cycle of silica with eutrophication. *Marine Ecology Progress Series*, 101, pp.179–192.

Cornwell, J.C. & Banahan, S., 1992. A silicon budget for an Alaskan arctic lake. *Hydrobiologia*, 240, pp.37–44.

Cowan, J.L.W. & Boynton, W., 1996. Sediment-water oxygen and nutrient exchanges along the longitudinal axis of Chesapeake Bay: Seasonal patterns,controlling factors and ecological significance. *Estuaries*, 19(3), pp.562–580.

Cowan, J.L.W., Pennock, J.R. & Boynton, W.R., 1996. Seasonal and interannual patterns of sediment-water nutrient and oxygen fluxes in Mobile Bay, Alabama (USA): regulating factors and ecological significance. *Marine Ecology Progress Series*, 141, pp.229–245.

D'Elia, C.F., Nelson, D.M. & Boynton, W.R., 1983. Chesapeake Bay nutrient and plankton dynamics: III. The annual cycle of dissolved silicon. *Geochimica et Cosmochimica Acta*, 47, pp.1945–1955.

Danielsson, A., 2014. Influence of hypoxia on silicate concentrations in the Baltic Proper (Baltic Sea). *Boreal Environment Research*, 19, pp.267–280.

Danielsson, Å., Papush, L. & Rahm, L., 2008. Alterations in nutrient limitations — Scenarios of a changing Baltic Sea. *Journal of Marine Systems*, 73, pp.263–283.

Davison, W., 1993. Iron and manganese in lakes. *Earth-Science Reviews*, 34, pp.119–163.

Degobbis, D., Gilmartin, M. & Degobbis Gilmartin, D.M., 1990. Nitrogen, phosphorus, and biogenic silicon budgets for the northern Adriatic Sea. *Oceanologica Acta*, 13(1), pp.31–45.

DeMaster, D.J., 1981. The supply and accumulation of silica in the marine environment. *Geochimica et Cosmochimica Acta*, 45, pp.1715–1732.

Denis, L. & Grenz, C., 2003. Spatial variability in oxygen and nutrient fluxes at the sediment-water interface on the continental shelf in the Gulf of Lions (NW Mediterranean). *Oceanologica Acta*, 26, pp.373–389.

Dermott, R. et al., 2007. *Assessment of lower food web in Hamilton Harbour, Lake Ontario, 2002-2004*, Burlington, Ontario.

Derry, L. a et al., 2005. Biological control of terrestrial silica cycling and export fluxes to watersheds. *Nature*, 433, pp.728–731.

Dietzel, M., 2000. Dissolution of silicates and the stability of polysilicic acid. *Geochimica et Cosmochimica Acta*, 64(19), pp.3275–3281.

Dove, A., 2009. Long-term trends in major ions and nutrients in Lake Ontario. *Aquatic Ecosystem Health & Management*, 12(3), pp.281–295.

Duan, S.-W. & Kaushal, S.S., 2013. Warming increases carbon and nutrient fluxes from sediments in streams across land use. *Biogeosciences*, 10, pp.1193–1207.

Egge, J.K. & Aksnes, D.L., 1992. Silicate as regulating nutrient in phytoplankton competition. *Marine Ecology Progress Series*, 83, pp.281–289.

Einsele, W., 1938. Uber chemische und kolloidchemische vorgange in eisen-phosphat-systemen unter limnochemischen und limnogeologischen gesichtspunkten. *Archiv fur Hydrobiologie*, 33, pp.361–387.

Einsele, W., 1936. Uber die beziehungen des eisenkreislaufs zum phosphatkreislauf im eutrophen see. *Archiv fur Hydrobiologie*, 29, pp.664–686.

Environmental Protection Agency, 1978. *Silica, dissolved (colorimetric)*,

Epstein, E., 1994. The anomaly of silicon in plant biology. *Proceedings of the National Academy of Sciences of the United States of America*, 91, pp.11–17.

Finenko, Z.Z. & Krupatkina-Akinina, D.K., 1974. Effect of inorganic phosphorus on the growth rate of diatoms. *Marine Biology*, 26, pp.193–201.

Freitas, R.M., Perilli, T.A.G. & Ladeira, A.C.Q., 2013. Oxidative precipitation of manganese from acid mine drainage by potassium permanganate. *Journal of Chemistry*, 2013, p.8.

Frings, P.J. et al., 2014. Lack of steady-state in the global biogeochemical Si cycle: Emerging evidence from lake Si sequestration. *Biogeochemistry*, 117, pp.255–277.

Froelich, P.N. et al., 1979. Early oxidation of organic matter in pelagic sediments of the eastern equatorial Atlantic: Suboxic diagenesis. *Geochemica et Cosmochimica Acta*, 43, pp.1075–1090.

Gaedke, U. & Schweizer, A., 1993. The first decade of oligotrophication in Lake Constance. *Oecologia*, 93, pp.268–275.

Gaillard, J. et al., 1987. Interstitial water and sediment chemistries of Lake Aiguebelette (Savoy, France). *Chemical Geology*, 63, pp.73–84.

Galloway, J.N. & Likens, G.E., 1978. The collection of precipitation for chemical analysis. *Tellus*, 30(1), pp.71–82.

Garnier, J. et al., 2002. Modelling the transfer and retention of nutrients in the drainage network of the Danube River. *Estuarine, Coastal and Shelf Science*, 54, pp.285–308.

Garnier, J. et al., 2010. N:P:Si nutrient export ratios and ecological consequences in coastal seas evaluated by the ICEP approach. *Global Biogeochemical Cycles*, 24(GB0A05), pp.1–12.

Gibson, C.E., Wang, G. & Foy, R.H., 2000. Silica and diatom growth in Lough Neagh: The importance of internal recycling. *Freshwater Biology*, 45, pp.285–293.

Glibert, P.M. et al., 1995. Dynamics of the 1990 winter/spring bloom in Chesapeake Bay. *Marine Ecology Progress Series*, 122, pp.27–43.

Gobler, C.J. et al., 2006. Nitrogen and silicon limitation of phytoplankton communities across an urban estuary : The East River-Long Island Sound system. *Estuarine, Coastal and Shelf Science*, 68, pp.127–138.

Haffner, G.D., Poulton, D.J. & Kohli, B., 1983. Physical processes and eutrophication. *Water Resources Bulletin*, 18(3), pp.457–464.

Hamblin, P.F. & He, C., 2003. Numerical models of the exchange flows between Hamilton Harbour and Lake Ontario. *Canadian Journal of Civil Engineering*, 180, pp.168–180.

Hamilton Harbour RAP Technical Team, 2010. *Contaminant loadings and concentrations to Hamilton Harbour: 2003-2007 update*,

Harrison, J.A. et al., 2012. Global importance, patterns, and controls of dissolved silica retention in lakes and reservoirs. *Global Biogeochemical Cycles*, 26, pp.1–12.

Harriss, R.C., 1966. Biological buffering of oceanic silica. *Nature*, 212, pp.275–276.

Hartikainen, H. et al., 1996. Co-occurrence and potential chemical competition of phosphorus and silicon in lake sediment. *Water Research*, 30(10), pp.2472–2478.

Harvey, F.E., Rudolph, D.L. & Frape, S.K., 2000. Estimating ground water flux into large lakes: application in the Hamilton Harbour, western Lake Ontario. *Groundwater*, 38(4), pp.550–565.

Heinen, E.A. & McManus, J., 2004. Carbon and nutrient cycling at the sediment-water boundary in Western Lake Superior. *Journal of Great Lakes Research*, 30(Suppl. 1), pp.113–132.

Hesslein, R.H., 1976. An in situ sampler for close interval pore water studies. *Limnology and Oceanography*, 21(6), pp.912–914.

Hingston, F.J. et al., 1967. Specific adsorption of anions. *Nature*, 215, pp.1459–1461.

Hiriart-Baer, V.P. et al., 2016. Hamilton Harbour over the last 25 years: Insights from a long-term comprehensive water quality monitoring program. *Aquatic Ecosystem Health and Management*, 19(2), pp.124–133.

Hiriart-Baer, V.P., Milne, J. & Charlton, M.N., 2009. Water quality trends in Hamilton Harbour: Two decades of

change in nutrients and chlorophyll a. *Journal of Great Lakes Research*, 35, pp.293–301.

Holmer, M. & Storkholm, P., 2001. Sulphate reduction and sulphur cycling in lake sediments: A review. *Freshwater Biology*, 46, pp.431–451.

Horn, H. & Uhlmann, D., 1995. Competitive growth of blue-greens and diatoms (Fragilaria) in the Saidenback reservoir, Saxony. *Water Science and Technology*, 32(4), pp.77–88.

Humborg, C. et al., 2000. Silicon retention in river basins: far-reaching effects on biogeochemistry and aquatic food webs in coastal marine environments. *Ambio*, 29(1), pp.45–50.

Hupfer, M. & Lewandowski, J., 2008. Oxygen controls the phosphorus release from lake sediments - A long-lasting paradigm in limnology. *International Review of Hydrobiology*, 93(4–5), pp.415–432.

Hyacinthe, C. & Van Cappellen, P., 2004. An authigenic iron phosphate phase in estuarine sediments: Composition, formation and chemical reactivity. *Marine Chemistry*, 91, pp.227–251.

International Joint Commission United States and Canada, 1987. *Revised Great Lakes Water Quality Agreement of 1978*, Ottawa.

Jickells, T.D., 1998. Nutrient biogeochemistry of the coastal zone. *Science*, 281, pp.217–222.

Johnson, T.C. & Eisenreich, S.J., 1978. Silica in Lake Superior: Mass balance considerations and a model for dynamic response to eutrophication. *Geochimica et Cosmochimica Acta*, 43, pp.77–91.

Justic, D. et al., 1995. Changes in nutrient structure of river-dominated coastal waters: Stoichiometric nutrient balance and its consequences. *Estuarine, Coastal and Shelf Science*, 40, pp.339–356.

Justic, D., Rabalais, N. & Turner, R.E., 1995. Stoichiometric nutrient balance and origin of coastal eutrophication. *Marine Pollution Bulletin*, 30(1), pp.41–46.

Kamatani, A., 1982. Dissolution rates of silica from diatoms decomposing at various temperatures. *Marine Biology*, 68, pp.91–96.

Kappler, A. & Straub, K.L., 2005. Geomicrobiological cycling of iron. *Reviews in Mineralogy and Geochemistry*, 59(1), pp.85–108.

Kelton, N. & Chow-Fraser, P., 2005. A simplified assessment of factors controlling phosphorus loading from oxygenated sediments in a very shallow eutrophic lake. *Lake and Reservoir Management*, 21(3), pp.223–230.

Kilham, S.S., 1975. Kinetics of silicon-limited growth in the freshwater diatom Asterionella formosa. *Journal of Phycology*, 11, pp.396–399.

Kinniburgh, D.G. & Cooper, D.M., 2011. *PhreePlot: Creating graphical output with PHREEQC*,

Klapwijk, A. & Snodgrass, W.J., 1985. Model for lake-bay exchange flow. *Journal of Great Lakes Research*, 11(1), pp.43–52.

Kling, H.J. et al., 2011. Bloom development and phytoplankton succession in lake winnipeg: A comparison of historical records with recent data. *Aquatic Ecosystem Health and Management*, 14(2), pp.219–224.

Koning, E. et al., 1997. Settling, dissolution and burial of biogenic silica in the sediments off Somalia (northwestern Indian Ocean). *Deep-Sea Research Part II: Topical Studies in Oceanography*, 44(6–7), pp.1341–1360.

Koning, E., Epping, E. & Van Raaphorst, W., 2002. Determining biogenic silica in marine samples by tracking silicate and aluminium concentrations in alkaline leaching solutions. *Aquatic Geochemistry*, 8(1), pp.37–67.

Koski-Vähälä, J., Hartikainen, H. & Tallberg, P., 2001. Phosphorus mobilization from various sediment pools in

response to increased pH and silicate concentration. *Journal of Environmental Quality*, 30, pp.546–552.

Kostka, J.E. & Luther III, G.W., 1994. Partitioning and speciation of solid phase iron in saltmarsh sediments. *Geochimica et Cosmochimica Acta*, 58(7), pp.1701–1710.

Krivtsov, V. et al., 2000. Interrelations between Si and P biogeochemical cycles - a new approach to the solution of the eutrophication problem. *Hydrobiological Processes*, 14, pp.283–295.

Laruelle, G.G. et al., 2009. Anthropogenic perturbations of the silicon cycle at the global scale : Key role of the land-ocean transition. *Global Biogeochemical Cycles*, 23, pp.1–17.

Lehrter, J.C. et al., 2012. Sediment-water fluxes of dissolved inorganic carbon, O2, nutrients, and N2 from the hypoxic region of the Louisiana continental shelf. *Biogeochemistry*, 109, pp.233–252.

Lehtimäki, M., Sinkko, H. & Tallberg, P., 2016. The role of oxygen conditions in the microbial dissolution of biogenic silica under brackish conditions. *Biogeochemistry*, 129, pp.355–371.

Li, M. et al., 2007. Long-term variations in dissolved silicate, nitrogen, and phosphorus flux from the Yangtze River into the East China Sea and impacts on estuarine ecosystem. *Estuarine, Coastal and Shelf Science*, 71, pp.3–12.

Ling, H., Diamond, M. & Mackay, D., 1993. Application of the QWASI fugacity/aquivalence model to assessing sources and fate of contaminants in Hamilton Harbour. *Journal of Great Lakes Research*, 19(3), pp.582–602.

Long, T. et al., 2014. Evaluation of stormwater and snowmelt inputs, land use and seasonality on nutrient dynamics in the watersheds of Hamilton Harbour, Ontario, Canada. *Journal of Great Lakes Research*, 40, pp.964–979.

Loucaides, S., Cappellen, P. Van & Behrends, T., 2008a. Dissolution of biogenic silica from land to ocean : Role of salinity and pH. , 53(4), pp.1614–1621.

Loucaides, S., Cappellen, P. Van & Behrends, T., 2008b. Dissolution of biogenic silica from land to ocean : Role of salinity and pH. *Limnology and Oceanography*, 53(4), pp.1614–1621.

Lovely, D.R. & Phillips, E.J.P., 1988. Novel mode of microbial energy metabolism: Organic carbon oxidation coupled to dissimilatory reduction of iron or manganese. *Applied and Environmental Microbiology*, 54(6), pp.1472–1480.

Lovely, D.R., Phillips, E.J.P. & Lonergan, D.J., 1991. Enzymatic versus nonenzymatic mechanisms for Fe(III) reduction in aquatic sediments. *Environmental Science & Technology*, 25, pp.1052–1067.

Lumsdon, D.G. & Evans, L.J., 1994. Surface complexation model parameters for geothite (a-FeOOH). *Journal of Colloid and Interface Science*, 164, pp.119–125.

Maavara, T. et al., 2015. Global phosphorus retention by river damming. *Proceedings of the National Academy of Sciences of the United States of America*, 112(51).

Maavara, T. et al., 2015. Reactive silicon dynamics in a large prairie reservoir (Lake Diefenbaker, Saskatchewan). *Journal of Great Lakes Research*, 41(Supplement 2), pp.100–109.

Maavara, T., Dürr, H.H. & Cappellen, P. Van, 2014. Worldwide retention of nutrient silicon by river damming: From sparse data set to global estimate. *AGU publications*, pp.1–14.

Mackenzie, F.T., Ver, L.M. & Lerman, A., 2000. Coastal-zone biogeochemical dynamics under global warming. *International Geology Review*, 42, pp.193–206.

Maguire, T.J. & Fulweiler, R.W., 2017. Fate and effect of dissolved silicon within wastewater treatment effluent. *Environmental Science and Technology*, 51, pp.7403–7411.

Maguire, T.J. & Fulweiler, R.W., 2016. Urban dissolved silica: Quantifying the role of groundwater and runoff in wastewater influent. *Environmental Science and Technology*, 50, pp.54–61.

Marvin, C.H. et al., 2004. Contaminants associated with suspended sediments in Lakes Erie and Ontario , 1997 – 2000. *Journal of Great Lakes Research*, 30(2), pp.277–286.

Mayer, T. & Johnson, M.G., 1994. History of anthropogenic activities in Hamilton Harbour as determined from the sedimentary record. *Environmental Pollution*, 86, pp.341–347.

Mayer, T.D. & Jarrell, W.M., 2000. Phosphorus sorption during iron(II) oxidation in the presence of dissolved silica. *Water Research*, 34(16), pp.3949–3956.

Ministry of the Environment, 2008. *Design guidelines for sewage works 2008*,

Ministry of the Environment and Climate Change, 2015. *Environmental Compliance Approval*,

Ministry of the Environment and Climate Change, 2014. *The determintation of molybdate reactive silicates and dissolved carbon in water, industrial waste, and precipitation by colorimetry*,

Miretzky, P. & Cirelli, A.F., 2004. Silica dynamics in a pampean lake (Lake Chascomús, Argentina). *Chemical Geology*, pp.109–122.

Mortimer, C.H., 1941. The exchange of dissolved substances between mud and water in lakes I. *Journal of Ecology*, 29(2), pp.280–329.

Mortimer, C.H., 1942. The exchange of dissolved substances between mud and water in lakes II. *Journal of Ecology*, 30(1), pp.147–201.

Moss, B., Stansfield, J. & Irvine, K., 1991. Development of daphnid communities in diatom- and cyanophyte-dominated lakes and their relevance to lake restoration by biomanipulation. *Journal of Applied Ecology*, 28, pp.586–602.

Munawar, M. et al., 2017. Phytoplankton ecology of a culturally eutrophic embayment : Hamilton Harbour, Lake Ontario. *Aquatic Ecosystem Health & Management*, 20(3), pp.201–213.

Murphy, J. & Riley, J.P., 1962. A modified single solution method for the determination of phosphate in natural waters. *Analytica Chimica Acta*, 27, pp.31–36.

Nelson, D.M. et al., 1995. Production and dissolution of biogenic silica in the ocean: revised global estimates, comparison with regional data and relationship to biogenic sedimentation. *Global Biogeochemical Cycles*, 9(3), pp.359–372.

Nriagu, J.O., 1978. Dissolved silica in pore waters of Lakes Ontario, Erie, Superior sediments. *Limnology and Oceanography*, 23(1), pp.53–67.

Obihara, C.H. & Russell, E.W., 1972. Specific adsorption of silicate and phosphate by soils. *Journal of Soil Sciences*, 23(1), pp.105–117.

Officer, C.B. & Ryther, J.H., 1980. The possible importance of silicon in marine eutrophication. *Marine Ecology Progress Series*, 3, pp.83–91.

Orihel, D.M. et al., 2017. Internal phosphorus loading in Canadian fresh waters: a critical review and data analysis. *Canadian Journal of Fisheries and Aquatic Sciences*, 0, pp.1–25.

Pallud, C. et al., 2007. The use of flow-through sediment reactors in biogeochemical kinetics : methodology and examples of applications. *Marine Chemistry*, 106, pp.256–271.

Pallud, C. & Van Cappellen, P., 2006. Kinetics of microbial sulfate reduction in estuarine sediments. *Geochimica et*

Cosmochimica Acta, 70, pp.1148–1162.

Parker, J.I., Conway, H.L. & Yeguchi, E.M., 1977. Dissolution of diatom frustules and recycling of amorphous silicon in Lake Michigan. *Journal of the Fisheries Research Board of Canada*, 34, pp.545–551.

Parkhurst, D.L. & Appelo, C.A.J., 1999. *User's guide to PHREEQC (version 2) - A computer program for speciation, batch-reaction, one-dimensional transport, and inverse geochemical calculations*, Reston, Virginia.

Parsons, C.T. et al., 2017. Sediment phosphorus speciation and mobility under dynamic redox conditions. *Biogeosciences*, 14, pp.3585–3602.

Parsons, M.L., Dortch, Q. & Turner, R.E., 2002. Sedimentological evidence of an increase in Pseudo-nitzschia (Bacillariophyceae) abundance in response to coastal eutrophication. *Limnol. Oceanogr.*, 47(2), pp.551–558.

Peeters, J.C.H. et al., 1991. Limiting factors for phytoplankton in the North Sea. *Water Science and Technology*, 24(10), pp.261–267.

Pernica, P., North, R.L. & Baulch, H.M., 2017. In the cold light of day: The potential importance of under-ice convective mixed layers to primary producers. *Inland Waters*, 7(2), pp.138–150.

Peterson Holm, N. & Armstrong, D.E., 1981. Role of nutrient limitation and competition in controlling the populations of Asterionella formosa and Microcystis aeruginosa in semicontinuous culture. *Limnology and Oceanography*, 26(4), pp.622–634.

Qin, C. et al., 2015. Bioavailability and characterization of dissolved organic nitrogen and dissolved organic phosphorus in wastewater effluents. *Science of the Total Environment*, 511, pp.47–53.

Rabalais, N.N. et al., 2010. Dynamics and distribution of natural and human-caused hypoxia. *Biogeosciences*, 7, pp.585–619.

Redfield, A.C., 1958. The biological control of chemical factors in the environment. *American Scientist*, 46(3), pp.205–221.

Regional Municipality of Halton, 2011. *Wastewater treatment systems 2010 performance report*,

Rocha, C., Galvao, H. & Barbosa, A., 2002. Role of transient silicon limitation in the development of cyanobacteria blooms in the Guadiana estuary, south-western Iberia. *Marine Ecology Progress Series*, 228, pp.35–45.

Rosa, F., 1985. Sedimentation and sediment resuspension in Lake Ontario. *Journal of Great Lakes Research*, 11(1), pp.13–25.

Rukavina, N.A. & Versteeg, J.K., 1996. Surficial sediments of Hamilton Harbour: physical properties and basin morphology. *Water Quality Research Journal of Canada*, 31(3), pp.529–551.

Sauer, D. et al., 2006. Review of methodologies for extracting plant-available and amorphous Si from soils and aquatic sediments. *Biogeochemistry*, 80, pp.89–108.

Savchuk, O.P., 2002. Nutrient biogeochemical cycles in the Gulf of Riga: Scaling up field studies with a mathematical model. *Journal of Marine Systems*, 32, pp.253–280.

Schelske, C.L., 1985. Biogeochemical silica mass balances in Lake Michigan and Lake Superior. *Biogeochemistry*, 1, pp.197–218.

Schelske, C.L. et al., 1983. Early eutrophication in the lower Great Lakes: new evidence from biogenic silica in sediments. *Science*, 222(4621), pp.320–322.

Schelske, C.L. et al., 1986. Phosphorus enrichment, silica utilization and biogeochemical silica depletion in the

Great Lakes. *Canadian Journal of Fisheries and Aquatic Sciences*, 43, pp.407–415.

Schelske, C.L. & Stoermer, E.F., 1971. Eutrophication, silica depletion, and predicted changes in algal quality in Lake Michigan. *Science*, 173(3995), pp.423–424.

Schelske, C.L. & Stoermer, E.F., 1972. Phosphorus, silica, and eutrophication of Lake Michigan G. E. Likens, ed. *American Society of Limnology and Oceanography Special Symposium*, 1, pp.157–171.

Schoelynck, J. et al., 2010. Silica uptake in aquatic and wetland macrophytes: A strategic choice between silica, lignin and cellulose? *New Phytologist*, 186, pp.385–391.

Schoelynck, J. & Struyf, E., 2016. The functional role of silicon in plant biology: Silicon in aquatic vegetation. *Functional Ecology*, 30, pp.1323–1330.

Schwertmann, U., 1991. Solubility and dissolution of iron oxides. *Plant and Soil*, 130, pp.1–25.

Seitzinger, S.P. et al., 2010. Global river nutrient export : A scenario analysis of past and future trends. *Global Biogeochemical Cycles*, 24(GB0A08).

Sferratore, A. et al., 2006. Diffuse and point sources of silica in the Seine River watershed. *Environmental Science and Technology*, 40(21), pp.6630–6635.

Sholkovitz, E., 1973. Interstitial water chemistry of the Santa Barbara Basin sediments. *Geochemica et Cosmochimica Acta*, 37, pp.2043–2073.

Sierszen, M.E. et al., 2012. A review of selected ecosystem services provided by coastal wetlands of the Laurential Great Lakes. *Aquatic Ecosystem Health and Management*, 15(1), pp.92–106.

Siipola, V. et al., 2013. Separating biogenic and adsorbed pools of silicon in sediments using bayesian inference. *Silicon*, 5(1), pp.53–65.

Siipola, V., Lehtimaki, M. & Tallberg, P., 2016. The effects of anoxia on Si dynamics in sediments. *Journal of Soils and Sediments*, 16, pp.266–279.

Singh, S.P. et al., 2015. Dissolved silicon and its isotopes in the water column of the Bay of Bengal: Internal cycling versus lateral transport. *Geochimica et Cosmochimica Acta*, 151, pp.172–191.

Slomp, C.P., Van der Gaast, S.J. & Van Raaphorst, W., 1996. Phosphorus binding by poorly crystalline iron oxides in North Sea sediments. *Marine Chemistry*, 52, pp.55–73.

Sommer, U., 1983. Algal nutrient competition in continuous culture. *Hydrobiological Bulletin*, 17(1), pp.21–27.

Sommer, U., 1994. Are marine diatoms favoured by high Si:N ratios? *Marine Ecology Progress Series*, 115, pp.309–315.

Sommer, U., 1985. Comparisons between steady state and non-steady state competition: Experiments with natural phytoplankton. *Limnology and Oceanography*, 30(2), pp.335–346.

Sommer, U., Katechakis, A. & Hansen, T., 2002. Pelagic food web configurations at different levels of nutrient richness and their implications for the ratio fish production. *Hydrobiologia*, 48, pp.11–20.

Sommer, U. & Stabel, H.-H., 1983. Silicon consumption and population density changes of dominant planktonic diatoms in Lake Constance. *Journal of Ecology*, 71, pp.119–130.

Søndergaard, M., Jensen, J.P. & Jeppesen, E., 2003. Role of sediment and internal loading of phosphorus in shallow lakes. *Hydrobiologia*, 506–509, pp.135–145.

Spears, B.M. et al., 2008. Effects of light on sediment nutrient flux and water column nutrient stoichiometry in a

shallow lake. *Water Research*, 42, pp.977–986.

Srithongouthai, S. et al., 2003. The influence of environmental variability on silicate exchange rates between sediment and water in a shallow-water coastal ecosystem, the Seto Inland Sea, Japan. *Marine Pollution Bulletin*, 47, pp.10–17.

Statistics Canada, 2017. Focus on Geography Series, 2016 Census - Hamilton, (CMA) - Ontario. Available at: http://www12.statcan.gc.ca/census-recensement/2016/as-sa/fogs-spg/Facts-cma-eng.cfm?LANG=Eng&GK=CMA&GC=537.

Stoermer, E.F., 1993. Evaluating diatom succession: some pecularities of the Great Lakes case. *Journal of Paleolimnology*, 8, pp.71–83.

Strayer, D.L. & Findlay, S.E.G., 2010. Ecology of freshwater shore zones. *Aquatic Science*, 72, pp.127–163.

Street-Perrott, F.A. & Barker, P.A., 2009. Biogenic silica: a neglected component of coupled global continental biogeochemical cycles of carbon and silicon. *Earth Surface Processes and Landforms*, 33, pp.1436–1457.

Struyf, E. et al., 2010. Historical land use change has lowered terrestrial silica mobilization. *Nature Communications*, 1(8), p.129.

Struyf, E. & Conley, D.J., 2012. Emerging understanding of the ecosystem silica filter. *Biogeochemistry*, 107, pp.9–18.

Struyf, E. & Conley, D.J., 2009. Silica: An essential nutrient in wetland biogeochemistry. *Frontiers in Ecology and the Environment*, 7(2), pp.88–94.

Tallberg, P. et al., 2009. Applicability of a sequential P fractionation procedure to Si in sediment. *Journal of Soils and Sediments*, 9, pp.594–603.

Tallberg, P. et al., 2012. Horizontal and vertical distribution of biogenic silica in coastal and profundal sediments of the Gulf of Finland (northeastern Baltic sea). *Boreal Environment Research*, 17, pp.347–362.

Tallberg, P. et al., 2008. Potentially mobile pools of phosphorus and silicon in sediment from the Bay of Brest: Interactions and implications for phosphorus dynamics. *Estuarine, Coastal and Shelf Science*, 76, pp.85–94.

Tallberg, P., 1999. The magnitude of Si dissolution from diatoms at the sediment surface and its potential impact on P mobilization. *Archiv fur Hydrobiologie*, 144(4), pp.429–438.

Tallberg, P. & Koski-Vahala, J., 2001. Silicate-induced phosphate release from surface sediment in eutrophic lakes. *Archiv fur Hydrobiologie*, 151(2), pp.221–245.

Terseleer, N., Gypens, N. & Lancelot, C., 2013. Factors controlling the production of domoic acid by Pseudo-nitzschia (Bacillariophyceae): A model study. *Harmful Algae*, 24, pp.45–53.

Thibault, P.-J. et al., 2009. Mineralogical confirmation of a near-P:Fe = 1:2 limiting stoichiometric ratio in colloidal P-bearing ferrihydrite-like hydrous ferric oxide. *Geochimica et Cosmochimica Acta*, 73, pp.364–376.

Thorel, M. et al., 2014. Interactive effects of irradiance and temperature on growth and domoic acid production of the toxic diatom Pseudo-nitzschia australis (Bacillariophyceae). *Harmful Algae*, 39, pp.232–241.

Tilman, D. & Kilham, S.S., 1976. Phosphate and silicate growth and uptake kinetics of the diatoms Asterionella formosa and Cyclotella meneghiniana in batch and semicontinuous culture. *Journal of Phycology*, 12, pp.375–383.

Treguer, P. et al., 1995. The silica balance in the world ocean: a reestimate. *Science*, 268, pp.375–379.

Tuominen, L. et al., 1998. Increases bioavaliability of sediment phosphorus due to silicate enrichment. *Water*

Research, 32(7), pp.2001–2008.

Turner, R.E. et al., 1998. Fluctuating silicate:nitrate ratios and coastal plankton food webs. *Proceedings of the National Academy of Sciences of the United States of America*, 95, pp.13048–13051.

Turner, R.E. et al., 2003. Future aquatic nutrient limitations. *Marine Pollution Bulletin*, 46, pp.1032–1034.

Urban, N., Dinkel, C. & Wehrli, B., 1997. Solute transfer across the sediment surface of a eutrophic lake: I. Porewater profiles from dialysis samplers. *Aquatic Science*, 59, pp.1–25.

Van Cappellen, P., 2003. Biomineralization and Global Biogeochemical Cycles. In *Reviews in Mineralogy and Geochemistry*. pp. 357–381.

Vandevenne, F. et al., 2012. Agricultural silica harvest: Have humans created a new loop in the global silica cycle? *Frontiers in Ecology and the Environment*, 10(5), pp.243–248.

Van Dokkum, H.P. et al., 2004. Emission, fate and effects of soluble silicates (waterglass) in the aquatic environment. *Environmental Science and Technology*, 38, pp.515–521.

Viaroli, P. et al., 2013. Factors affecting dissolved silica concentrations, and DSi and DIN stoichiometry in a human impacted watershed (Po River, Italy). *Silicon*, 5, pp.101–114.

Willen, E., 1991. Planktonic diatoms - An ecological review. *Algological Studies*, 62, pp.69–106.

Winter, T.C., 1981. Uncertainties in estimating the water balance of lakes. *Journal of the American Water Resources Association*, 17(1), pp.82–115.

Wright, J.L.C. et al., 1989. Identification of domoic acid, a neuroexcitatory amino acid, in toxic mussels from eastern Prince Edward Island. *Canadian Journal of Chemistry*, 67, pp.481–490.

Zhou, X. et al., 2016. Warming increases nutrient mobilization and gaseous nitrogen removal from sediments across cascade reservoirs. *Environmental Pollution*, 219, pp.490–500.

Appendix 1

Hamilton Harbour Si Data Set

A1 Table 1. Hamilton Harbour monthly and annual water budget ± uncertainty.

Water Source/Sink	Discharge (10^3 m^3 day^{-1})					
	Jan.	Feb.	Mar.	Apr.	May	Jun.
Tributaries	140 ± 21	168 ± 25	271 ± 41	258 ± 39	159 ± 24	112 ± 17
Cootes' Paradise	273 ± 68	293 ± 73	538 ± 135	511 ± 128	257 ± 64	168 ± 42
WWTP	435 ± 4	447 ± 4	501 ± 5	496 ± 5	444 ± 4	419 ± 4
CSO	13 ± 3	13 ± 3	13 ± 3	13 ± 3	13 ± 3	13 ± 3
Steel mill intake	646 ± 97	627 ± 94	623 ± 93	656 ± 98	675 ± 101	726 ± 109
Steel mill discharge	646 ± 97	627 ± 94	623 ± 93	656 ± 98	675 ± 101	726 ± 109
Groundwater	58 ± 29	58 ± 29	58 ± 29	58 ± 29	58 ± 29	58 ± 29
Precipitation	39 ± 7	44 ± 7	44 ± 8	53 ± 9	59 ± 10	52 ± 9
Evaporation	0	0	0	49 ± 20	73 ± 29	90 ± 36
L. Ontario inflow	829 ± 94	829 ± 94	829 ± 94	829 ± 94	5098 ± 579	5098 ± 579
H. Harbour outflow	1789 ± 221	1852 ± 229	2255 ± 278	2170 ± 268	6016 ± 743	5830 ± 720

Water Source/Sink	Discharge (10^3 m^3 day^{-1})					
	July	August	September	October	November	December
Tributaries	75 ± 11	58 ± 9	47 ± 7	72 ± 11	82 ± 12	112 ± 17
Cootes' Paradise	87 ± 22	79 ± 20	66 ± 17	151 ± 38	210 ± 52	285 ± 71
WWTP	398 ± 4	385 ± 4	398 ± 4	411 ± 4	401 ± 4	431 ± 4
CSO	13 ± 3	13 ± 3	13 ± 3	13 ± 3	13 ± 3	13 ± 3
Steel mill intake	775 ± 116	757 ± 114	736 ± 110	690 ± 104	658 ± 99	665 ± 100
Steel mill discharge	775 ± 116	757 ± 114	736 ± 110	690 ± 104	658 ± 99	665 ± 100
Groundwater	58 ± 29	58 ± 29	58 ± 29	58 ± 29	58 ± 29	58 ± 29
Precipitation	57 ± 10	62 ± 11	58 ± 10	50 ± 8	65 ± 11	50 ± 8
Evaporation	90 ± 36	71 ± 28	39 ± 15	15 ± 6	0	0
L. Ontario inflow	5098 ± 579	5098 ± 579	5098 ± 579	5098 ± 579	829 ± 94	829 ± 94
H. Harbour outflow	5696 ± 703	5682 ± 702	5699 ± 704	5837 ± 721	1660 ± 205	1779 ± 220

A1 Table 2. Dissolved silicon (DSi), soluble reactive silicon (SRSi), and total dissolved phosphorus (TDP) concentrations measured at sites 1, 2, 3, and 4 across Hamilton Harbour from 1 m below the surface (epilimnion). Concentrations of DSi and SRSi were not significantly different. Epilimnion DSi concentrations between sites were not significantly different. DSi concentrations at site 2 were significantly different between the epilimnion and hypolimnion. Epilimnion TDP concentrations between sites were not significantly different. TDP concentrations at site 2 were significantly different between the epilimnion and hypolimnion. All significant differences were determined by one-way ANOVA at the $\alpha = 0.05$ level, followed by a Tukey HSD test.

Date	**Concentration (µmol L^{-1})**								
(D/M/Y)	Site 1 (70270)			Site 2 (258)			Site 3 (7007)		
Epilimnion	DSi	SRSi	TDP	DSi	SRSi	TDP	DSi	SRSi	TDP
20/04/16	1.82		1.14	0.82		0.98	2.43		0.93
4/05/16	0.86		1.04	0.45		1.15	0.79		1.52
18/05/16	1.02		0.78	2.10		1.16	1.85		1.82
31/05/16	3.71	3.76	0.85	3.51	3.26	1.37	3.03	2.96	0.71
14/06/16	3.38	3.99	0.75	7.34		0.57	4.84		0.52
29/06/16	2.34	3.23	0.73	1.64	1.61	0.62	2.96		1.02
12/07/16	4.28		1.27	4.50		0.74	5.81	4.94	0.97
26/07/16	3.78		0.97	2.58	3.29	0.08	4.64		0.65
11/08/16	9.10	11.15	0.39	10.17		0.51	10.62	10.20	-
24/08/16	15.03	15.25	0.35	11.85	14.35	0.57	14.45		0.70
08/09/16	7.06		0.70	4.64		0.33	4.05	3.98	0.41
20/09/16	9.61		0.10	6.99		0.24	9.37		0.51
05/10/16	18.18	18.45	1.51	19.27	19.63	1.50	19.01	19.58	1.60
19/10/16	23.54		1.84	20.46		1.74	19.39		1.24
04/11/16	22.04		1.31	22.37		1.42	23.16	22.08	1.13
Mean	8.38		0.92	7.91		0.87	8.43		0.98

Date	**Concentration (µmol L^{-1})**				
(D/M/Y)	Site 4 (W3)			Mean All Sites	
Epilimnion	DSi	SRSi	TDP	DSi	TDP
20/04/16	4.45	4.81	0.98	2.38	1.01
4/05/16	4.95		1.18	1.76	1.22
18/05/16	2.32		1.32	1.82	1.27
31/05/16	6.72	7.89	2.34	4.24	1.32
14/06/16	6.97		1.03	5.64	0.72
29/06/16	2.35		1.49	2.32	0.96
12/07/16	4.51	5.90	0.75	4.78	0.93
26/07/16	4.72	5.58	1.07	3.93	0.69
11/08/16	10.02	11.69	0.17	9.98	0.36
24/08/16	11.32		1.55	13.16	0.79
08/09/16	7.70		0.75	5.86	0.55
20/09/16	10.13		0.48	9.03	0.33
05/10/16	24.08	24.83	1.85	20.13	1.61
19/10/16	21.85		1.87	21.31	1.67
04/11/16	22.70	22.58	1.30	22.57	1.29
Mean	9.65		1.21	8.59	0.98

A1 Table 3. Dissolved silicon (DSi), soluble reactive silicon (SRSi), and total dissolved phosphorus (TDP) concentrations measured at sites 1, 2, 3, and 4 across Hamilton Harbour from 1 m above the sediment water interface (hypolimnion), which was between 10 and 11 m depth for site 1, between 19 and 23.5 m depth for site 2, between 10 and 11 m depth for site 3, and between 8.5 and 19 m depth for site 4. Concentrations of DSi and SRSi were not significantly different. Hypolimnion DSi concentrations were significantly different between sites 2 and 3. DSi concentrations at site 2 were significantly different between the epilimnion and hypolimnion. Hypolimnion TDP concentrations were significantly different between sites 1 and 2 and between sites 2 and 3. TDP concentrations at site 2 were significantly different between the epilimnion and hypolimnion. All significant differences were determined by one-way ANOVA at the $\alpha = 0.05$ level, followed by a Tukey HSD test.

Date (D/M/Y)	**Concentration (µmol L^{-1})**								
	Site 1 (70270)			Site 2 (258)			Site 3 (7007)		
	DSi	SRSi	TDP	DSi	SRSi	TDP	DSi	SRSi	TDP
20/04/16	0.82		0.86	6.29	6.37	0.98	7.40		0.97
4/05/16	1.33		0.80	1.76		0.87	1.89		0.63
18/05/16	1.24		1.22	3.60		0.62	2.51		0.84
31/05/16	4.67		0.96	7.94	10.26	1.14	4.80		0.58
14/06/16	7.35	8.76	0.54	14.38		1.24	8.11		0.57
29/06/16	10.27		1.05	14.69		0.97	7.69	7.65	1.08
12/07/16	12.05	14.92	0.95	27.58	33.69	1.30	13.84		0.94
26/07/16	20.26	22.15	0.82	23.41	26.51	0.82	14.17	14.04	0.65
11/08/16	14.27		0.80	32.49	37.08	1.89	17.84		0.83
24/08/16	23.26		1.34	32.65		2.92	16.92		0.51
08/09/16	19.58		0.72	31.40	37.47	3.62	14.02		0.53
20/09/16	18.94	18.35	0.56	44.95		6.54	14.40	14.63	0.77
05/10/16	18.98		1.25	28.89		2.93	22.11		1.99
19/10/16	23.42	24.12	1.43	39.64	41.87	2.73	20.29	20.95	1.25
04/11/16	22.97	22.25	1.46	24.03	23.81	1.32	23.33		1.21
Mean	13.29		0.98	22.25		1.99	12.62		0.89

Date (D/M/Y)	**Concentration (µmol L^{-1})**				
	Site 4 (W3)			Mean All Sites	
	DSi	SRSi	TDP	DSi	TDP
20/04/16	4.26	4.14	1.02	4.69	0.96
4/05/16	2.04		0.83	1.75	0.78
18/05/16	3.23		0.86	2.65	0.88
31/05/16	7.38		0.94	6.20	0.90
14/06/16	10.34	12.69	0.70	10.04	0.76
29/06/16	8.79	4.26	1.07	10.36	1.04
12/07/16	12.37		1.11	16.46	1.07
26/07/16	8.83		0.95	16.67	0.81
11/08/16	12.31	13.75	0.66	19.23	1.12
24/08/16	15.73	14.10	1.07	22.14	1.46
08/09/16	34.66	35.07	3.59	24.92	2.12
20/09/16	10.87		0.38	22.29	2.06
05/10/16	23.48		1.71	23.37	1.97
19/10/16	21.05	21.53	1.59	26.10	1.75
04/11/16	21.43		1.21	22.94	1.30
Mean	13.12		1.18	15.32	1.27

A1 Table 4. Wt% Si, total suspended solids (TSS) and RPSi concentrations measured at sites 1, 2, 3, and 4 across Hamilton Harbour from 1 m below the surface (epilimnion). Samples were extracted in groups in order to have enough suspended particulate matter and the resulting wt% Si is the mean of sample group. RPSi concentrations showed no significant differences between the 4 sites or with depth in a one-way ANOVA at the $\alpha = 0.05$ level.

Date (D/M/Y)	**Site 1 (70270)**			**Site 2 (258)**		
	Wt% Si	TSS (mg L^{-1})	RPSi (µmol L^{-1})	Wt% Si	TSS (mg L^{-1})	RPSi (µmol L^{-1})
20/04/16	6.12	6.10	13.29	7.92	4.88	13.75
4/05/16	5.07	3.25	5.87	7.92	2.17	6.12
18/05/16	5.07	2.13	3.84	4.89	3.09	5.37
31/05/16	5.07	1.23	2.23	4.89	1.72	5.37
14/06/16	7.17	1.96	5.00	5.28	1.97	3.70
29/06/16	7.17	0.69	1.75	5.28	0.59	1.11
12/07/16	7.17	1.96	5.00	5.28	1.59	2.98
26/07/16	7.17	1.27	3.25	5.28	1.07	2.02
11/08/16	3.38	2.41	2.90	2.96	3.09	3.25
24/08/16	3.38	0.40	0.48	2.96	0.68	0.72
08/09/16	3.38	1.09	1.31	2.96	2.39	2.51
20/09/16	9.49	1.62	5.48	6.59	0.97	2.27
05/10/16	9.49	0.50	1.68	6.59	1.48	3.48
19/10/16	9.49	1.26	4.26	6.59	1.18	2.77
04/11/16	9.49	1.49	5.04	6.59	0.99	2.32
Mean			**4.09**			**3.85**

Date (D/M/Y)	**Site 3 (7007)**			**Site 4 (W3)**			**Mean All Sites**
	Wt% Si	TSS (mg L^{-1})	RPSi (µmol L^{-1})	Wt% Si	TSS (mg L^{-1})	RPSi (µmol L^{-1})	RPSi (µmol L^{-1})
20/04/16	9.41	3.84	12.85	8.50	4.71	14.25	13.54
4/05/16	9.41	1.75	5.88	8.50	2.76	8.35	8.06
18/05/16	6.15	2.73	5.98	4.16	2.44	3.62	4.30
31/05/16	6.15	1.35	2.95	4.16	2.84	4.20	4.14
14/06/16	3.50	12.70	15.82	4.61	2.45	4.02	7.13
29/06/16	3.50	0.50	0.63	4.61	0.98	1.61	1.27
12/07/16	3.50	1.61	2.00	4.61	1.46	2.39	3.09
26/07/16	3.50	1.00	1.24	4.61	1.71	2.81	2.33
11/08/16	3.24	2.63	3.03	3.56	2.76	3.50	3.17
24/08/16	3.24	1.20	1.38	3.56	2.86	3.62	1.55
08/09/16	3.24	1.07	1.23	3.56	2.22	2.81	1.97
20/09/16	6.23	2.15	4.77	5.48	2.20	4.30	4.20
05/10/16	6.23	0.98	2.18	5.48	0.78	1.52	2.21
19/10/16	6.23	0.85	1.89	5.48	1.58	3.08	3.00
04/11/16	6.23	1.33	2.95	5.48	1.37	2.67	3.25
Mean			**4.32**			**4.18**	**4.21**

A1 Table 5. Wt% Si, total suspended solids (TSS) and RPSi concentrations measured at sites 1, 2, 3, and 4 across Hamilton Harbour from 1 m above the sediment water interface (hypolimnion), which was between 10 and 11 m depth for Site 1, between 19 and 23.5 m depth for Site 2, between 10 and 11 m depth for Site 3, and between 8.5 and 19 m depth for Site 4. Samples were extracted in groups in order to have enough suspended particulate matter and the resulting wt% Si is the mean of sample group. RPSi concentrations showed no significant differences between the 4 sites or with depth in a one-way ANOVA at the $\alpha = 0.05$ level.

Date (D/M/Y)	**Site 1 (70270)**			**Site 2 (258)**		
	Wt% Si	TSS (mg L^{-1})	RPSi (µmol L^{-1})	Wt% Si	TSS (mg L^{-1})	RPSi (µmol L^{-1})
20/04/16	6.58	5.07	11.88	7.07	3.86	9.73
4/05/16	5.06	2.24	4.04	7.07	2.01	9.73
18/05/16	5.06	2.32	4.18	7.46	2.74	7.27
31/05/16	5.06	6.84	12.33	7.46	2.02	5.36
14/06/16	6.86	2.15	5.24	3.21	1.25	1.42
29/06/16	6.86	1.09	2.67	3.21	5.61	6.40
12/07/16	6.86	1.80	4.39	3.21	0.60	0.69
26/07/16	6.86	2.26	5.52	3.21	1.20	1.37
11/08/16	6.71	1.96	4.68	1.29	2.42	1.12
24/08/16	6.71	1.83	4.38	1.29	1.46	0.67
08/09/16	6.71	1.18	2.83	1.29	1.09	0.50
20/09/16	7.89	1.08	3.02	5.76	3.40	6.97
05/10/16	7.89	1.16	3.27	5.76	1.48	3.03
19/10/16	7.89	1.71	4.80	5.76	5.09	10.44
04/11/16	7.89	2.00	5.62	5.76	1.79	3.67
Mean			5.26			4.56

Date (D/M/Y)	**Site 3 (7007)**			**Site 4 (W3)**			**Mean All Sites**
	Wt% Si	TSS (mg L^{-1})	RPSi (µmol L^{-1})	Wt% Si	TSS (mg L^{-1})	RPSi (µmol L^{-1})	RPSi (µmol L^{-1})
20/04/16	9.25	4.79	15.78	8.23	4.91	14.38	11.44
4/05/16	9.25	2.37	7.81	8.23	2.39	6.99	7.09
18/05/16	7.27	2.95	7.63	6.79	3.28	7.92	6.75
31/05/16	7.27	1.73	4.48	6.79	2.22	5.38	6.89
14/06/16	5.38	1.79	3.43	1.26	1.38	0.62	2.68
29/06/16	5.38	0.69	1.33	1.26	18.61	8.35	4.69
12/07/16	5.38	5.09	9.75	1.26	1.12	0.50	3.83
26/07/16	5.38	0.88	1.69	1.26	1.57	0.70	2.32
11/08/16	10.35	1.55	5.73	3.80	1.57	2.13	3.41
24/08/16	10.35	0.00	0.00	3.80	1.66	2.25	1.83
08/09/16	10.35	1.06	3.90	3.80	2.23	3.02	2.56
20/09/16	10.10	0.98	3.53	6.49	1.76	4.08	4.40
05/10/16	10.10	0.49	1.75	6.49	0.93	2.14	2.55
19/10/16	10.10	1.47	5.28	6.49	1.81	4.19	6.18
04/11/16	10.10	1.39	4.98	6.49	2.11	4.88	4.79
Mean			5.14			4.50	4.76

A1 Table 6. Monthly gross sedimentation downflux, wt% Si, and RPSi flux from May to November 2016. Suspended sediments were unable to be collected from site 1 in August and from site 2 in September and October.

Month	Site 1 (9031)			Site 2 (9032)		
	Wt% Si	Down-flux (g cm^{-2} day^{-1})	RPSi (mmol m^{-2} day^{-1})	Wt% Si	Down-flux (g cm^{-2} day^{-1})	RPSi (mmol m^{-2} day^{-1})
May	4.89	27.04	47.05	7.49	22.42	59.81
Jun.	3.32	33.41	39.50	4.75	21.40	36.22
Jul.	3.56	31.26	39.61	7.15	9.22	23.49
Aug.				3.94	14.84	20.79
Sept.	3.00	39.17	41.78			
Oct.	3.39	15.95	19.23			
Nov.	4.66	43.91	72.94	7.37	82.40	216.35

Month	Site 3 (9030)			Site 4 (9033)			Mean All Sites
	Wt% Si	Down-flux (g cm^{-2} day^{-1})	RPSi (mmol m^{-2} day^{-1})	Wt% Si	Down-flux (g cm^{-2} day^{-1})	RPSi (mmol m^{-2} day^{-1})	RPSi (mmol m^{-2} day^{-1})
May	6.26	31.01	69.18	4.37	54.88	85.29	65.33
Jun.	4.38	12.77	19.93	3.29	18.69	21.92	29.39
Jul.	5.71	10.91	22.18	3.78	29.80	40.07	31.34
Aug.	3.88	14.16	19.57	2.80	32.30	32.21	24.19
Sept.	3.43	21.63	26.38	2.49	28.71	25.45	31.20
Oct.	3.53	10.83	13.63	3.46	14.58	17.96	16.94
Nov.	4.36	35.25	54.74	4.14	73.40	108.29	113.08

A1 Table 7. Concentrations of DSi, SRSi, and TDP and Si:P ratios measured at WWTP 1. No significant differences were found between DSi and SRSi (t-test at the $\alpha = 0.05$ level).

Date	Concentration (µmol L^{-1})			Si:P
(D/M/Y)	DSi	SRSi	TDP	
04/11/2015	75.06		4.49	16.72
10/11/2015	60.01	67.26	4.83	12.42
18/11/2015	63.85		4.63	13.79
23/11/2015	59.62	67.39	7.37	8.09
03/12/2015	66.61	70.55	11.62	5.73
22/12/2015	69.96	75.27	5.30	13.20
29/12/2015	78.77	82.89	3.41	23.10
05/01/2016	84.48	86.92	1.94	43.55
10/02/2016	80.41	83.68	1.79	44.92
17/02/2016	73.81	75.30	1.16	63.63
24/02/2016	71.36	72.67	1.40	50.97
02/03/2016	90.04	89.94	1.28	70.34
08/03/2016	92.17	98.25	1.04	88.63
16/03/2016	101.60		1.08	94.07
23/03/2016	91.29	97.21	2.34	39.01
30/03/2016	108.25		1.15	94.13
06/04/2016	105.15	114.78	0.98	107.30
20/04/2016	91.14	93.59	1.06	85.98
01/06/2016	57.59	68.99	6.92	8.32
08/06/2016	55.88	67.51	4.33	12.91
06/07/2016	44.16	50.57	2.74	16.12
13/07/2016	47.32		3.55	13.33
20/07/2016	53.25		3.84	13.87
27/07/2016	58.90	65.71	4.29	13.73
03/08/2016	57.58		3.00	19.19
10/08/2016	52.32	57.85	4.04	12.95
17/08/2016	73.25	81.72	2.95	24.83
24/08/2016	68.07	74.53	3.03	22.47
31/08/2016	70.43		2.22	31.73
05/10/2016	59.69	61.44	2.81	21.24
12/10/2016	61.84		3.21	19.26
19/10/2016	51.90	53.27	7.99	6.50
26/10/2016	65.81		3.32	19.82
09/11/2016	67.36		1.89	35.64
17/11/2016	65.19	68.89	2.40	27.16
23/11/2016	66.05		1.74	37.96
30/11/2016	70.28		2.39	29.41

A1 Table 8. Wt% Si, total suspended solids (TSS) and RPSi concentrations measured at WWTP1. Samples were grouped by month and extracted together. Samples were not collected in September 2016.

Year	Month	Wt% Si	TSS (mg/L)	RPSi (µmol L^{-1})
2015	November	3.53	3.77	4.74
	December	1.39	8.16	4.05
2016	January	1.52	1.50	0.81
	February	3.36	1.60	1.92
	March	3.12	1.92	2.13
	April	1.55	1.50	0.83
	May	2.24	2.38	1.90
	June	1.77	2.69	1.69
	July	1.94	1.14	0.79
	August	2.79	1.16	1.15
	September			
	October	2.14	0.60	0.46
	November	1.45	2.01	1.04

A1 Table 9. Concentrations of DSi, SRSi, and TDP and Si:P ratios measured at WWTP 2. No significant differences were found between DSi and SRSi (t-test at the $\alpha = 0.05$ level).

Date (D/M/Y)	Sample number	Concentration (μmol L^{-1})					Si:P
		DSi	SRSi	TDP	Mean DSi	Mean TDP	
11/11/2015	1	85.86		5.16	69.33	5.22	13.28
	2	85.97	95.07	5.14			
	3	36.16		5.35			
26/11/2015	1	65.45	70.80	11.75	65.20	11.68	5.58
	2	65.06		11.53			
	3	65.10		11.77			
06/01/2016	1	77.61	81.70	13.89	78.21	13.67	5.72
	2	79.71	81.81	13.77			
	3	77.29	80.55	13.36			
03/02/2016	1	63.36		3.03	64.55	3.06	21.09
	2	64.76	64.40	3.22			
	3	65.12		3.04			
	4	64.98	64.53	2.96			
10/03/2016	1	110.65	113.62	6.83	110.92	6.59	16.83
	2	109.93		6.37			
	3	109.93		6.56			
	4	113.18		6.61			
07/04/2016	1	117.06	124.10	1.79	118.32	1.74	68.00
	2	117.60		1.69			
	3	120.30		1.75			
27/04/2016	1	82.01	86.36	4.24	81.34	4.23	19.23
	2	80.45		4.45			
	3	81.14	86.53	3.90			
	4	81.74		4.32			
26/05/2016	1	68.11		16.80	68.43	17.26	3.96
	2	68.42		17.13			
	3	67.76		17.56			
	4	69.43		17.55			
22/06/2016	1	56.21	67.27	11.91	55.83	11.94	4.68
	2	55.52		12.03			
	3	55.72		11.78			
	4	55.88	66.42	12.01			
21/07/2016	1	51.31	61.69	12.15	51.12	12.32	4.15
	2	51.42		12.75			
	3	50.86		12.19			
	4	50.89		12.19			
18/08/2016	1	66.26	74.68	6.61	65.75	6.68	9.84
	2	65.36		6.30			
	3	65.48		7.11			
	4	65.88	73.80	6.72			
03/10/2016	1	74.80	82.59	1.43	74.76	1.75	42.72
	2	75.04		1.93			
	3	74.92		1.80			
	4	74.28		1.85			
03/11/2016	1	40.49	41.52	8.83	41.10	8.05	5.11
	2	12.10		5.95			
	3	55.94		8.71			
	4	55.87		8.69			

A1 Table 9. Continued

Date (D/M/Y)	Sample number	Concentration (µmol L^{-1})					Si:P
		DSi	SRSi	TDP	Mean DSi	Mean TDP	
30/11/2016	1	67.68		5.99	67.94	6.14	11.07
	2	68.22		6.25			
	3	67.92	71.92	6.22			
	4	67.92		6.09			

A1 Table 10. Wt% Si, total suspended solids (TSS) and RPSi concentrations measured at WWTP 2. Grab samples taken on the same date were combined and extracted together.

Date (D/M/Y)	Wt% Si	TSS (mg L^{-1})	RPSi (µmol L^{-1})
26/11/2015	0.56	3.82	0.76
06/01/2016	0.41	7.75	1.13
03/02/2016	0.78	16.85	4.67
10/03/2016	0.43	5.76	0.89
07/04/2016	0.36	16.60	2.12
27/04/2016	0.41	13.01	1.90
26/05/2016	0.39	11.53	1.59
22/06/2016	0.68	3.54	0.86
21/07/2016	0.73	2.38	0.61
18/08/2016	0.52	7.60	1.41
03/10/2016	0.60	9.05	1.94
03/11/2016	1.27	19.28	8.69
30/11/2016	0.43	4.85	0.74

A1 Table 11. Concentrations of DSi, SRSi, and TDP and Si:P ratios measured at steel mill intake and one steel mill discharge point (contact water). No significant differences were found between DSi and SRSi for either site (t-test at the $\alpha = 0.05$ level).

Date (D/M/Y)	Concentration (μmol L^{-1})						Si:P	
	Intake			Discharge			Intake	Discharge
	DSi	SRSi	TDP	DSi	SRSi	TDP		
02/11/2015	8.73	9.94	1.26	12.28		1.71	6.93	7.18
09/11/2015	5.04		1.03	9.59	10.27	1.26	4.89	7.61
16/11/2015	5.13	5.70	1.12	9.18	9.77	1.29	4.58	7.12
23/11/2015	20.23	10.73	1.13	9.55	10.47	1.85	17.90	5.16
30/11/2015	8.65	9.79	1.09	12.84	13.72	1.69	7.94	7.60
07/12/2015	9.77	10.94	1.00	10.41	11.40	1.33	9.77	7.83
14/12/2015	15.84	16.88	0.95	10.19	11.24	1.29	16.67	7.90
21/12/2015	9.30	10.44	1.36	12.24	13.24	1.62	6.84	7.56
28/12/2015				18.20		2.42		7.52
04/01/2016	10.68	9.48	1.42	13.24		1.18	7.52	11.22
11/01/2016	11.53		1.63	15.54	14.84	7.17	7.07	2.17
18/01/2016	9.65	9.34	1.40	11.57		1.03	6.89	11.23
25/01/2016	9.42		1.11	11.93	11.28	1.13	8.49	10.56
01/02/2016	7.70		1.07	10.13		1.06	7.20	9.56
15/02/2016	5.31	4.10	1.38	9.70	8.70	1.13	3.85	8.58
22/02/2016	4.66	3.63	1.15	6.87	6.07	1.24	4.05	5.54
29/02/2016	6.12	6.21	1.16	10.06	10.82	1.14	5.28	8.82
07/03/2016	2.95		0.87	5.98		1.07	3.39	5.59
14/03/2016	2.19	2.07	0.96	6.33	6.57	1.04	2.28	6.09
21/03/2016	2.58		0.50	5.54		0.81	5.16	6.84
28/03/2016	7.55	7.70	0.73	12.49	13.16	0.87	10.34	14.36
11/04/2016	11.21	11.14	1.17	13.83	14.07	1.06	9.58	13.05
18/04/2016	4.52		1.02	8.48		1.15	4.43	7.37
25/04/2016	5.66		0.95	6.79		1.03	5.96	6.59
16/05/2016	7.90		1.64	9.10		2.06	4.82	4.42
23/05/2016	6.35		1.43	7.27		0.96	4.44	7.57
30/05/2016	8.02	9.78	1.34	9.87	11.46	1.86	5.99	5.31
06/06/2016	9.90	11.99	1.83	10.48	12.46	2.47	5.41	4.24
13/06/2016	8.03		0.97	10.63		1.23	8.28	8.64
20/06/2016	8.20	8.11	1.50	12.02		1.79	5.47	6.72
27/06/2016	12.92		1.12	14.28	16.39	1.35	11.54	10.58
04/07/2016	12.57		1.04	16.59		1.36	12.09	12.20
11/07/2016	14.87	14.11	1.32	16.09	17.60	1.63	11.27	9.87
18/07/2016	12.66	13.48	1.33	15.15	15.34	1.16	9.52	13.06
25/07/2016	14.11		0.69	18.40	19.29	0.84	20.45	21.90
01/08/2016	15.09	16.15	0.80	21.43		0.70	18.86	30.61
08/08/2016	14.78	15.38	0.81	19.41	20.49	1.92	18.25	10.11
29/08/2016	20.19		0.90	23.21		0.90	22.43	25.79
05/09/2016	18.37		0.38	22.38	24.43	0.83	48.34	26.96
12/09/2016	16.34	17.64	0.90	18.40		0.87	18.16	21.15
19/09/2016	24.02		0.65	23.86	25.81	0.99	36.95	24.10
26/09/2016	16.36	17.39	1.23	18.94		1.02	13.30	18.57
03/10/2016	25.68	26.01	1.31	30.28	31.06	1.86	19.60	16.28
10/10/2016	21.50		1.47	26.54		1.17	14.63	22.68
24/10/2016	26.70	27.19	1.56	33.27		2.28	17.12	14.59
31/10/2016	25.54		10.32	33.32		1.62	2.47	20.57
07/11/2016	22.61	22.44	1.23	25.52		1.43	18.38	17.85

A1 Table 11. Continued

Date (D/M/Y)	Concentration (µmol L^{-1})						Si:P	
	Intake			Discharge			Intake	Discharge
	DSi	SRSi	TDP	DSi	SRSi	TDP		
14/11/2016	22.68		1.36	30.15		1.87	16.68	16.12
21/11/2016	24.63		1.39	29.64	30.79	1.74	17.72	17.03
28/11/2016	18.18		0.98	21.85		1.13	18.55	19.34

A1 Table 12. Wt% Si, total suspended solids (TSS) and RPSi concentrations measured at steel mill intake and one steel mill discharge point (contact water). Samples were grouped by month and extracted together.

Year	Month	Intake			Discharge		
		Wt% Si	TSS ($mg\ L^{-1}$)	RPSi ($\mu mol\ L^{-1}$)	Wt% Si	TSS ($mg\ L^{-1}$)	RPSi ($\mu mol\ L^{-1}$)
2015	Nov.	15.27	0.87	4.73	14.37	2.19	11.19
	Dec.	5.59	0.79	1.57	5.48	1.87	3.65
2016	Jan.	7.65	1.00	2.73	7.67	2.24	6.12
	Feb.	13.74	1.21	5.92	14.46	1.76	9.08
	Mar.	11.62	2.35	9.74	13.23	2.45	11.53
	Apr.	8.43	3.16	9.48	8.52	2.65	8.04
	May	5.96	1.69	3.59	6.47	3.27	7.52
	Jun.	7.09	1.33	3.37	5.99	1.52	3.24
	Jul.	11.27	1.05	4.21	9.57	1.52	5.18
	Aug.	10.80	0.39	1.50	4.94	1.74	3.05
	Sept.	7.54	1.14	3.07	11.36	0.73	2.97
	Oct.	5.92	2.31	4.86	4.35	3.07	4.76
	Nov.	7.66	2.10	5.73	5.52	2.92	5.75

A1 Table 13. May to November 2016 monthly DSi fluxes ± uncertainty. A positive value of net uptake indicates net assimilation of DSi to RPSi, and negative value for net uptake indicates net dissolution of RPSi to DSi. DSi sources are tributaries, Cootes' Paradise, WWTPs, CSOs, steel mill discharge, groundwater, precipitation, net dissolution, internal loading, and Lake Ontario (L. Ontario) inflow. DSi sinks are net uptake, steel mill withdrawal and Hamilton Harbour (H. H.) outflow.

DSi Flux	**DSi Flux (10^3 moles day^{-1})**			
	May	Jun.	Jul.	Aug.
Tributaries	8.4 ± 3.8	7.3 ± 3.3	5.0 ± 2.3	3.9 ± 1.8
Cootes' Paradise	10.4 ± 5.7	13.3 ± 7.3	2.5 ± 1.4	5.1 ± 2.8
WWTPs	31.1 ± 6.5	22.7 ± 4.8	20.3 ± 4.3	25.0 ± 5.2
CSOs	0.9 ± 0.9	0.9 ± 0.9	0.9 ± 0.9	0.9 ± 0.9
Steel mill withdrawal	5.0 ± 1.8	7.1 ± 2.5	9.7 ± 3.4	15.4 ± 5.4
Steel mill discharge	5.3 ± 1.9	7.6 ± 2.7	10.6 ± 3.7	16.4 ± 5.7
Groundwater	10.6 ± 7.4	10.6 ± 7.4	10.6 ± 7.4	10.6 ± 7.4
Precipitation	0.2 ± 0.2	0.2 ± 0.2	0.2 ± 0.2	0.2 ± 0.2
Net uptake/dissolution	145.7 ± 58.3	69.2 ± 27.7	38.1 ± 15.3	-37.9 ± 15.2
Internal loading	31.2 ± 12.5	38.7 ± 15.5	41.1 ± 16.4	43.6 ± 17.5
L. Ontario inflow	67.0 ± 24.4	53.9 ± 19.6	46.7 ± 17.0	14.6 ± 5.3
H. H. outflow	18.5 ± 4.1	41.3 ± 9.2	59.6 ± 13.3	91.6 ± 20.5

DSi Flux	**DSi Flux (10^3 moles day^{-1})**		
	Sept.	Oct.	Nov.
Tributaries	2.6 ± 1.2	5.5 ± 2.5	5.8 ± 2.6
Cootes' Paradise	3.1 ± 1.7	11.4 ± 6.3	12.7 ± 7.0
WWTPs	28.7 ± 6.0	17.9 ± 3.8	27.3 ± 5.7
CSOs	0.9 ± 0.9	0.9 ± 0.9	0.9 ± 0.9
Steel mill withdrawal	12.7 ± 4.4	12.4 ± 4.3	10.5 ± 3.7
Steel mill discharge	13.3 ± 4.6	13.5 ± 4.7	11.1 ± 3.9
Groundwater	10.6 ± 7.4	10.6 ± 7.4	10.6 ± 7.4
Precipitation	0.2 ± 0.2	0.2 ± 0.2	0.2 ± 0.2
Net uptake/dissolution	42.1 ± 16.8	-60.0 ± 24.0	71.3 ± 28.5
Internal loading	48.4 ± 19.3	49.1 ± 19.6	34.0 ± 13.6
L. Ontario inflow	29.8 ± 10.8	41.0 ± 14.9	17.1 ± 6.2
H. H. outflow	88.5 ± 19.8	132.7 ± 29.7	37.8 ± 8.4

A1 Table 14. May to November 2016 monthly RPSi fluxes ± uncertainty. A positive value of net uptake indicates net assimilation of DSi to RPSi, and negative value for net uptake indicates net dissolution of RPSi to DSi. RPSi sources are tributaries, Cootes' Paradise, WWTPs, CSOs, steel mill discharge, net uptake, resuspension, and Lake Ontario (L. Ontario) inflow. RPSi sinks are net dissolution, steel mill withdrawal, sedimentation, burial and Hamilton Harbour (H. H.) outflow.

RPSi Flux	**Flux (10^3 moles day^{-1})**			
	May	Jun	Jul	Aug
Tributaries	1.6 ± 0.7	1.4 ± 0.6	1.0 ± 0.4	0.7 ± 0.3
Cootes' Paradise	2.0 ± 1.1	2.5 ± 1.4	0.5 ± 0.3	1.0 ± 0.5
WWTPs	0.7 ± 0.2	0.4 ± 0.1	0.3 ± 0.1	0.6 ± 0.1
CSOs	0.2 ± 0.2	0.3 ± 0.3	0.3 ± 0.3	0.2 ± 0.2
Steel mill discharge	3.4 ± 1.2	2.4 ± 0.9	3.5 ± 1.3	2.5 ± 0.9
Steel mill withdrawal	2.4 ± 0.9	2.4 ± 0.9	3.3 ± 1.2	2.5 ± 0.9
Net uptake	145.7 ± 58.3	69.2 ± 27.7	38.1 ± 15.3	-37.9 ± 15.2
Sedimentation	1490.0 ± 461.9	650.2 ± 201.5	784.7 ± 243.2	553.6 ± 171.6
Resuspension	1309.4 ± 405.9	568.1± 176.1	741.2 ± 229.8	589.5 ± 182.7
Burial	149.5 ± 46.3	43.3 ± 13.4	2.4 ± 0.7	79.5 ± 24.7
L. Ontario inflow	10.1 ± 4.8	10.1 ± 4.8	10.1 ± 4.8	10.1 ± 4.8
H. H. outflow	37.3 ± 12.4	23.0 ± 7.7	16.5 ± 5.5	14.2 ± 4.7

RPSi Flux	**Flux (10^3 moles day^{-1})**		
	Sept.	Oct.	Nov.
Tributaries	0.5 ± 0.2	1.1 ± 0.5	1.1 ± 0.5
Cootes' Paradise	0.6 ± 0.3	2.2 ± 1.2	2.4 ± 1.3
WWTPs	1.3 ± 0.3	1.3 ± 0.3	2.6 ± 0.6
CSOs	0.2 ± 0.2	0.2 ± 0.2	0.9 ± 0.9
Steel mill discharge	3.1 ± 1.1	3.2 ± 1.2	4.3 ± 1.5
Steel mill withdrawal	2.5 ± 0.9	3.2 ± 1.2	3.4 ± 1.2
Net uptake	42.1 ± 16.8	-60.0 ± 24.0	71.3 ± 28.5
Sedimentation	678.4 ± 210.3	365.2 ± 113.2	2309.6 ± 716.0
Resuspension	649.2 ± 201.2	432.6 ± 134.1	2240.5 ± 694.5
Burial	19.1 ± 5.9	116.4 ± 36.1	35.1 ± 10.9
L. Ontario inflow	10.1 ± 4.8	10.1 ± 4.8	1.6 ± 0.8
H. H. outflow	18.7 ± 6.2	20.3 ± 6.8	6.7 ± 2.2

Appendix 2

Uncertainty Analysis

A2 Table 1. Water budget uncertainty. ε denotes relative uncertainty as a percent.

Water Source	Sources of uncertainty	Assigned ε (%)	Reference/Calculation	Total ε (%)
Grindstone Creek	Current meter	5	Winter (1981)	**15**
	Stage-discharge relationship	5	Winter (1981)	
	Channel bias	5	Winter (1981)	
Redhill Creek	Current meter	5	Winter (1981)	**15**
	Stage-discharge relationship	5	Winter (1981)	
	Channel bias	5	Winter (1981)	
Indian Creek	Current meter	5	Winter (1981)	**25**
	Stage-discharge relationship	5	Winter (1981)	
	Channel bias	5	Winter (1981)	
	Regression relationship	10	Tanya Long, personal communication	
Cootes' Paradise	Current meter	5	Winter (1981)	**25**
	Stage-discharge relationship	5	Winter (1981)	
	Channel bias	5	Winter (1981)	
	Regression relationship	10	Tanya Long, personal communication	
WWTPs	Flow meter	1	Ministry of the Environment (2008); City of Hamilton (2011); Regional Municipality of Halton (2011)	**1**
CSO	MIKE URBAN Model	20	City of Hamilton (2017)	**20**
Steel Mill	Flow meter	15	Ministry of the Environment and Climate Change (2015)	**15**
Groundwater	Hydraulic conductivity estimation methods	50	Estimate	**50**
Precipitation	Gage type	2	Winter (1981)	**17**
	Gage placement	5	Winter (1981)	
	Gage density	10	Winter (1981)	
Lake Ontario Inflow	Model uncertainty	11.35	Hamblin & He (2003)	**11.35**
Evaporation	Measurement error	10	Winter (1981)	**40**
	Pan to lake coefficient	15	Winter (1981)	
	Areal averaging	15	Winter (1981)	
Hamilton Harbour Outflow	Sum of Δ of all water sources divided by total discharge	12.35	Calculated	**12.35**

A2 Table 2. DSi concentration uncertainty. ε denotes relative uncertainty as a percent.

DSi Source/Sink	Sources of uncertainty	Assigned ε	Reference/Calculation	Total ε
Grindstone Creek	Analytical uncertainty	10	Ministry of the Environment and Climate Change (2014)	**30**
	Partitioning of DSi and RPSi	20	Conley (1997)	
Redhill Creek	Analytical uncertainty	10	Ministry of the Environment and Climate Change (2014)	**30**
	Partitioning of DSi and RPSi	20	Conley (1997)	
Indian Creek	Analytical uncertainty	10	Ministry of the Environment and Climate Change (2014)	**30**
	Partitioning of DSi and RPSi	20	Conley (1997)	
Cootes' Paradise	Analytical uncertainty	10	Ministry of the Environment and Climate Change (2014)	**30**
	Partitioning of DSi and RPSi	20	Conley (1997)	
WWTPs	Analytical uncertainty	15	Performance of QA/QC samples	**20**
	Sample storage time	5	Estimated from difference of DSi measured in sample stored for 1 week versus stored for 8 weeks	
CSO	Analytical uncertainty	15	Performance of QA/QC samples	**80**
	Sample storage	15	Estimated from difference of DSi measured in sample stored for 1 week versus stored for 8 weeks	
	Spatial uncertainty	50	Estimate	
Steel Mill	Analytical uncertainty	15	Performance of QA/QC samples	**20**
	Sample storage time	5	Estimated from difference of DSi measured in sample stored for 1 week versus stored for 8 weeks	
Groundwater	Analytical uncertainty	10	Ministry of the Environment and Climate Change (2014)	**20**
	Spatial uncertainty	10	Difference in DSi between 2 wells	
Precipitation	Analytical uncertainty	10	Ministry of the Environment and Climate Change (2014)	**80**
	Sampling uncertainty	20	Estimated based on Galloway & Likens (1978)	
	Spatial uncertainty	50	Estimated based on Galloway & Likens (1978)	
Lake Ontario Inflow	Analytical uncertainty	10	Ministry of the Environment and Climate Change (2014)	**25**
	Spatial variability	15	Estimated from difference in DSi concentration between 2 monitoring sites	
Hamilton Harbour Outflow	Analytical uncertainty	15	Performance of QA/QC samples	**20**
	Sample storage time	5	Estimated from difference of DSi measured in sample stored for 1 week versus stored for 8 weeks	
Internal loading	Analytical uncertainty	15	Performance of QA/QC samples	**15**

A2 Table 3. RPSi concentration uncertainty. ε denotes relative uncertainty as a percent.

RPSi Source/Sink	Sources of uncertainty	Assigned ε	Reference/Calculation	Total ε
Grindstone Creek	Analytical uncertainty	10	Ministry of the Environment and Climate Change (2014)	**30**
	Partitioning of DSi and RPSi	20	Conley (1997)	
Redhill Creek	Analytical uncertainty	10	Ministry of the Environment and Climate Change (2014)	**30**
	Partitioning of DSi and RPSi	20	Conley (1997)	
Indian Creek	Analytical uncertainty	10	Ministry of the Environment and Climate Change (2014)	**30**
	Partitioning of DSi and RPSi	20	Conley (1997)	
Cootes' Paradise	Analytical uncertainty	10	Ministry of the Environment and Climate Change (2014)	**30**
	Partitioning of DSi and RPSi	20	Conley (1997)	
WWTPs	Extraction uncertainty	21	Average difference between measured and published value for reference material Conley (1998)	**21**
CSO	Spatial uncertainty	50	Estimate	**86**
	Extraction uncertainty	21	Average difference between measured and published value for reference material (Conley 1998)	
	Use of WWTP 2 concentration	15	Estimate	
Steel Mill	Extraction uncertainty	21	Average difference between measured and published value for reference material (Conley 1998)	**21**
Lake Ontario Inflow	Extraction uncertainty	21	Average difference between measured and published value for reference material (Conley 1998)	**36**
	Use of Hamilton Harbour concentration	15	Estimate	
Hamilton Harbour Outflow	Extraction uncertainty	21	Average difference between measured and published value for reference material (Conley 1998)	**21**
Sedimentation	Extraction uncertainty	21	Average difference between measured and published value for reference material (Conley 1998)	**21**

A2 Table 4. Reactive Si flux uncertainty. ε denotes relative uncertainty as a percent.

Si Flux	Sources of uncertainty	Assigned ε	Reference/ Calculation	Total DSi Flux ε	Total RPSi Flux ε
Tributaries	Discharge	15	See A2 Table 1	**45**	**45**
	DSi Concentration	30	See A2 Table 2		
	RPSi Concentration	30	See A2 Table 3		
Cootes' Paradise	Discharge	25	See A2 Table 1	**55**	**55**
	DSi Concentration	30	See A2 Table 2		
	RPSi Concentration	30	See A2 Table 3		
WWTPs	Discharge	1	See A2 Table 1	**21**	**22**
	DSi Concentration	20	See A2 Table 2		
	RPSi Concentration	21	See A2 Table 3		
CSO	Discharge	20	See A2 Table 1	**100**	**106**
	DSi Concentration	80	See A2 Table 2		
	RPSi Concentration	86	See A2 Table 3		
Steel mill intake and discharge	Discharge	15	See A2 Table 1	**35**	**36**
	DSi Concentration	20	See A2 Table 2		
	RPSi Concentration	21	See A2 Table 3		
Groundwater	Discharge	50	See A2 Table 1	**70**	
	DSi Concentration	20	See A2 Table 2		
Precipitation	Discharge	80	See A2 Table 1	**90**	
	DSi Concentration	10	See A2 Table 2		
Lake Ontario inflow	Discharge	11.35	See A2 Table 1	**36.35**	**47.35**
	DSi Concentration	25	See A2 Table 2		
	RPSi Concentration	36	See A2 Table 3		
Hamilton Harbour outflow	Discharge	12.35	See A2 Table 1	**22.35**	**33.35**
	DSi Concentration	20	See A2 Table 2		
	RPSi Concentration	21	See A2 Table 3		
Internal loading	DSi Concentration Temperature relationship	15 25	See A2 Table 2 Difference in flux calculated from lower and upper 95% confidence intervals	**40**	
Net uptake	Uncertainties of other fluxes	40	Average relative uncertainties of other DSi flux except CSO and precipitation because so small	**40**	
Sedimentation	RPSi Concentration	21	See A2 Table 3		**31**
	Catch efficiency	10	Estimated based on Boyce et al. (1990)		
Resuspension	Uncertainties of other fluxes	31	Same as sedimentation (same order of magnitude)		**31**
Burial	Uncertainties of benthic flux, sedimentation, and resuspension	31	Same as sedimentation and resuspension which exert larger influence than internal loading		**31**